SPECIAL REPORT 03-02

ENCLOSURE 5

FRAMATOME ANP REPORT 51-5027436-00
"EXAMINATION OF DIABLO CANYON UNIT 2 SG TUBES – FINAL REPORT"

20440-9 (2/2002)

FRAMATOME ANP

ENGINEERING INFORMATION RECORD

Document Identifier 51 - 5027436 - 00

Title EXAMINATION OF DIABLO CANYON UNIT 2 SG TUBES - FINAL REPORT

PREPARED BY:	REVIEWED BY:
Name PA SHERBURNE	Name MG POP
Signature PA Sherburne Date 6/04/03	Signature Mike J. Pop Date 6/04/03

Technical Manager Statement: Initials MR L.S.Lamanna

Reviewer is Independent.

Remarks:

RECORD OF REVISION

DATE	REV.	SECTION	DESCRIPTION
6/04/2003	00	All	Original Release

Examination of Diablo Canyon Unit 2 Steam Generator Tubes

51-5027436-00

Final Report, May 2003

Citations

This report was prepared by

Framatome ANP, Inc.
155 Mill Ridge Road
Lynchburg, Virginia 24502-4341

Principal Investigator
P. A. Sherburne, P.E.
Advisory Engineer

Examination of Diablo Canyon Unit 2 Steam Generator Tubes; May 2003. FRA-ANP Document No. 51-5027436-00.

Acknowledgements

The author would like to acknowledge and thank the following people for their significant contributions to this project: Bob Allen, Jim Begley, Ben Blankinship, Jeff Fleck, Eddie Grubbs, Greg Pillow, Mike Pop, Tom Ribaric, and Steve Jensen and Woody White of BWXT.

EXECUTIVE SUMMARY

Sections of 2 Alloy 600 steam generator (SG) tubes were removed from Diablo Canyon Power Plant Unit 2 (DCPP-2) during the 2R11 outage in February 2003. These tubes were removed from SG 24 to meet the three-cycle frequency requirement of EPRI Report No. 1006255. Both tubes had eddy current (EC) indications representative of axially oriented OD stress corrosion cracks (ODSCC) at the 2nd TSP (2H) intersections.

Laboratory examinations of the pulled tubes were subsequently conducted in support of NRC GL 95-05 requirements for voltage-based alternate repair criteria (ARC) for axial ODSCC. The primary objectives of the examinations were the following:

- To physically characterize the tube degradation for correlation with field NDE results and to verify that the degradation morphology is consistent with the assumptions made in NRC GL 95-05.
- To determine the effect of degradation on the burst strength of the tubing and the leak rate under main steam line break (MSLB) conditions.

These examinations included receipt inspection and verification of identity, eddy current testing, dimensional measurements, ambient temperature leak rate and burst testing, visual and stereovisual inspections and photography, scanning electron microscopy (SEM) including energy dispersive spectroscopy (EDS) and wavelength dispersive spectroscopy (WDS), fractography, metallography, and tensile testing.

The laboratory examinations confirmed axial intergranular stress corrosion cracking (IGSCC) in the 2H TSP regions of these 2 tubes. 100% through wall defects were present in both tubes as confirmed by leak rate testing and later by SEM fractography. In addition, both tubes had secondary IGSCC cracks at one other circumferential location.

The 2H TSP section from tube number R35C57 contained a 0.52" long axial crack with 0.23" through wall extent, and burst at 5,961 psi. The 2H TSP section from tube R44C45 contained a 0.7" long axial crack with 0.47" through wall extent, and burst at 4,226 psi. The corresponding free span regions burst at 12,769 psi for tube number R35C57, and 12,269 psi for tube number R44C45.

SEM/EDS/WDS analysis revealed the presence of sulfur and lead in spalled areas on the OD surface near the defect location of R35C57, as well as on the burst rupture surface itself. This is consistent with results from the 2R8 tube pull examination conducted in 1998.[3] Sulfur and lead are known to be detrimental to Alloy 600 and have been previously implicated in ODSCC.

Table of Contents

List of Tables

List of Figures

1 Introduction

1.1 Background

Diablo Canyon Power Plant Unit 2 (DCPP-2) is one of two pressurized water reactor plants operated by the Pacific Gas and Electric Company. Unit 2 is an 1130 MWe plant that went into commercial operation in March 1986 and has since operated for 14+ effective full power years (EFPY). DCPP-2 has four Westinghouse Model 51 recirculating steam generators with 3388 U-tubes each. The tubing material is 7/8 inch OD mill annealed Alloy 600, with a nominal wall thickness of 0.050 inch. The tubes were initially roll expanded into the tubesheet several inches from the primary side. Before unit startup, the tubes were expanded along the full tubesheet depth using the WEXTEX explosive process to eliminate the tube to tubesheet crevice. The tubes are supported along their length by drilled-hole carbon steel tube support plates (TSP).

During the scheduled 2R11 outage in February 2003, sections of 2 tubes – R35C57 and R44C45 - were removed from steam generator 24 to meet the three-cycle frequency requirement of EPRI Report No. 1006255. Both tubes had field bobbin coil eddy current (EC) indications at the 2nd TSP (2H) intersections. These indications were confirmed by rotating coil EC to be axially oriented OD stress corrosion cracks (ODSCC). The indication in tube no. R44C45 was believed to be a through wall defect.

1.2 Examinations Performed

Laboratory examinations of the pulled tubes were conducted by Framatome ANP, Inc. (FANP) and by BWX Technologies, Inc. (BWXT) under contract to FANP, in support of NRC GL 95-05 requirements for voltage-based alternate repair criteria (ARC) for axial ODSCC. The primary objectives of the examinations were the following:

- To characterize tube degradation (i.e., morphology, size, and extent) for correlation with field NDE results and to verify that the degradation morphology is consistent with the assumptions made in NRC GL 95-05.
- To determine the effect of degradation on the burst strength of the tubing and the leak rate under main steam line break (MSLB) conditions.

These examinations included receipt inspection and verification of identity, eddy current testing, dimensional measurements, leak rate and burst testing, visual and stereovisual inspections and photography, scanning electron microscopy (SEM) including energy dispersive spectroscopy (EDS) and wavelength dispersive spectroscopy (WDS), fractography, metallography, and tensile testing. Data from these examinations[1] are summarized and discussed in this report.

[1]Destructive examination data included in this report is from the following document: *Examinations of Diablo Canyon Unit 2 Steam Generator Tube Sections from 35-57 and 44-45,* BWX Report No. 1140-028-03-09, May 2003.

In addition, an evaluation of the through wall crack profiles was completed by J.M. Begley and transmitted to Westinghouse in FANP Document No. 51-5028414-01, *DCPP 2R11 DE Input Transmittal to Westinghouse.* This evaluation is included in Appendix A.

1.3 Quality Assurance

All examinations were performed as Safety Related work in accordance with Framatome ANP QA Program and Quality Management Manual 56-5015885-01. This program meets the requirements of 10CFR50, Appendix B. A QA Data Package for this work will be maintained by FANP in accordance with applicable procedures.

2 Tube Failure Analysis

2.1 Receipt Visual Inspection

Sections of tube numbers R35C57 and R44C45 from Diablo Canyon SG 2-4 were received at the Framatome ANP (FANP) SERF-4 facility on Monday, March 10, 2003. The tube sections removed and their relative location in the steam generator are illustrated in Figure 1. Since the region of interest in both tubes was the 2H TSP elevation, only those sections and the sections above the 2H elevation were unpacked and inspected.[1] Results of the receipt inspection are summarized in Table 1.

Figures 2 and 3 illustrate the typical appearance of tube numbers R35C57 and R44C45 at the 2H intersections. As can be seen in the photographs, the locations at which the support plates contacted the tubes are clearly visible.

Note the axial scrape marks and almost complete absence of scale on the OD of R35C57 (Figure 2). With the exception of the 2H TSP location, the OD of all sections of R44C45 inspected were uniformly covered with a black scale. Portions of this scale had spalled away from the tube surface above and below the TSP elevation during tube removal operations (Figure 3).

During the receipt inspection, a reference notch was placed on the bottom of each tube section. In subsequent examinations, all field and laboratory axial positions are referenced from the bottom end of the tube segments and all angular orientations are referenced to the notch, with angles increasing in the clockwise (CW) direction looking at the bottom end of the tube.

2.2 Eddy Current Inspection

Following receipt inspection and prior to leak rate testing, tube sections R35C57-8 and R44C45-13 were inspected with bobbin coil and 3-coil rotating pancake coil (RPC). These inspections used a Zetec 0.720" diameter M/ULC bobbin coil and a Zetec 0.720" diameter 3-coil RPC containing a 0.115" diameter pancake coil, a +Point coil, and a 0.080" diameter high frequency pancake coil. Zetec EDDYNET 98 software (Version 2.38 for examination and Version 2.40 for analysis) was utilized. The Examination Technique Specification Sheets (ETSS's) in PG&E Procedure NDE ET-7 Rev. 2 were followed for all data acquisition and analysis. Complete details of the examinations, including graphics, can be found in Reference 2.

Results of the receipt inspection are summarized and compared with data from both the initial examination and the platform (post tube pull) examination in Tables 2 and 3. In Table 3, the angular orientation of the indication in degrees is included in the "Call" column as measured clockwise (CW) from the reference notch in the bottom of the tube section.

The following paragraphs discuss the results for each tube section inspected.

R35C57-8, 2H

The field bobbin coil inspection identified a 5.09 volt (V) DOS[2] indication approximately in the middle of the 2H TSP. The +Point coil identified the indication as a 4.01V single axial indication (SAI). Following tube pull, the voltages increased to 7.18V and 5.08V for the bobbin and +Point coils, respectively. These increases in voltage may have occurred as a result of ligament tearing between micro cracks and/or a change in the width of the crack following removal of the tube from the steam generator; i.e., the primary crack may have opened up slightly when no longer constrained by the TSP or deposits within the TSP. The SAI was estimated to be near through wall and positioned 202° from the reference notch.

In addition, an 8.76V dent (DNT) signal was detected at the 2H location following tube pull. This signal was not present prior to tube pull. The location of the dent signal in the laboratory inspection was measured at 0.44 inches below the DOS indication. No visible evidence of OD damage was observed during the receipt visual inspection that would explain the presence of denting.

R44C45, 2H

The field bobbin coil inspection identified a 21.5V DOS indication at 0.14" above the middle of the 2H TSP. The +Point coil identified two axial indications (SAI) at the 2H TSP. Following tube pull, the bobbin coil voltage increased by ~50% to 32.31V (on platform) and to 35.73V (in lab). No dent signal was observed either before or after the tube pull for this tube. The larger of the two axial indications also exhibited an increase in voltage from 12.12V (field) to 17.37V (on platform) and to 15.58V (in lab). The larger of the two indications was estimated to be 98% through wall and positioned 73° from the reference notch. The smaller indication was estimated to be 57% through wall and positioned 25° from the reference notch.

2.3 Leak Rate Testing

Room temperature leak rate testing was performed per EPRI guidelines[4] on the two sections of tubing containing the 2H TSP intersection. The test setup used the Framatome ANP insitu pressure test system and consisted of a full length tool head locked into the bottom end of each sample as a water supply probe and a full length tool head locked into the top end of each tube as a vent and stopper probe.

Test pressures included 1750 psi (normal operating pressure corrected for temperature and gauge effects), 2250 psi (intermediate pressure), and 2750 psi (MSLB pressure corrected for gage effects and for the effect of temperature on material properties). The tests were conducted with approximately 5 minute hold periods at each of these pressures. Results of the leak test are summarized in Table 4.

[2] A "DOS" indication is defined as a distorted support plate signal with a possible OD indication.

The test pressure and leak rate versus time (time in seconds) results for R35C57 are shown in Figure 4. Leakage initiated at approximately 2200 psi but decreased with time over the hold period and again increased with the increase in pressure to the MSLB condition. The maximum MSLB leak rate measured during this test was 0.0368 gpm at the start of the hold period at the MSLB pressure differential. Over the hold time at MSLB conditions with approximately constant pressure, the leak rate decreased by about a factor of three. Although deionized water was used in the tests to minimize the potential for particles in the water, it's possible that particulates in the pulled tube test specimen may have deposited within the crack.

The test pressure and leak rate versus time (time in seconds) for R44C45 are shown in Figure 5. Upon reaching the MSLB pressure differential, the leak rate increased to a maximum of 0.88 gpm. This spike in leak rate might have been due to a transient in the flow meter following the rapid increase in leakage with increasing pressure. Following the spike, the leak rate remained essentially constant for the remainder of the 5 minute hold time.

Complete details of the leak rate tests can be found in Reference 5.

Following leak rate testing, the tube sections were reexamined and subjected to repeat eddy current inspection with the 3-coil rotating probe. Figure 6 is a photograph of the 2H intersection of tube no. R44C45 at ~75°, showing the axial crack that was not visible before leak rate testing. The visible portion of the crack was ~0.55 inches long.

The axial crack at the 2H intersection of Tube R35C57 was not visible even after leak rate testing.

The eddy current inspection results before and after leak rate testing are summarized in Table 5. Line by line phase sizing comparisons for the field EC, the lab receipt EC, and the post leak rate test EC inspections are shown in Figures 7 through 9 for the 3 single axial indications. In the figures, the phrase "normalized length" means that the first data point recorded was set to x = 0.0 for all 3 data sets, so that all 3 records begin at the same point. Note that the indicated flaw lengths increased for the primary defects following leak rate testing.

2.4 Furnace Oxidation

Because both 2H intersections leaked and thus may have experienced ligament tearing during the leak rate test, the two tube sections were placed in an atmospheric furnace and held at 900°F for 1 hour to heat tint/oxidize any torn ligaments. The objective was to allow any tearing that occurred during leak rate testing to be distinguished from tearing that would occur later during burst testing. The time and minimum temperature required to oxidize the ligaments were selected based on a qualification test program carried out in advance of the leak rate testing.[6] Figure 10 is a photograph of tube no. R44C45 following the oxidation step. As expected, the magnetite scale took on a burnished color as a result of oxidation.

2.5 Post Oxidation Inspections

Low magnification photographs were taken at 45° intervals at the 2H TSP regions on both tubes to document their overall condition following the oxidation step. These photographs are provided in Figures 11-26. The bottom end of each tube segment is always to the left in these photographs.

Stereovisual examinations detected an axial crack on R35C57-8B at ~170°, starting about 0.2" above the bottom of the 2H TSP region. A photo mosaic of this crack is provided in Figure 27. A large axial crack was located on R44C45-13A at ~90°, which was ~0.6" long and ended just below the top of the 2H TSP region. A photograph of this crack is provided in Figure 28. Another small area of secondary cracking was also noted on R44C45-13A at ~25° within the TSP region.

Heavy black deposits were generally present on tube R44C45, whereas the deposits on R35C57 had generally been scraped off during removal from the steam generator.

2.6 Sectioning Diagrams

Detailed sectioning diagrams for all the tube sections examined are provided in Figures 29-36. Also included are schematic diagrams showing the location and extent of the cracks found in the 2H TSP regions.

In the following discussions of test results, reference will be made to specific tube sections as defined in these diagrams.

2.7 Burst Testing

Following the post oxidation inspections, the two 2H tube sections (R35C57-8B and R44C45-13A2) were subjected to burst testing at room temperature in accordance with EPRI guidelines for leak and burst testing[7], along with a free span region from each tube (R35C57-9B and R44C45-13B2). In addition, a control sample of virgin tubing was tested for baseline purposes. The burst tests were performed simulating free span conditions with no supports enveloping the tube segments. Silicon plastic bladders were used in all the samples, and 0.006" thick brass shims were used at the defect locations in accordance with the EPRI guidelines. These guidelines also stipulated a pressurization rate of 20 - 500 psi/sec, which was measured between ~2,000 psi and ~6,000 psi (prior to yield), or up until the point of rupture in the case of the defect specimens.

During initial testing on R44C45-13A2, a pressure of 3,403 psi was reached before the pressure started to decrease and the test was stopped. Subsequent examinations revealed that the brass shim had slipped out of place, and that leakage was occurring through a breach in the plastic bladder at the defect location. The defect location had opened slightly as shown in Figure 37, to a maximum opening width of ~0.022". In accordance with the EPRI guidelines[3], which allow pressurization rates of up to 2000 psi/sec under special

[3] Higher pressurization rates pose less challenge to the seal used to prevent leakage through the defect prior to burst.

circumstances, the sample was reshimmed and retested at a pressurization rate of 1,956 psi/sec to ensure that a fish mouth rupture would occur. This test was successful and resulted in a burst pressure of 4,226 psi. It should be noted that prior to the issuance of the latest EPRI guidelines, a pressurization rate of 200-2000 psi/sec was specified, so testing at these higher pressurization rates is consistent with earlier test results.

Burst test results are summarized in Table 6. Dimensional measurements required by the EPRI guidelines are provided in Tables 7 - 11. All fish mouth burst openings were axially oriented. R33C57-8B burst at 5,961 psi and R44C45-13A2 burst at 4,226 psi, whereas the associated free span specimens burst at 12,769 psi (R35C57-9B) and 12,269 psi (R44C45-13B2). The virgin tube control sample burst at 10,020 psi.

2.8 Macro Photography/Stereovisual Examinations of Post-burst Regions

Following burst testing, visual inspections were performed at low magnification to characterize the burst ruptures and associated areas of interest. Low magnification photographs were taken at 45° intervals in the TSP regions of the two tubes, and of the burst opening on the free span sections of tubing. Photographs were taken of additional selected areas during the stereovisual examinations of these tube sections as described in the following paragraphs. The bottom end of each tube segment is always to the left in these photographs.

R35C57-8B (2H TSP)

Macro photographs of this tube section in 45° intervals are provided in Figures 38-45, and a similar photograph centered over the fish mouth opening at 170° is provided in Figure 46. Higher magnification photographs of the fracture surfaces showing the extent of oxidation from the post-leak oxidation process is provided in Figures 47 and 48. The burst region was at approximately 170°, with the bottommost extent of the oxidized defect region at ~0.2" from the bottom of the TSP. SEM fractography (Section 2.9) later revealed a total axial extent of ~0.52", and a through wall length of ~0.23".

There was also a secondary crack located at ~180°, which was parallel to the burst rupture, and which was ~0.55" long beginning ~0.2" from the bottom of the TSP. This can be seen in Figure 47.

R35C57-9B (Free span)

The fish mouth rupture on free span specimen R35C57-9B occurred near 135°, and a photograph of the burst rupture is provided in Figure 49. As described in Section 2.9, SEM fractography later verified that the failure was completely ductile, with no IGSCC.

A photograph of typical mottled deposits adhering to the surface after burst testing is provided in Figure 50.

R44C45-13-A2B1 (2H TSP)

Macro photographs of this tube section in 45° intervals are provided in Figures 51-58, and a similar photograph centered over the fish mouth opening at 90° is

provided in Figure 59. Higher magnification photographs of the fracture surfaces showing the extent of oxidation from the post-leak oxidation process is provided in Figures 60 and 61. The burst region was at approximately 90°, with the bottommost extent of the oxidized defect region at ~0.04" from the bottom of the TSP. SEM fractography (Section 2.9) later revealed a total axial IGSCC extent of ~0.7" (OD), and a through wall IGSCC length of ~0.47".

There was also some secondary cracking ~0.35" long and located near 25°, which was parallel to the burst rupture and located from ~0.05" to 0.4" from the bottom of the TSP. Macro photographs of this crack are provided in Figures 62 and 63 after sectioning had already occurred. This crack corresponds to the second eddy current defect indication on this tube. It was later decided to perform SEM fractography on the two halves of this crack, so additional sectioning was performed to expose the defect surfaces. Stereovisual photographs of all the defect surfaces are provided in Figures 64 through 67, which clearly show the oxidized IGSCC regions. The CCW surfaces were subsequently chosen for SEM fractography, and analyses revealed a maximum through wall depth of ~78%.

R44C45-13B2 (Free span)

The fish mouth rupture on the free span section R44C45-13B2 occurred near 135°, and a photograph of the burst rupture is provided in Figure 68. As described in Section 2.9, SEM fractography later verified that the failure was completely ductile, with no IGSCC.

A photograph of typical mottled deposits adhering to the surface of this tube after burst testing is provided in Figure 69.

2.9 SEM Fractography

R35C57-8B2B (Through wall 2H defect)

A low magnification photo mosaic of the counterclockwise (CCW) fracture surface from R35C57-8B2B is provided in Figure 70. Surface details are largely obscured due to the heavy oxide layer on this surface (the majority of which is believed to have occurred in service, and not as a result of the post-leak oxidation process). The black rectangles in this photo mosaic are from calibrated depth measurements made on the SEM.

Standard internal distance calibrations on the SEM are routinely performed at 1000X. To ensure that these calibrations were still valid at the 50X range used to obtain the photo mosaics, a section of metallic ruler that could be placed in the SEM was photographed adjacent to a calibrated stage micrometer used on the metallograph. Comparisons between the calibrated stage micrometer, the section of ruler, and the internal SEM calibrations, provided traceability and indicated that the measurements were accurate to $\pm$2% (±0.001" for a 0.050" nominal wall thickness).

Higher magnification photographs typifying the areas at the bottom, center, and top of the fracture surface are provided in Figures 71-76. The actual depth measurements of IGSCC and ductile regions were obtained from photographs

such as these. This data is tabulated in Table 12. The starting point for these measurements was at the bottom edge of the IGSCC, and axial lengths were measured at the mid-wall of the tubing. Areas of IGSCC, oxidized ductile regions that tore during the leak test, and nonoxidized ductile regions that tore during the burst test are also tabulated and compared to the nominal cross-sectional area as a check.

Based upon these measurements, the total axial extent of IGSCC was 0.52", with a maximum depth of 100% through wall. The axial extent of through wall IGSCC was 0.23". There were 0.0208 square inches of IGSCC, a very minimal amount of ductile tearing during the leak test (0.000055 square inches), and 0.0055 square inches of nonoxidized ductile region.

R44C45-13A2B1 (Through wall 2H defect)

A low magnification photo mosaic of the counterclockwise (CCW) fracture surface from R44C45-13A2B1 is provided in Figure 77. Surface details are largely obscured due to the heavy oxide layer on this surface (most of which is believed to have occurred in service, and not from the post-leak oxidation process). The black rectangles in this photo mosaic are from calibrated depth measurements made on the SEM.

Higher magnification photographs typifying the areas at the bottom, center, and top of the fracture surface are provided in Figures 78-83 (the photographs are oriented so as to keep the bottom of the tube to the left). The actual depth measurements of IGSCC and ductile regions were obtained from photographs such as these. This data is tabulated in Table 13. The starting point for these measurements was at the bottom edge of the IGSCC, and axial lengths were measured at the mid-wall of the tubing. Areas of IGSCC, oxidized ductile regions that tore during the leak test (very minimal), and nonoxidized ductile regions that tore during the burst test are also tabulated and compared to the nominal cross-sectional area as a check.

Based on these measurements, the axial extent of IGSCC was 0.701" with a maximum depth of 100% through wall. The axial extent of through wall IGSCC was 0.47". There were 0.0305 square inches of IGSCC, a very minimal amount of ductile tearing during the leak test (0.00023 square inches), and 0.0039 square inches of nonoxidized ductile region.

As can be seen in Figures 82 and 83, there is a small region of intergranular corrosion that is ~0.025 inches out-of-plane from the main crack. This region is typical of the main fracture surface, which is made up of several small crack segments joined together by intergranular corrosion. More discussion of the features observed in this region can be found in Appendix A.

R44C45-A2B2A and R44C45-A2B3A (Non through wall crack at 25°)

The partial through wall crack at 25° was originally cut in two to provide circumferential metallographic information in the 2H TSP region as described in Section 9. It was later decided to perform SEM fractography on this non through

wall defect region, primarily to provide comparison data for the eddy current signal at this location.

A photo mosaic of the two sections are provided in Figure 84. The missing saw kerf[4] between these two sections is ~0.02", and it is apparent that the very bottommost portion of IGSCC was cut into during the section removal process. However, the extent of this IGSCC is believed to be very minimal, based upon the small amount at the edge of the cut and visual examinations of the OD surface prior to removal.

Measurements of the IGSCC depth profile are provided in Table 14. Based on these data, the length of the crack was ~0.36", with a maximum depth of 78% through wall.

R35C57-9B (Free span)

SEM photographs showing the ductile nature of the nondefect free span burst sample from R35C57-9B are provided in Figures 85 and 86. Photo mosaics were not obtained in this instance because the fracture mode was 100% ductile, with no IGSCC.

R44C45-13B2 (Free span)

SEM photographs showing the ductile nature of the nondefect free span burst sample from R44C45-13B2 are provided in Figures 87 and 88. Photo mosaics were not obtained in this instance because the fracture mode was 100% ductile, with no IGSCC.

2.10 EDS/WDS Defect and Outer Surface Characterization

EDS/WDS analysis was performed in the IGSCC regions of the burst rupture surfaces on R35C57-8B, and on the adjacent outer surface deposits in the TSP regions, to characterize the elements that were present in these regions. This was done for comparison to similar analysis performed in 1998 on the TSP defect regions of tube nos. R02C66 and R37C53 from the 24 steam generator[3]. It should be noted that after the defect specimens from R35C57 and R44C45 were leak tested, they were oxidized at 900°F for one hour to heat tint any ductile tear regions that may have occurred during the leak test. The tubes examined in 1998 were not subjected to this process, which may have affected the surface chemistry.

R35C57-8B (2H TSP Region)

A spalled area on the OD surface near the burst rupture was examined on sample R35C57-8B. This area is shown as Area 1 in Figure 89. As shown in the WDS analysis in Figure 90, both sulfur (predominant) and lead (lesser amounts) were detected. Both of these elements were similarly detected during the examinations in 1998[3].

SEM fractography and EDS analysis in the IGSCC fracture surface region is provided in Figure 91 and 92. Significant amounts of silicon were detected

[4] The term "saw kerf" refers to the width of the saw blade used in cutting the specimen.

(some of which may have come from the silicon bladder used during burst testing) in addition to the base constituents and minor amounts of various elements. Overlapping peaks for S/Mo/Pb required WDS analysis as shown in Figures 93 and 94 to resolve. Similar to the results from the OD surface, both sulfur and lead were detected.

2.11 Defect Metallography

Transverse metallographic cross-sections were prepared through both of the TSP defect regions (see Figures 29-36 for detailed sectioning diagrams). The axial location of each of these metallographic cross-sections was selected to coincide with the apex of the fish mouth rupture in the center of the defect region. This provided information on the extent and depth of IGSCC around the circumference of the tube away from the actual burst region. Serial grinding was not performed on these samples.

R35C57-8B2B

Figure 95 is a polished cross-section showing the rupture surface at 170°, along with a secondary crack at 180° that was near, if not completely, 100% through wall. Figure 96 shows the intergranular nature of the secondary crack near the ID surface. The nearness of these two cracks at 170° and 180° prevented their differentiation by eddy current inspection techniques.

There were no other incipient cracks around the circumference of the tube at this location.

R44C45-13A2B2

Figures 97 and 98 are polished and etched cross-sections showing the rupture surface along with numerous intergranular stress corrosion cracks in the nearby vicinity. In addition, two closely-spaced secondary cracks were present near 25° as shown in the transverse cross section of Figure 99. The two cracks shown in this view were 0.027" (53% TW) and 0.033" (65% TW) deep based on a 0.051" nominal wall thickness for this tube. SEM fractography of this region after the tube section was bent open revealed a maximum penetration of 78% TW (see Section 2.9 and Figure 84). This region of IGSCC corresponds to the 57% TW single axial indication (SAI) detected in the lab (with the +Point coil) prior to leak rate testing and the 67% TW SAI after leak rate testing.

2.12 Tube Deposit Analysis

Approximately 8 grams of free span deposits were collected from free span sample R44C45-14C after tensile testing. There were insufficient deposits available from the OD surface of R35C57, or from either of the 2H TSP regions to allow for analysis. Inductively Coupled Plasma (ICP) spectroscopy was performed on the free span deposits from R44C45-14C and the results are tabulated in Table 15. The major constituent was iron (oxide), with significant amounts of copper, zinc, nickel, and manganese. These results are very similar to results found in earlier examinations[3].

2.13 Material Properties

Tensile Testing

Two free span regions from each tube were tensile tested at ambient temperature. As shown in Table 16, the sample from tube R35C57 had a slightly higher yield and tensile strength than the sample from tube R44C45. The engineering stress/strain curves for these tube specimens are provided in Figures 100 and 101.

Bulk Chemistry

One piece from each tube was sectioned and decontaminated for bulk chemical analysis. The analysis results are presented in Table 16.

Microstructure

Longitudinal metallographic samples were prepared from the free span regions of each tube as shown in the sectioning diagrams in Figures 29 – 36. A dual etch procedure using phosphoric and nital acid solutions was used on these samples to characterize the carbide distribution and grain microstructure. The results are shown in Figures 102 and 103 for tube R35C57, and Figures 104 and 105 for tube R44C45. In both instances the carbide distribution along the grain boundaries was relatively light, as is typical for mill annealed Alloy 600 tubing. Intragranular matrix carbides were also present in both cases, sometimes in the form of longitudinally oriented bands.

Hilliard Circular intercept measurements indicated an ASTM grain size of 9.75 for tube R35C57 (12.6 μm average grain diameter) and 10.0 (11 μm average grain diameter) for tube R44C45.

Summary

The material properties discussed above are summarized and compared with the material test report values and with the ASME specification for SB-163 (Alloy 600) in Tables 17 and 18. As can be seen in the tables, the material properties for tube nos. R35C57 and R44C45 are in agreement with both the material test reports and the ASME specification.

3 Summary of Laboratory Examinations

The following summary observations were made based on the results of the laboratory examinations documented in this report:

- Tube nos. R35C57 and R44C45 both developed leaks at the 2H TSP location when subjected to leak rate testing. The maximum room temperature leak rate recorded for tube no. R35C57 was 0.0368 gpm at a pressure differential of 2750 psi (MSLB pressure corrected for gauge effects and for the effect of temperature on material properties). The maximum room temperature leak rate recorded for tube no. R44C45 was 0.88 gpm at a pressure differential of 2750 psi.
- The 2H TSP defect specimen from tube no. R35C57 contained a 0.52" long axial crack (characterized as IGSCC, 0.23" of which was through wall) and burst at 5,961 psi. The 2H TSP defect specimen from tube no. R44C45 contained a 0.7" long axial crack (characterized as IGSCC, 0.47" of which was through wall) and burst at 4,226 psi. In both cases, prior leak testing had confirmed that the IGSCC was 100% through wall. The corresponding free span regions without defects burst at 12,769 psi for tube no. R35C57, and 12,269 psi for tube no. R44C45.
- The IGSCC in these tube specimens was generally isolated, with the majority of the circumference unaffected. In both 2H TSP regions, only one other area of axially oriented IGSCC was identified in addition to the primary defect. In the case of tube no. R35C57, the second region of IGSCC was located ~10° from the primary crack and was ~100% through wall. In the case of tube no. R44C45, the secondary IGSCC was located ~65° away from the primary crack and was 78% through wall.
- SEM fractography confirmed that very little ductile tearing occurred during the leak rate test for either tube section.
- SEM/EDS/WDS analysis revealed the presence of sulfur and lead in spalled areas on the OD surface near the defect location on tube no. R35C57, as well as on the burst rupture surface itself. This is consistent with results from similar examinations conducted in 1998. Both of these materials are detrimental to Alloy 600.[8]
- Quantitative ICP analysis of deposits from a free span region indicated that iron (oxide) was the major constituent. Significant concentrations of copper, zinc, nickel, and manganese were also present.
- Material properties for both tubes were in agreement with the material test report values and with the ASME SB-163 specification.

4 Conclusions

Axially oriented IGSCC was confirmed in the 2H TSP regions of these tube numbers R35C57 and R44C45. 100% through wall defects were present in both tubes as confirmed by leak rate testing and later by SEM fractography. These defects were detected by eddy current testing in both the field and the laboratory. In addition, both tubes had secondary IGSCC cracks at one other circumferential location. On tube number R35C57, the secondary crack was also ~100% TW and located parallel to and in close proximity (~10° or ~0.024") to the primary defect. The second crack in this tube was not distinguishable from the primary crack by eddy current because of its close proximity to the primary crack.

In tube number R44C45, the second region of IGSCC was located ~65° from the primary crack and readily detected by eddy current. The maximum through wall penetration of this region of IGSCC was 78%.

In general, there was good agreement between the eddy current results and the laboratory results.

The 2H TSP section from tube number R35C57 contained a 0.52" long axial crack with 0.23" through wall extent, and burst at 5,961 psi. The 2H TSP section from tube R44C45 contained a 0.7" long axial crack with 0.47" through wall extent, and burst at 4,226 psi. In both cases, the leak rate testing had confirmed that the defects were 100% through wall. The corresponding free span regions burst at 12,769 psi for tube number R35C57, and 12,269 psi for tube number R44C45.

SEM/EDS/WDS analysis revealed the presence of sulfur and lead in spalled areas on the OD surface near the defect location on R35C57, as well as on the burst rupture surface itself. This is consistent with results from the 2R8 tube pull examination conducted in 1998.[3] Sulfur and lead are known to be detrimental to Alloy 600 and have been previously implicated in ODSCC.

5 References

1. Quality Control Inspection Report No. 6022977, 3/13/2003.
2. FANP Document No. 51-5025823-00, "Eddy Current Tube Pull Examination for PG&E Diablo Canyon Unit 2 - March 2003," 4/15/2003.
3. FANP Document No. 51-1269247-00, "Diablo Canyon Unit 2 Steam Generator Pulled Tube Examinations," January 1999.
4. *Steam Generator In Situ Pressure Test Guidelines*, EPRI TR-107620-R1, Final Report, June 1999.
5. FANP Document No. 51-5025756-00, "Diablo Canyon Unit 2 Tube Pull Leak Rate Test Results," 3/18/2003.
6. FANP Document No. 51-5025213-00, "7/8" OD RSG Tube (Alloy 600) Oxidation Test Results," 3/12/2003.
7. *Steam Generator Tubing Burst Testing and Leak Rate Testing Guidelines*, EPRI Report No. 1006783, Final Report, December 2002.
8. *PWR Secondary Water Chemistry Guidelines – Revision 5,* EPRI TR-102135-R5, Final Report, May 2000.

Table 1. Receipt Inspection Summary

Sample Identification	As-received Length (inches)	On-site Length (inches)	Distance to landmark from bottom of tube section, inches	Landmark	Comments
R35C57-9	33 5/8	33 5/16	N/A	N/A	Section is somewhat bowed in an "S" shape, with the point of inflection ~23" from the bottom. Axial scrape marks full length/360°. Most deposit has been scraped off.
R35C57-8	21 7/8	21 7/8	7 3/4	Bottom of 2H TSP	Contact with 2H TSP clearly visible. No visible evidence of OD cracking. Most deposit was scraped off OD during tube removal. Circumferential saw cut at 21⅛ inches from bottom. Photographs taken at 0, 90, 180, and 270 degree orientations.
R44C45-15	12 1/4	12 3/8	N/A	N/A	Covered with thick black scale; no removal damage observed.
R44C45-14	17 1/8	17 1/8	15½ and 16⅞	Saw Cuts (~¼ inch square)	Covered with thick black scale; no removal damage observed.
R44C45-13	23	23	5 1/4	Bottom of 2H TSP	Contact with 2H TSP clearly visible. No visible evidence of OD cracking. Large areas of spalled deposit above (@90°) and below (@45°) 2H TSP. Photographs taken at 0, 90, 180, and 270 degrees.

Table 2. Bobbin Eddy Current Inspection Results Summary

Tube Sample No.	Location in SG	Field Exam			Post Tube Pull			In Lab		
		Call	Volts	Phase	Call	Volts	Phase	Call	Volts	Phase
R35C57-8	2H + 0.07"	DOS	5.09	60	DOS DNT	7.18 8.76	56 188	91% DNT	7.75 9.40	55 188
R44C45-13	2H + 0.14"	DOS	21.5	54	DOS	32.31	53	93%	35.73	51

Table 3. Rotating Coil Eddy Current Inspection Summary

Tube Sample No.	Location in SG	Field Exam			Post Tube Pull (On Platform)			In Lab		
		Call	Volts	Phase	Call	Volts	Phase	Call	Volts	Phase
R35C57-8	2H + 0.03"	SAI	4.01	53	SAI	5.08	53	SAI 91% TW @ 202° (CW rotation from reference notch)	5.00	54
R44C45-13	2H + 0.04"	SAI	12.12	38	SAI	17.37	36	SAI 98% TW @ 73°	15.58	39
	2H – 0.09"	SAI	0.29	98	SAI	0.27	95	SAI 57% TW @ 25°	0.28	98

Table 4. Summary of Leak Rate Tests

Tube Sample No.	Pressure Hold Points, psi	Hold Time minutes	Maximum Leak Rate, gpm	Avg. Pressurization Rate, psi/sec
R35C57-8	1750	2	0.0000	16
	2250	5	0.0016	12
	2750	5	0.0368	11
R44C45-13	1750	5	0.1680	23
	2250	5	0.3200	14
	2750	5	0.8800	10

Table 5. Rotating Coil Eddy Current Inspection Pre and Post Leak Comparisons

Tube Sample No.	Location in SG	Pre Leak Test			Post Leak Test		
		Call	Volts	Phase	Call	Volts	Phase
R35C57-8	2H + 0.03"	SAI 91% TW 202°	5.00	54	SAI 91% TW 202°	6.39	50
R44C45-13	2H + 0.04"	SAI 98% TW 73°	15.58	39	SAI 98% TW 73°	15.30	38
	2H – 0.09"	SAI 57% TW 25°	0.28	98	SAI 67% TW 25°	0.38	86

Table 6. Room Temperature Burst Test Results

Tube Sample No.	Sample length inches	Pressurization Rate psi/sec	Burst Pressure psi
Control tube		199	10,020
R35C57-9B (free span)	12 1/16	389	12,769
R35C57-8B (2H)	11 ⅞	425	5,961
R44C45-13B2 (free span)	10 ½	337	12,269
R44C45-13A2 (2H)	11 7/16	1956	4,226

Table 7. Burst Test Dimensional Measurements – Control Specimen

Sample: Virgin
Defect Angle: NA

INITIAL LENGTH 12 1/16"		Instrument = Ruler	Calibration Due = NA
INITIAL DIAMETERS:			
Bottom End, 0°or Defect	0.875	Instrument = BW 100003714 Calibration Due: 9/19/03	
Bottom end, ditto+90°	0.875		
Center, 0°or Defect	0.875		
Center, ditto+90°	0.876		
Top End, 0°or Defect	0.875		
Top end, ditto+90°	0.875		
INITIAL WALL THICKNESSES:			
Bottom End, 0°or Defect	0.05240	Instrument = BW 1006009 Calibration Due: 4/29/03	
Bottom end, ditto+90°	0.05075		
Bottom end, ditto+180°	0.05200		
Bottom end, ditto+270°	0.05285		
Top End, 0°or Defect	0.05220		
Top end, ditto+90°	0.05170		
Top end, ditto+180°	0.05165		
Top end, ditto+270°	0.05230		

POSTTEST DIAMETERS:		
Remote, aligned w/Rupture	1.010	Instrument = BW 10003549 Calibration Due: 9/19/03
Remote, ditto+90°	1.006	
Burst (C/L - 1"), at rupture	1.048	
Burst (C/L- 1"), ditto+90°	1.085	
@ Burst, at rupture	1.273	
@ Burst, ditto+90°	1.113	
Burst (C/L+ 1"), at rupture	1.049	
Burst (C/L+ 1"), ditto+90°	1.085	
BURST DIMENSIONS		
Burst Rupture Length	1.880	
Burst Maximum Width	0.378	
Distance From Bottom of Tube to Bottom of Burst Region	5.625	
Burst Position, angle	120°	

Table 8. Burst Test Dimensional Measurements – R35C57-8B (2H)

Sample: 35-57-8B
Defect Angle: 170°

INITIAL LENGTH 11 7/8"		Instrument = Ruler	Calibration Due = NA
INITIAL DIAMETERS:			
Bottom End, 0°or Defect	0.873	Instrument = BW 100003714 Calibration Due: 9/19/03	
Bottom end, ditto+90°	0.875		
Center, 0°or Defect	0.876		
Center, ditto+90°	0.875		
Top End, 0°or Defect	0.876		
Top end, ditto+90°	0.875		
INITIAL WALL THICKNESSES:			
Bottom End, 0°or Defect	0.0514	Instrument = BW 1006009 Calibration Due: 4/29/03	
Bottom end, ditto+90°	0.0519		
Bottom end, ditto+180°	0.0525		
Bottom end, ditto+270°	0.0511		
Top End, 0°or Defect	0.0512		
Top end, ditto+90°	0.0511		
Top end, ditto+180°	0.0529		
Top end, ditto+270°	0.0519		

POSTTEST DIAMETERS:		
Remote, aligned w/Rupture	0.876	Instrument = BW 10003549 Calibration Due: 9/19/03
Remote, ditto+90°	0.876	
Burst (C/L - 1"), at rupture	0.872	
Burst (C/L- 1"), ditto+90°	0.880	
@ Burst, at rupture	1.008	
@ Burst, ditto+90°	0.988	
Burst (C/L+ 1"), at rupture	0.873	
Burst (C/L+ 1"), ditto+90°	0.880	
BURST DIMENSIONS		
Burst Rupture Length	0.908	
Burst Maximum Width	0.210	
Distance From Bottom of Tube to Bottom of Burst Region	5.25	
Burst Position, angle	170°	

Table 9. Burst Test Dimensional Measurements – R35C57-9B (Free Span)

Sample: 35-57-9B
Defect Angle: NA

INITIAL LENGTH 12 1/16"		Instrument = Ruler	Calibration Due = NA
INITIAL DIAMETERS:			
Bottom End, 0°or Defect	0.874	Instrument = BW 100003714 Calibration Due: 9/19/03	
Bottom end, ditto+90°	0.874		
Center, 0°or Defect	0.873		
Center, ditto+90°	0.875		
Top End, 0°or Defect	0.872		
Top end, ditto+90°	0.874		
INITIAL WALL THICKNESSES:			
Bottom End, 0°or Defect	0.0532	Instrument = BW 1006009 Calibration Due: 4/29/03	
Bottom end, ditto+90°	0.0506		
Bottom end, ditto+180°	0.0514		
Bottom end, ditto+270°	0..0528		
Top End, 0°or Defect	0.0535		
Top end, ditto+90°	0.0508		
Top end, ditto+180°	0.0510		
Top end, ditto+270°	0.0522		

POSTTEST DIAMETERS:		
Remote, aligned w/Rupture	1.000	Instrument = BW 10003549 Calibration Due: 9/19/03
Remote, ditto+90°	0.995	
Burst (C/L - 1"), at rupture	1.025	
Burst (C/L- 1"), ditto+90°	1.057	
@ Burst, at rupture	1.237	
@ Burst, ditto+90°	1.095	
Burst (C/L+ 1"), at rupture	1.03	
Burst (C/L+ 1"), ditto+90°	1.051	
BURST DIMENSIONS		
Burst Rupture Length	1.929	
Burst Maximum Width	0.380	
Distance From Bottom of Tube to Bottom of Burst Region	2.625	
Burst Position, angle	135°	

Table 10. Burst Test Dimensional Measurements – R44C45-13A2 (2H)

Sample: 44-45-13A2
Defect Angle: 90°

INITIAL LENGTH 11 7/16"		Instrument = Ruler	Calibration Due = NA
INITIAL DIAMETERS:			
Bottom End, 0°or Defect	0.877		
Bottom end, ditto+90°	0.876	Instrument = BW 100003714	
Center, 0°or Defect	0.878		
Center, ditto+90°	0.875	Calibration Due: 9/19/03	
Top End, 0°or Defect	0.876		
Top end, ditto+90°	0.875		
INITIAL WALL THICKNESSES:			
Bottom End, 0°or Defect	0.0509		
Bottom end, ditto+90°	0.0545	Instrument = BW 1006009	
Bottom end, ditto+180°	0.0547		
Bottom end, ditto+270°	0.0485	Calibration Due: 4/29/03	
Top End, 0°or Defect	0.0479		
Top end, ditto+90°	0.0526		
Top end, ditto+180°	0.0527		
Top end, ditto+270°	0.0485		

POSTTEST DIAMETERS:		
Remote, aligned w/Rupture	0.882	
Remote, ditto+90°	0.880	Instrument = BW 10003549
Burst (C/L - 1"), at rupture	0.875	
Burst (C/L- 1"), ditto+90°	0.889	Calibration Due: 9/19/03
@ Burst, at rupture	1.000	
@ Burst, ditto+90°	0.886	
Burst (C/L+ 1"), at rupture	0.882	
Burst (C/L+ 1"), ditto+90°	0.890	
BURST DIMENSIONS		
Burst Rupture Length	1.091	
Burst Maximum Width	0.190	
Distance From Bottom of Tube to Bottom of Burst Region	4.563	
Burst Position, angle	90°	

Table 11. Burst Test Dimensional Measurements – R44C45-13B2 (Free Span)

Sample: 44-45-13B2
Defect Angle: NA

INITIAL LENGTH 10.5"		Instrument = Ruler	Calibration Due = NA
INITIAL DIAMETERS:			
Bottom End, 0°or Defect	0.876	Instrument = BW 100003714 Calibration Due: 9/19/03	
Bottom end, ditto+90°	0.877		
Center, 0°or Defect	0.886		
Center, ditto+90°	0.885		
Top End, 0°or Defect	0.875		
Top end, ditto+90°	0.876		
INITIAL WALL THICKNESSES:			
Bottom End, 0°or Defect	0.0484	Instrument = BW 1006009 Calibration Due: 4/29/03	
Bottom end, ditto+90°	0.0520		
Bottom end, ditto+180°	0.0545		
Bottom end, ditto+270°	0.0505		
Top End, 0°or Defect	0.0489		
Top end, ditto+90°	0.0497		
Top end, ditto+180°	0.0534		
Top end, ditto+270°	0.0525		

POSTTEST DIAMETERS:		
Remote, aligned w/Rupture	0.988	Instrument = BW 10003549 Calibration Due: 9/19/03
Remote, ditto+90°	0.989	
Burst (C/L - 1"), at rupture	0.996	
Burst (C/L- 1"), ditto+90°	1.033	
@ Burst, at rupture	1.216	
@ Burst, ditto+90°	1.049	
Burst (C/L+ 1"), at rupture	0.988	
Burst (C/L+ 1"), ditto+90°	1.028	
BURST DIMENSIONS		
Burst Rupture Length	2.020	
Burst Maximum Width	0.374	
Distance From Bottom of Tube to Bottom of Burst Region	3.125	
Burst Position, angle	0°	

Table 12. Defect Burst Specimen Fractography Measurements – R35C57-8B2B

Point	Incremental Length Segment (")	Cumulative Length (")	Measured Oxidized IGA (")	Depth (") Oxidized IGA	Measured Oxidized Ductile (")	Depth (") Oxidized Ductile	Measured Non-oxidized Ductile (")	Depth (") Non-oxidized Ductile
0	0.0000	0.0000	0.3310	0.0032	0.0000	0.0000	3.6660	0.0350
1	0.0066	0.0066	1.3755	0.0132	0.0000	0.0000	3.1375	0.0300
1A	0.0052	0.0118	1.6355	0.0156	0.0000	0.0000	3.0570	0.0292
2	0.0023	0.0141	1.8730	0.0179	0.2670	0.0026	2.6260	0.0251
3	0.0073	0.0214	2.1535	0.0206	0.3400	0.0033	2.4520	0.0234
4	0.0077	0.0290	2.4055	0.0230	0.3915	0.0037	2.2160	0.0212
5	0.0023	0.0313	2.6215	0.0251	0.0000	0.0000	2.4315	0.0232
6	0.0088	0.0401	3.5480	0.0339	0.0000	0.0000	1.6815	0.0161
7	0.0137	0.0537	4.2420	0.0406	0.0000	0.0000	1.1085	0.0106
8	0.0190	0.0727	4.3980	0.0420	0.0000	0.0000	0.9755	0.0093
9	0.0216	0.0944	4.8150	0.0460	0.0000	0.0000	0.8020	0.0077
10	0.0216	0.1160	4.8925	0.0468	0.0000	0.0000	0.7845	0.0075
11	0.0111	0.1271	4.9590	0.0474	0.0000	0.0000	0.7630	0.0073
12	0.0218	0.1489	5.7925	0.0554	0.0000	0.0000	0.0000	0.0000
13	0.0094	0.1582	5.8020	0.0555	0.0000	0.0000	0.0000	0.0000
14	0.0182	0.1764	5.7910	0.0554	0.0000	0.0000	0.0000	0.0000
15	0.0182	0.1946	5.7645	0.0551	0.0000	0.0000	0.0000	0.0000
16	0.0293	0.2239	5.7835	0.0553	0.0000	0.0000	0.0000	0.0000
17	0.0249	0.2488	5.7825	0.0553	0.0000	0.0000	0.0000	0.0000
18	0.0271	0.2759	5.7555	0.0550	0.0000	0.0000	0.0000	0.0000
19	0.0249	0.3008	5.7520	0.0550	0.0000	0.0000	0.0000	0.0000
20	0.0282	0.3289	5.7180	0.0547	0.0000	0.0000	0.0000	0.0000
21	0.0221	0.3510	5.7175	0.0547	0.0000	0.0000	0.0000	0.0000
22	0.0152	0.3662	5.6715	0.0542	0.0000	0.0000	0.0000	0.0000
23	0.0117	0.3778	4.7815	0.0457	0.0000	0.0000	0.7455	0.0071
24	0.0077	0.3855	4.3770	0.0418	0.0000	0.0000	1.0310	0.0099
25	0.0166	0.4022	3.3190	0.0317	0.0000	0.0000	1.8630	0.0178
26	0.0270	0.4292	2.4935	0.0238	0.0000	0.0000	2.2810	0.0218
27	0.0086	0.4378	2.1030	0.0201	0.0000	0.0000	2.5275	0.0242
28	0.0093	0.4471	1.7110	0.0164	0.0000	0.0000	2.7480	0.0263
29	0.0179	0.4650	0.7895	0.0075	0.0000	0.0000	3.4530	0.0330
30	0.0068	0.4719	1.1430	0.0109	0.0000	0.0000	2.9365	0.0281
31	0.0069	0.4787	0.7490	0.0072	0.0000	0.0000	3.2245	0.0308
32	0.0135	0.4922	0.6790	0.0065	0.0000	0.0000	3.4555	0.0330
33	0.0091	0.5013	0.3650	0.0035	0.0000	0.0000	3.7695	0.0360
34	0.0131	0.5145	0.4405	0.0042	0.0000	0.0000	3.6940	0.0353
35	0.0049	0.5194	0.0000	0.0000	0.0000	0.0000	4.1345	0.0395
Totals	0.5194							

Note: Starting reference point was at axial bottom of crack.
Check: 0.050" nominal wt X 0.5194" crack length = 0.026 sq inches. Sum of areas (IGA and ductile) = 0.026 sq inches

Table 13. Defect Burst Specimen Fractography Measurements – R44C45-13A2B1

Point	Incremental Length Segment (")	Cumulative Length (")	Measured Oxidized IGA (")	Depth (") Oxidized IGA	Measured Oxidized Ductile (")	Depth (") Oxidized Ductile	Measured Non-oxidized Ductile (")	Depth (") Non-oxidized Ductile
0	0.0000	0.0000	0.4035	0.0039	0.0000	0.0000	3.1315	0.0300
1	0.0063	0.0063	1.0425	0.0100	0.0000	0.0000	2.9655	0.0284
2	0.0055	0.0118	1.0310	0.0099	0.2945	0.0028	2.7580	0.0264
3	0.0020	0.0138	1.1345	0.0109	0.7250	0.0069	2.2280	0.0213
4	0.0106	0.0244	1.1205	0.0107	0.4425	0.0042	1.9335	0.0185
5	0.0050	0.0294	1.2850	0.0123	0.3145	0.0030	2.6725	0.0256
6	0.0012	0.0305	1.5775	0.0151	0.0000	0.0000	2.6645	0.0255
7	0.0031	0.0336	1.3280	0.0127	0.0000	0.0000	2.9565	0.0283
8	0.0127	0.0463	2.6155	0.0250	0.0000	0.0000	1.8315	0.0175
9	0.0116	0.0579	2.9920	0.0286	0.0000	0.0000	1.6330	0.0156
10	0.0263	0.0843	3.6770	0.0352	0.0000	0.0000	1.1535	0.0110
11	0.0151	0.0993	4.0935	0.0392	0.0000	0.0000	0.5450	0.0052
12	0.0233	0.1226	3.9285	0.0376	0.0000	0.0000	0.6885	0.0066
13	0.0223	0.1449	4.4240	0.0423	0.0000	0.0000	0.4745	0.0045
14	0.0169	0.1618	5.2655	0.0504	0.0000	0.0000	0.0000	0.0000
15	0.0115	0.1733	5.4395	0.0521	0.0000	0.0000	0.0000	0.0000
16	0.0176	0.1909	reference point- nm		reference point - nm			
17	0.0127	0.2036	5.4665	0.0523	0.0000	0.0000	0.0000	0.0000
18	0.0253	0.2288	5.4420	0.0521	0.0000	0.0000	0.0000	0.0000
19	0.0085	0.2373	reference point - nm					
20	0.0229	0.2603	5.3325	0.0510	0.0000	0.0000	0.0000	0.0000
21	0.0305	0.2908	5.3020	0.0507	0.0000	0.0000	0.0000	0.0000
22	0.0260	0.3168	5.3025	0.0507	0.0000	0.0000	0.0000	0.0000
23	0.0312	0.3481	5.5230	0.0529	0.0000	0.0000	0.0000	0.0000
24	0.0074	0.3555	5.5335	0.0530	0.0000	0.0000	0.0000	0.0000
25	0.0469	0.4023	5.4325	0.0520	0.0000	0.0000	0.0000	0.0000
26	0.0151	0.4174	reference point - nm					
27	0.0174	0.4348	5.4660	0.0523	0.0000	0.0000	0.0000	0.0000
28	0.0359	0.4707	5.5715	0.0533	0.0000	0.0000	0.0000	0.0000
29	0.0292	0.4999	reference point - nm					
30	0.0246	0.5244	5.5130	0.0528	0.0000	0.0000	0.0000	0.0000
31	0.0455	0.5699	5.5870	0.0535	0.0000	0.0000	0.0000	0.0000
32	0.0232	0.5931	reference point - nm					
33	0.0129	0.6060	5.6080	0.0537	0.0000	0.0000	0.0000	0.0000
34	0.0092	0.6152	5.6000	0.0536	0.0000	0.0000	0.0000	0.0000
35	0.0115	0.6267	4.3545	0.0417	0.0000	0.0000	1.1845	0.0113
36	0.0127	0.6394	3.7845	0.0362	0.0000	0.0000	1.3255	0.0127
37	0.0145	0.6539	1.8560	0.0178	0.0000	0.0000	2.6890	0.0257
38	0.0145	0.6684	1.2485	0.0119	0.0000	0.0000	3.1345	0.0300
39	0.0064	0.6747	1.1350	0.0109	0.0000	0.0000	3.1160	0.0298
39a	0.0054	0.6801	0.5920	0.0057	0.874	0.0084	2.6220	0.0251
40	0.0058	0.6859	1.4305	0.0137	0.3945	0.0038	2.3285	0.0223
41	0.0097	0.6956	0.5125	0.0049	0.7700	0.0074	3.1185	0.0298
42	0.0054	0.7010	0.0000	0.0000	0.0000	0.0000	4.3640	0.0418
Totals	0.7010							

Note: Blank cells appear where there was a length segment to a reference point used to connect individual printed photos.
Note: Starting reference point was at axial bottom of crack.
Check: 0.050" nominal wt X 0.7" crack length = 0.035 sq inches. Sum of areas (IGA and ductile) = 0.035 sq inches

Table 14. Defect Burst Specimen Fractography Measurements – R44C45-13A2B2A and R44C45-3A2B3A

44-45-13A2B2A

Point	Incremental Length Segment (")	Cumulative Length (")	Measured Oxidized IGA (")	Depth (") Oxidized IGA	Measured Oxidized Ductile (")	Depth (") Oxidized Ductile	Measured Non-oxidized Ductile (")
0	0.0000	0.0000	1.1115	0.0105	0.0000	0.0000	4.4655
1	0.0182	0.0182	2.0720	0.0195	0.0000	0.0000	3.3435
2	0.0159	0.0341	2.8620	0.0269	0.0000	0.0000	2.4355
3	0.0385	0.0726	3.3675	0.0317	0.0000	0.0000	2.3065
4	0.0116	0.0842	3.2375	0.0305	0.0000	0.0000	2.3845
5	0.0117	0.0958	2.2740	0.0214	0.0000	0.0000	3.3970
6	0.0254	0.1213	3.5050	0.0330	0.0000	0.0000	2.0705
7	0.0201	0.1413	4.2730	0.0402	0.0000	0.0000	1.2245
8	0.0142	0.1555	4.3925	0.0414	0.0000	0.0000	1.2535
9	0.0175	0.1730	3.9750	0.0374	0.0000	0.0000	1.5820
10	0.0286	0.2017	3.2740	0.0308	0.0000	0.0000	2.2860
11	0.0193	0.2210	3.5990	0.0339	0.0000	0.0000	2.0290
12	0.0174	0.2384	3.1025	0.0292	0.0000	0.0000	2.4280
Saw kerf	0.0200	0.2584	NM	NM	NM	NM	NM

44-45-13A2B3A

0	0.0000	0.2584	1.5170	0.0143	0.0000	0.0000	4.3400
1	0.0101	0.2684	2.0170	0.0190	0.0000	0.0000	3.8400
2	0.0106	0.2790	2.1045	0.0199	0.0000	0.0000	3.7525
3	0.0153	0.2943	1.5860	0.0150	0.0000	0.0000	4.2710
4	0.0106	0.3049	1.1535	0.0109	0.0000	0.0000	4.7035
5	0.0261	0.3311	0.8810	0.0083	0.0000	0.0000	4.9760
6	0.0120	0.3431	0.7375	0.0070	0.0000	0.0000	5.1195
7	0.0126	0.3556	0.0000	0.0000	0.0000	0.0000	5.8570
Totals	0.3556						

Note: Starting reference point was at axial bottom of crack.
Note: Could not check areas because of missing area in saw kerf.

(The term "saw kerf" refers to the width of the saw blade used in cutting the specimen.)

Table 15. Tube Free Span Deposit Chemistry Based on ICP

Element	wt %
Fe	64.50
Si	0.051
Al	0.022
Ti	0.008
Ca	<0.014
Mg	<0.006
Ni	0.301
Cr	0.045
Mo	0.006
V	0.005
Co	0.009
Mn	0.211
Cu	1.120
Zn	0.487
Pb	0.010
Sn	0.011
Zr	<0.006
Na	<0.011
S	<0.002
K	<0.036
As	0.017

Note: Where the operator < (less than) appears, it means that the concentration is less than the given minimum detection limit.

Table 16. Tensile Test Results

Property	35-57-9C2	44-45-14C
Yield Strength (psi)	58,148	54,525
Tensile Strength (psi)	105,398	99,661
Total Elongation (%)	39.39	36.59
Reduction in Area (%)	41.5	48.5

Table 17. Bulk Chemistry Analysis

Element	Sample 35-57-9C1 (wt. %)	Sample 44-45-14B (wt. %)
Ni	Balance (76.6)	Balance (76.0)
Cr	15.33	15.56
Fe	6.86	6.98
Al	0.34	0.53
C	0.079	0.073
Co	<0.05	<0.05
Cu	<0.05	<0.05
Mn	0.22	0.23
P	0.011	0.010
Si	0.33	0.35
S	<0.001	<0.001
Ti	0.26	0.30

Table 18. Summary Material Properties for Tube No. R35C57

Property		R35C57	Mill Test Report T02690[2]	ASME SB-163 Specification[3]
Heat Number		96B3	96B3	-
Yield Strength, psi		58,148	49,000 – 52,000	-
Ultimate Tensile Strength, psi		105,398	98,000 – 102,000	-
Total Elongation, %		39.39	40 - 41	-
Reduction in Area, %		41.5	Not available	-
ASTM Grain Size		9.75	-	-
Rockwell Hardness, RB		Not determined	87 - 88	-
Carbide Distribution		(Note 1)	-	-
Composition, wt%	Al	0.34	0.04	-
	C	0.079	0.04	0.15 max
	Co	<0.05	0.04	Added to Ni
	Cr	15.33	15.66	14.0 – 17.0
	Cu	<0.05	0.02	0.5 max
	Fe	6.86	6.98	6.0 – 10.0
	Mn	0.22	0.22	1.0 max
	Mo	<0.05	-	-
	Ni	76.6	78.85	72.0 min (+Co)
	P	0.011	-	-
	S	<0.001	0.007	0.015 max
	Si	0.33	0.20	0.5 max
	Ti	0.26	0.33	-

Table 2-2 Notes:

(1) Carbides were primarily intragranular with some longitudinal banding present.

(2) Attachment to John Arhar e-mail to Joe Crockett, et.al., dated 2/24/2003, "FW: A few more heat numbers".

(3) ASME Metals handbook Vol. 1, 10th Edition, Materials Park, OH, March 1990.

Table 19. Summary Material Properties for Tube No. R44C45

Property		R44C45	Mill Test Report T02690[2]	ASME SB-163 Specification[3]
Heat Number		95B2	95B2	-
Yield Strength, psi		54,525	50,000 – 51,000	-
Ultimate Tensile Strength, psi		99,661	100,000 – 101,000	-
Total Elongation, %		36.59	41 - 42	-
Reduction in Area, %		48.5	Not available	-
ASTM Grain Size		10.0	-	-
Rockwell Hardness, RB		Not determined	83 - 87	-
Carbide Distribution		(Note 1)	-	-
Composition, wt%	Al	0.53	0.18	-
	C	0.073	0.05	0.15 max
	Co	<0.05	0.05	Added to Ni
	Cr	15.15	15.66	14.0 – 17.0
	Cu	<0.05	0.10	0.5 max
	Fe	6.98	7.26	6.0 – 10.0
	Mn	0.23	0.22	1.0 max
	Mo	<0.05	-	-
	Ni	76.6	76.96	72.0 min (+Co)
	P	0.010	-	-
	S	<0.001	0.007	0.015 max
	Si	0.35	0.20	0.5 max
	Ti	0.30	0.28	-

Table 2-2 Notes:

1. Carbides were primarily intragranular with some longitudinal banding present.
2. Attachment to John Arhar e-mail to Joe Crockett, et.al., dated 2/24/2003, "FW: A few more heat numbers".
3. ASME Metals handbook Vol. 1, 10th Edition, Materials Park, OH, March 1990.

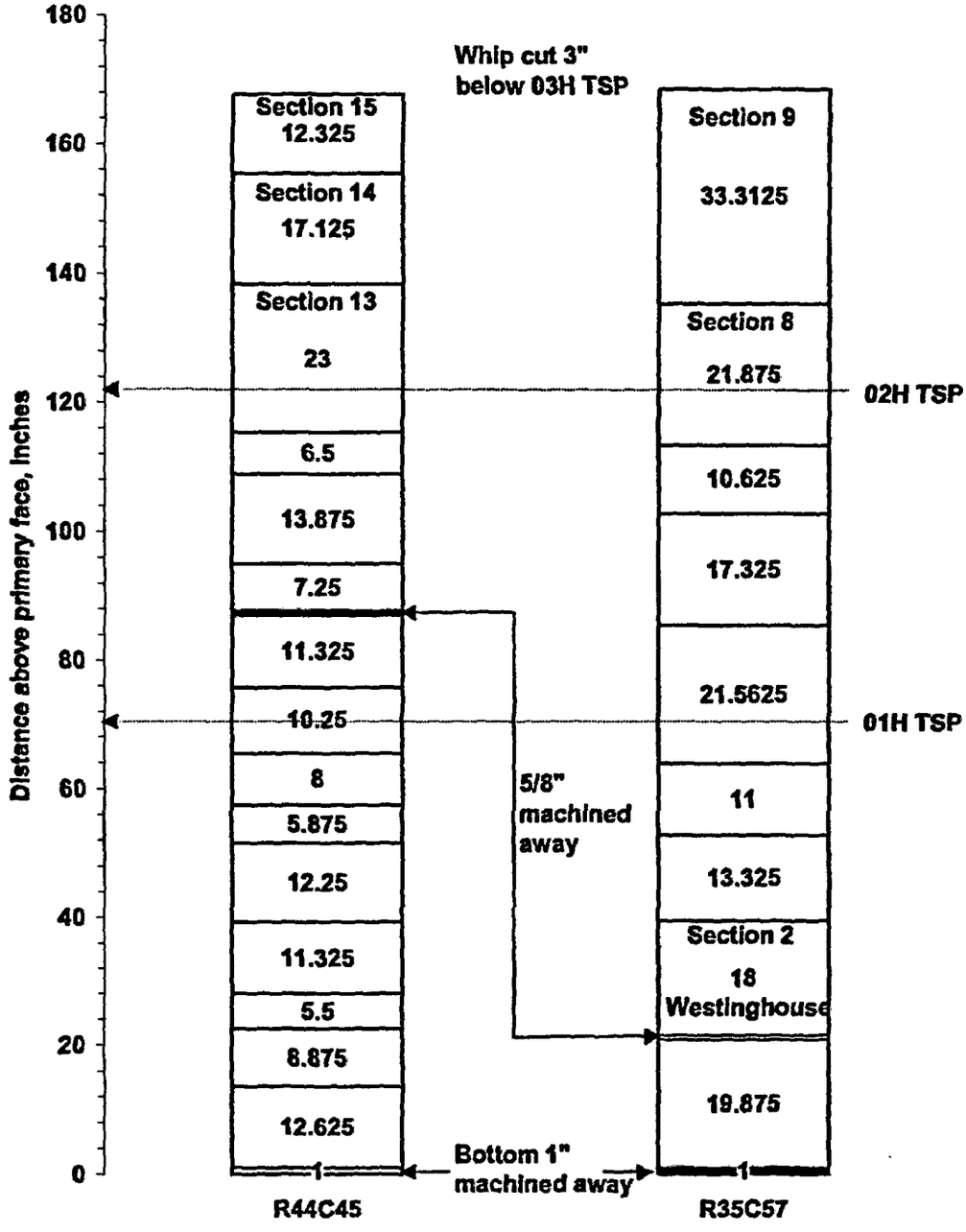

Figure 1. Pulled tube diagrams

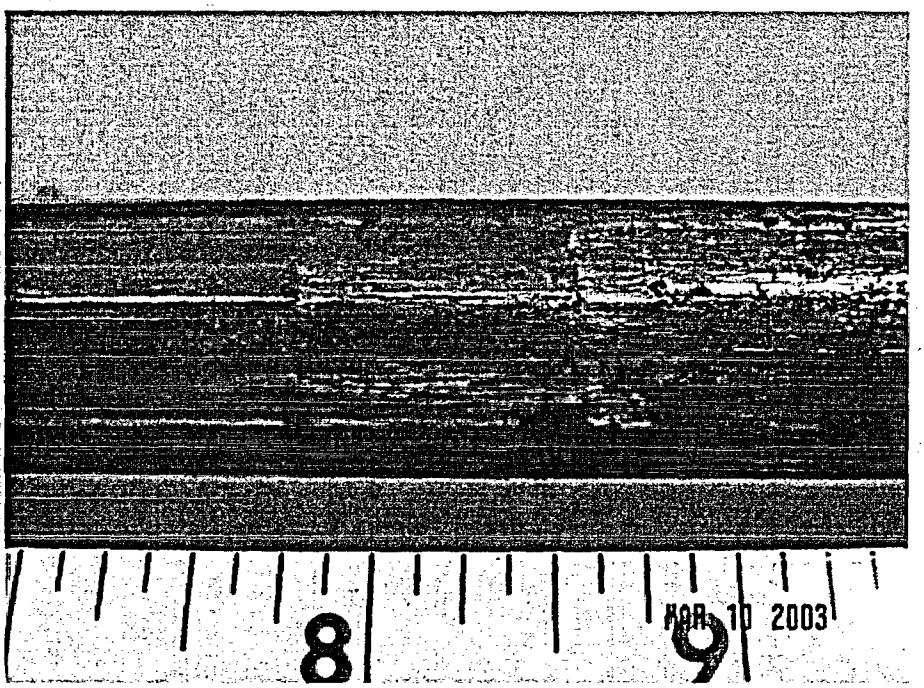

Figure 2. Receipt photograph of 02H TSP intersection at ~180° of tube no. R35C57 (section 8). Top (in SG) is to the right.

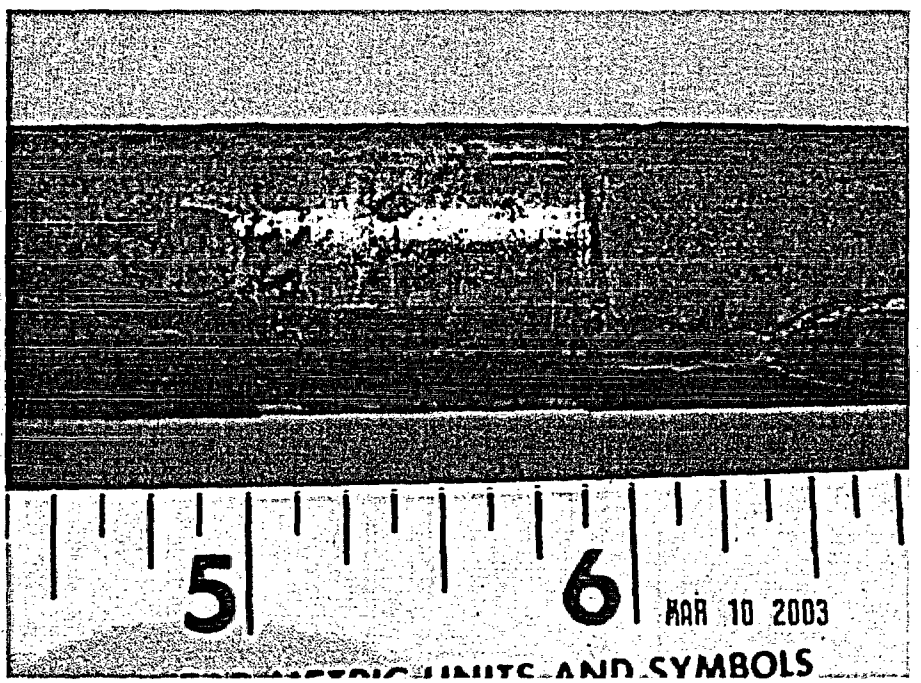

Figure 3. Receipt photograph of 02H TSP intersection at ~90° of tube no. R44C45 (section 13). Top (in SG) is to the right. Note spalled deposit above and below the TSP intersection.

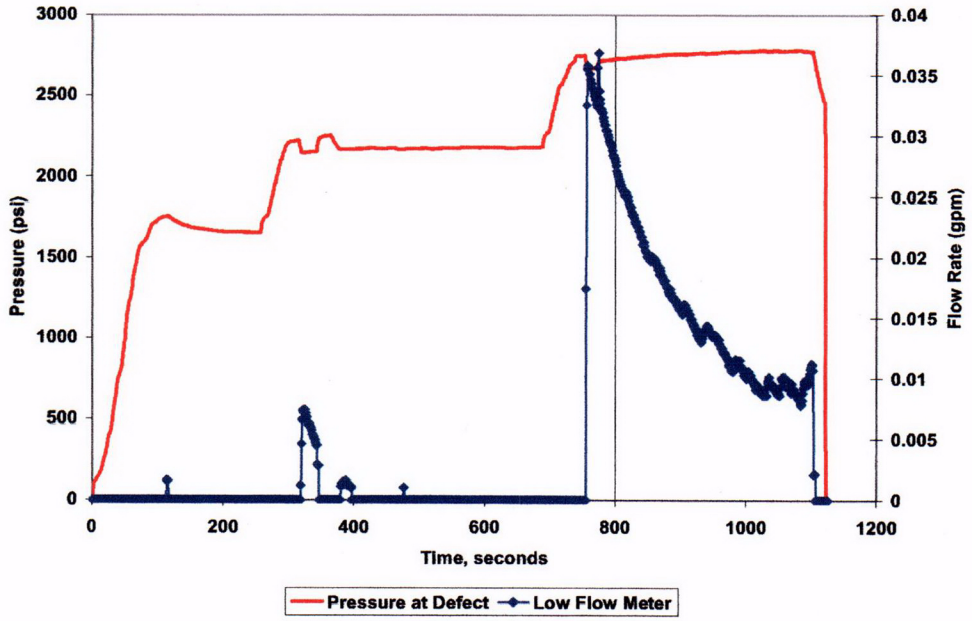

Figure 4. Room temperature leak rate for SG 24 tube no. R35C57, section 8 (02H TSP)

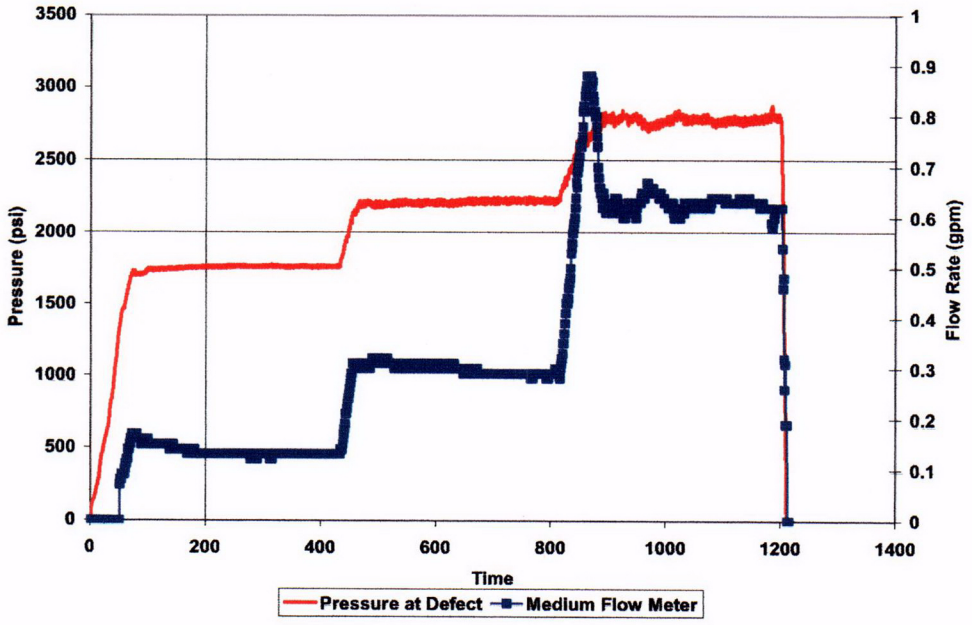

Figure 5. Room temperature leak rate for SG 24 tube no. R44C45, section 13 (02H TSP)

C01

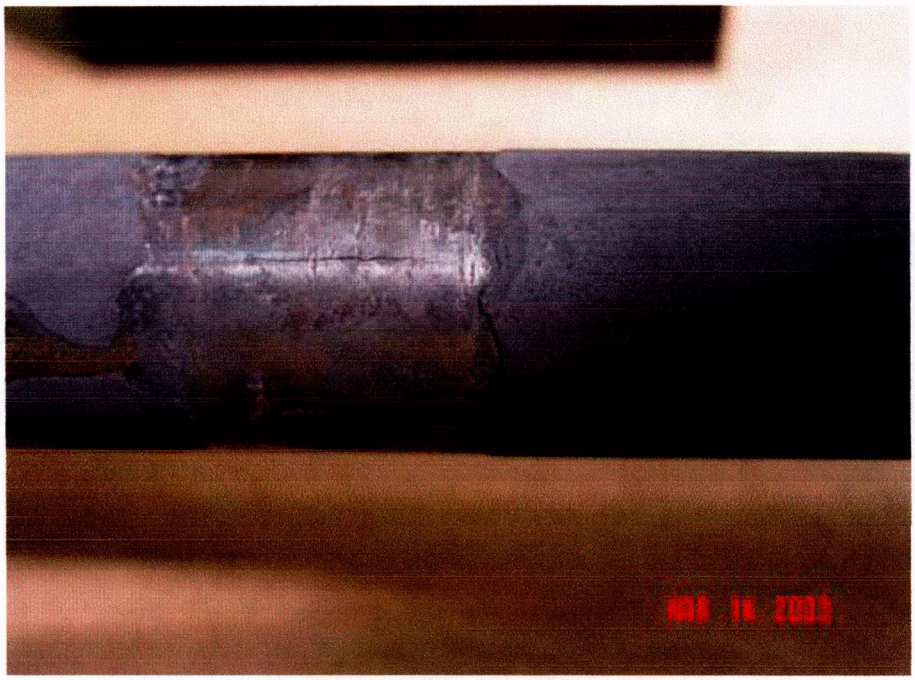

Figure 6. Post leak rate test photograph of axial crack at ~75° in 02H TSP intersection of tube no. R44C45. The top (in SG) of the tube section is to the right.

C02

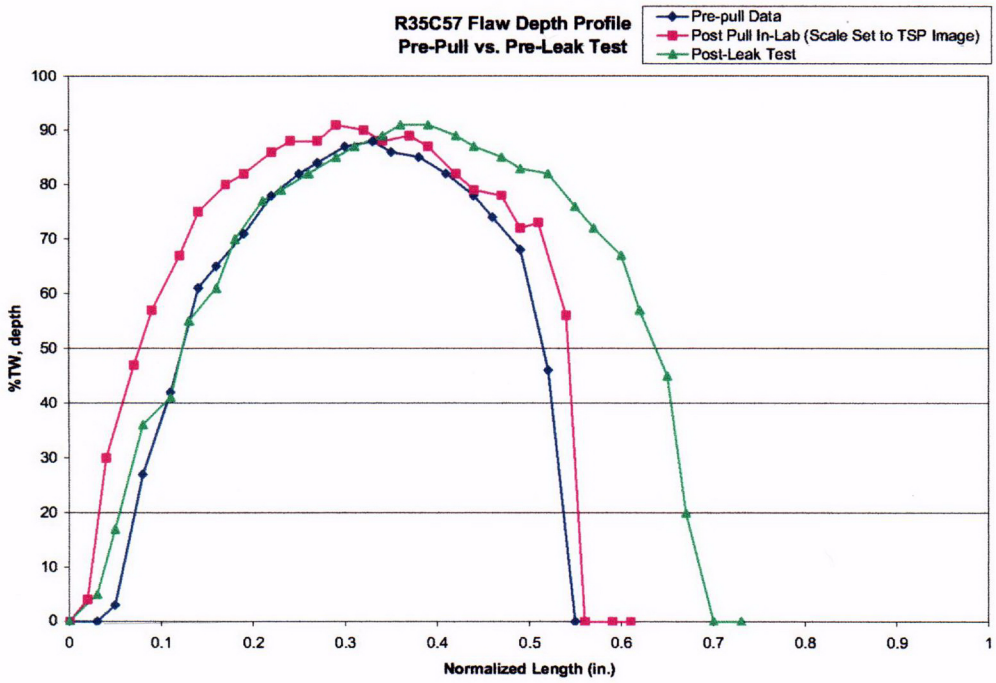

Figure 7. Axial crack NDE profile at 02H TSP location for tube no. R35C57

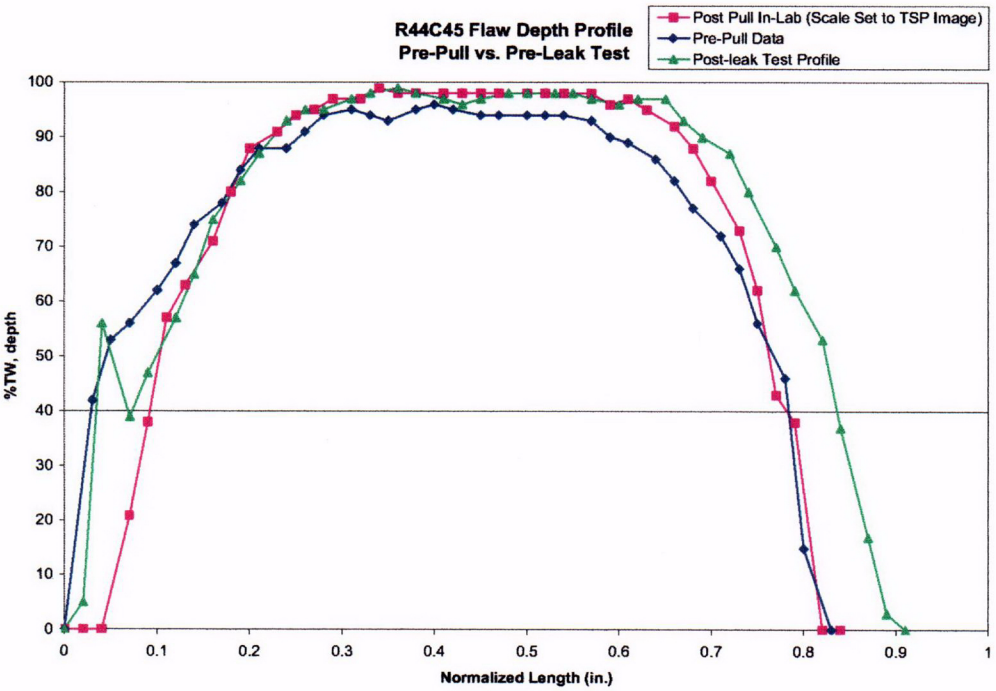

Figure 8. Axial crack NDE profile at 73° at 02H TSP location for tube no. R44C45

C03

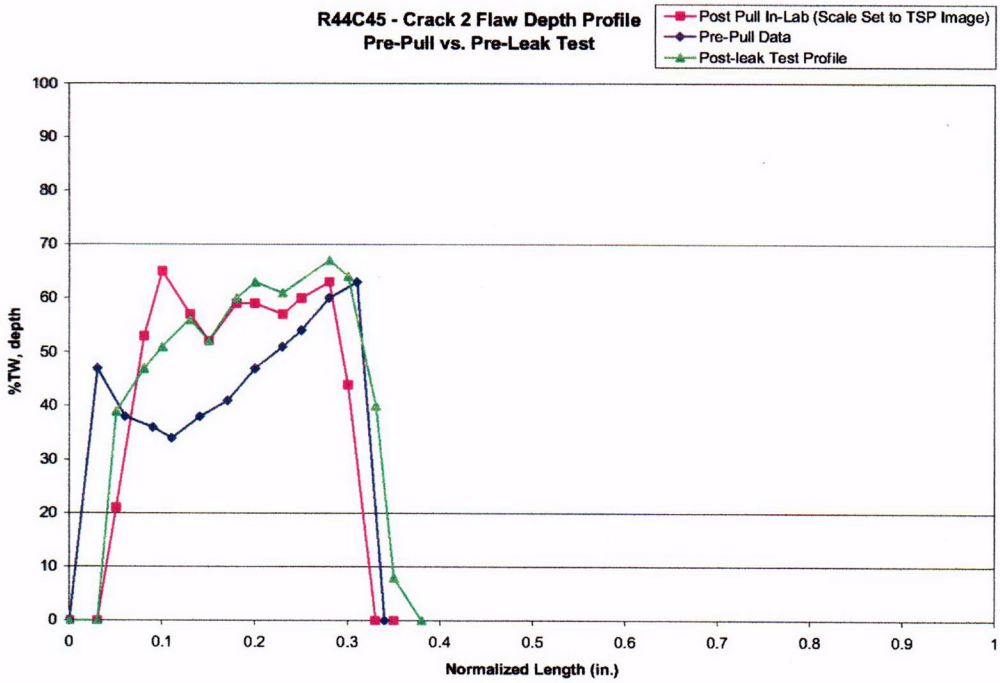

Figure 9. Axial crack NDE profile at 25° at 02H TSP location for tube no. R44C45

Figure 10. Post oxidation view of axial crack at ~75° in tube no. R44C45 at 02H TSP intersection.

C04

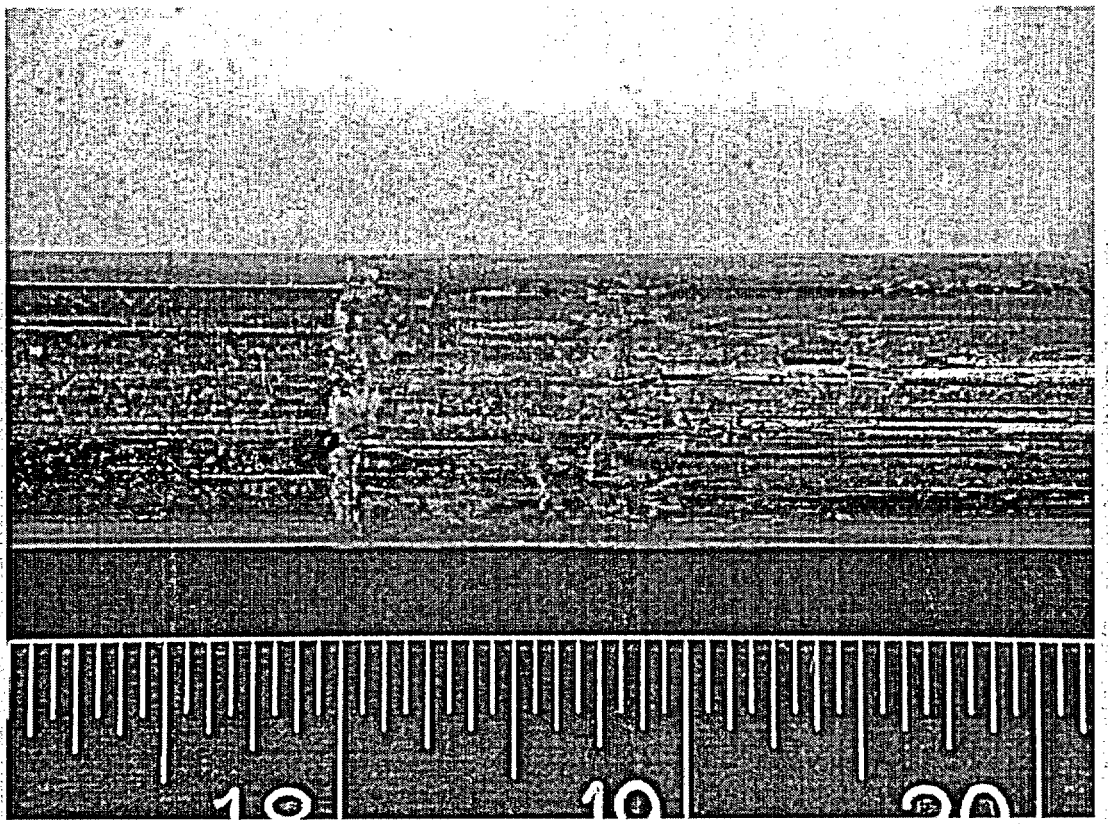

Figure 11. R35C57-8B at 0° 1.9X

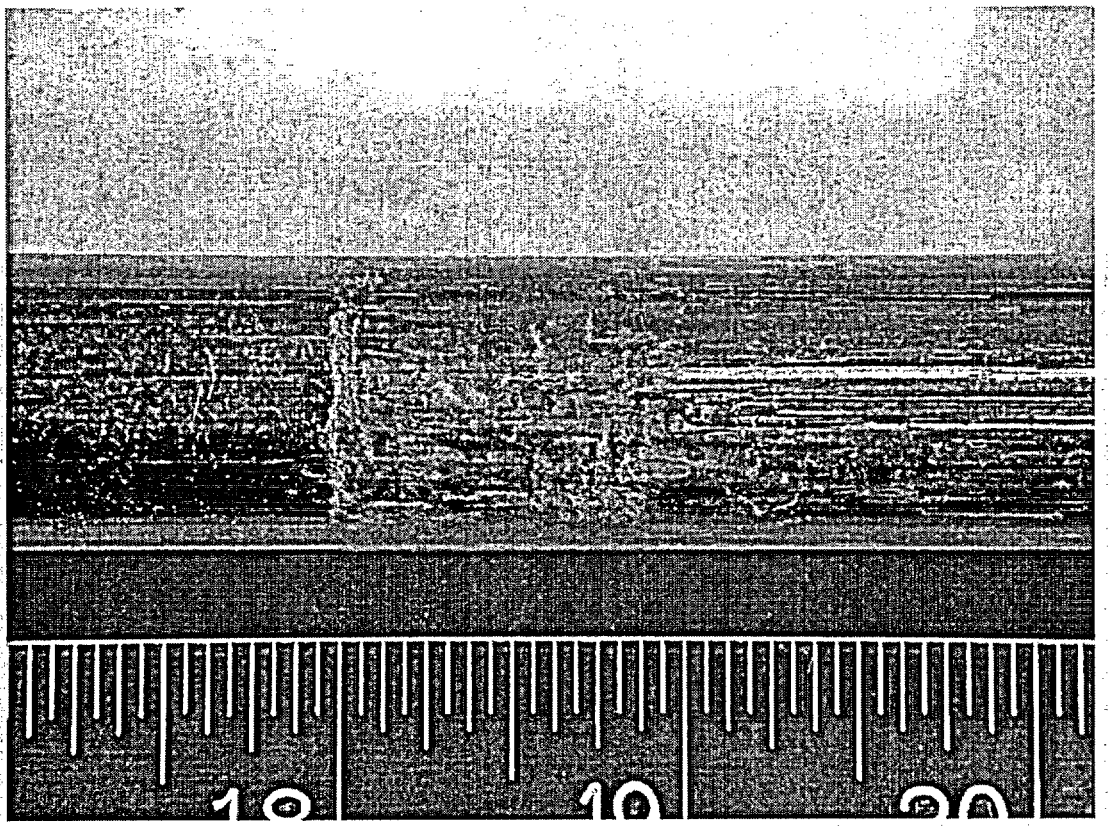

Figure 12. R35C57-8B at 45° 1.9X

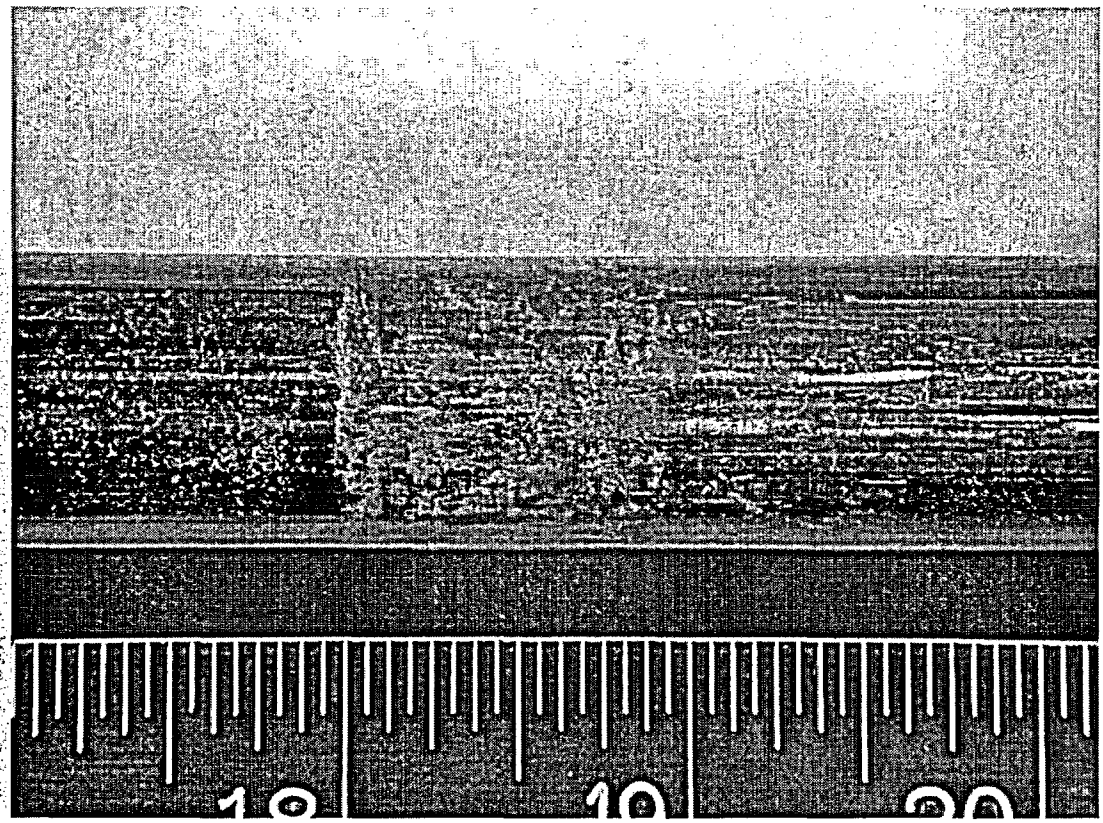

Figure 13. R35C57-8B at 90° 1.9X

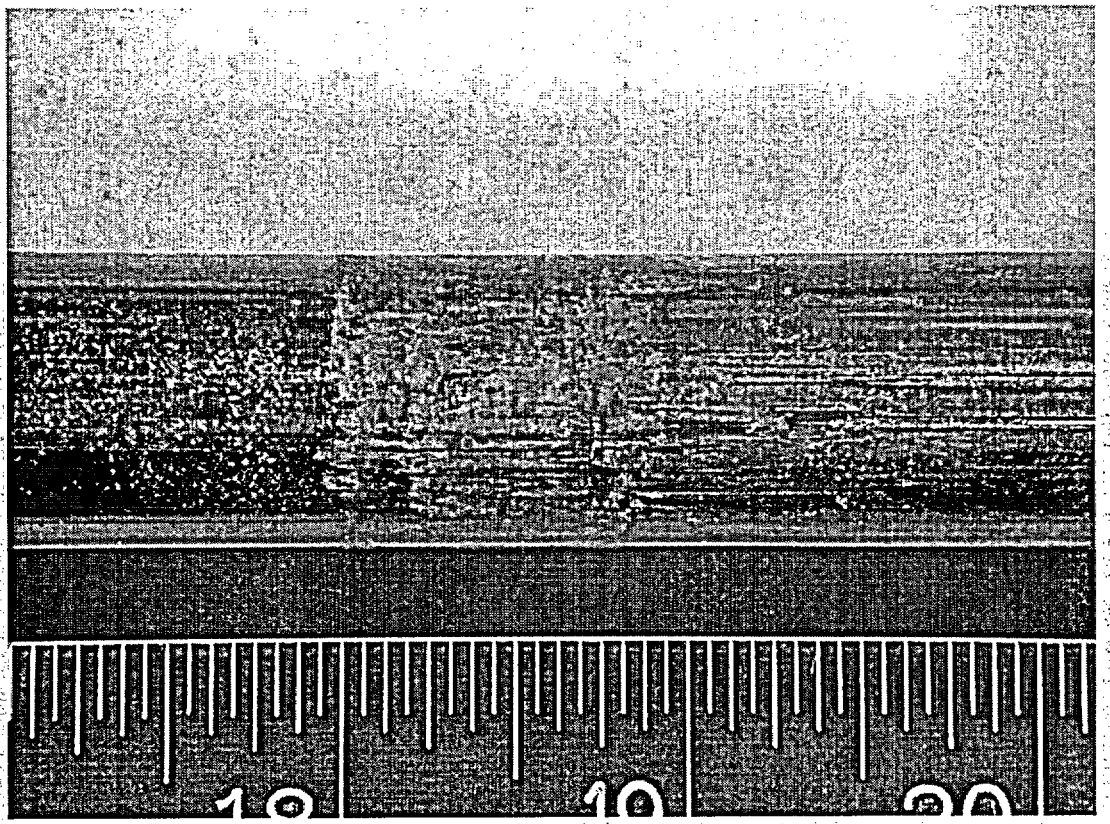

Figure 14. R35C57-8B at 135° 1.9X

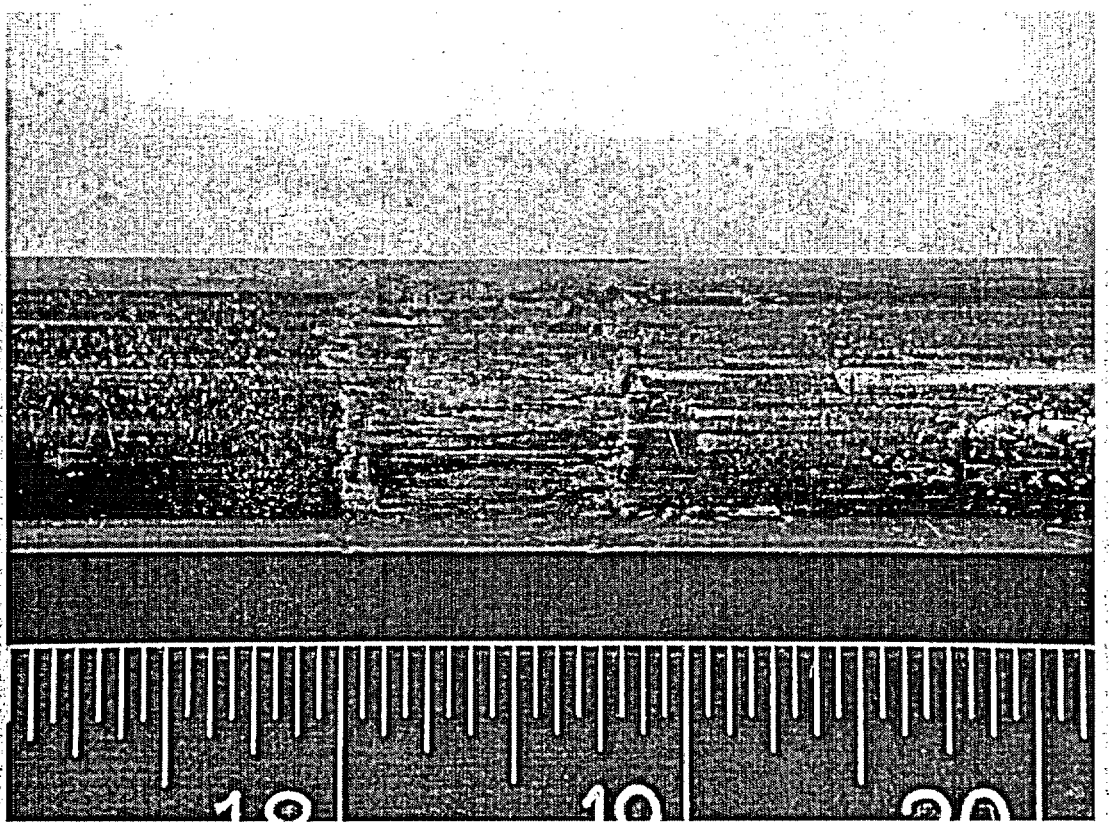

Figure 15. R35C57-8B at 180° 1.9X

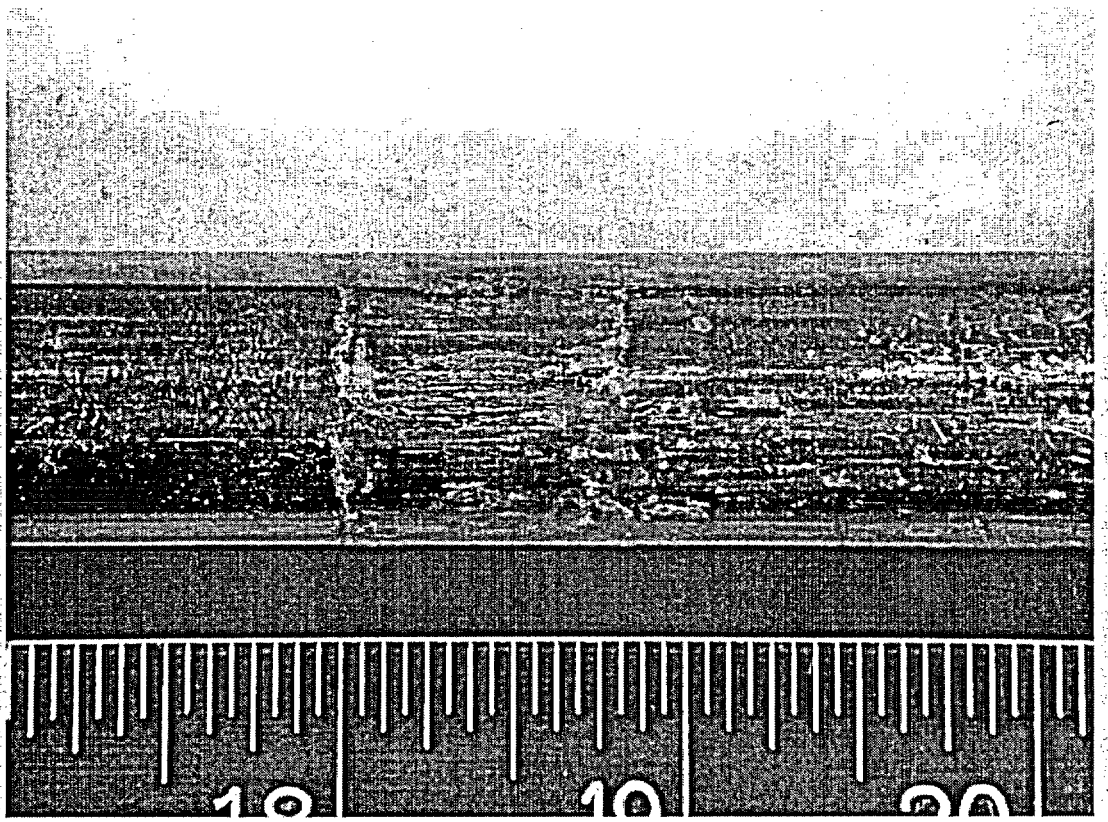

Figure 16. R35C57-8B at 225° 1.9X

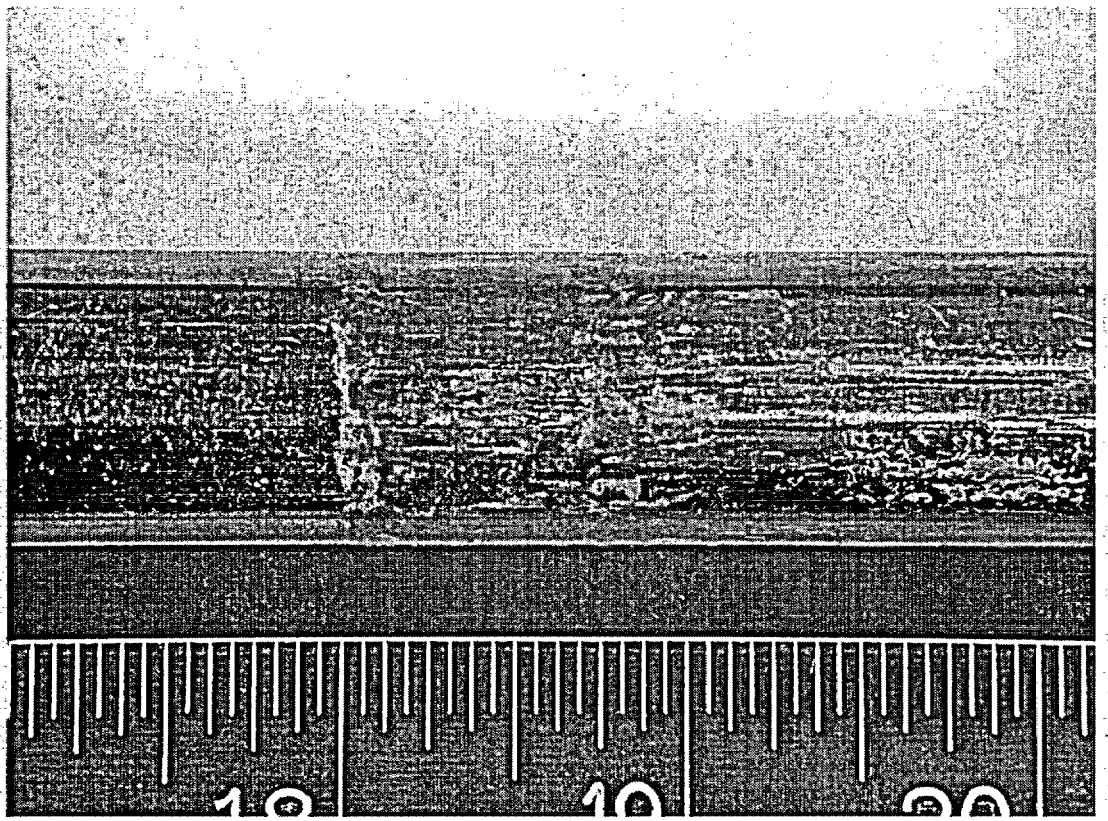

Figure 17. R35C57-8B at 270° 1.9X

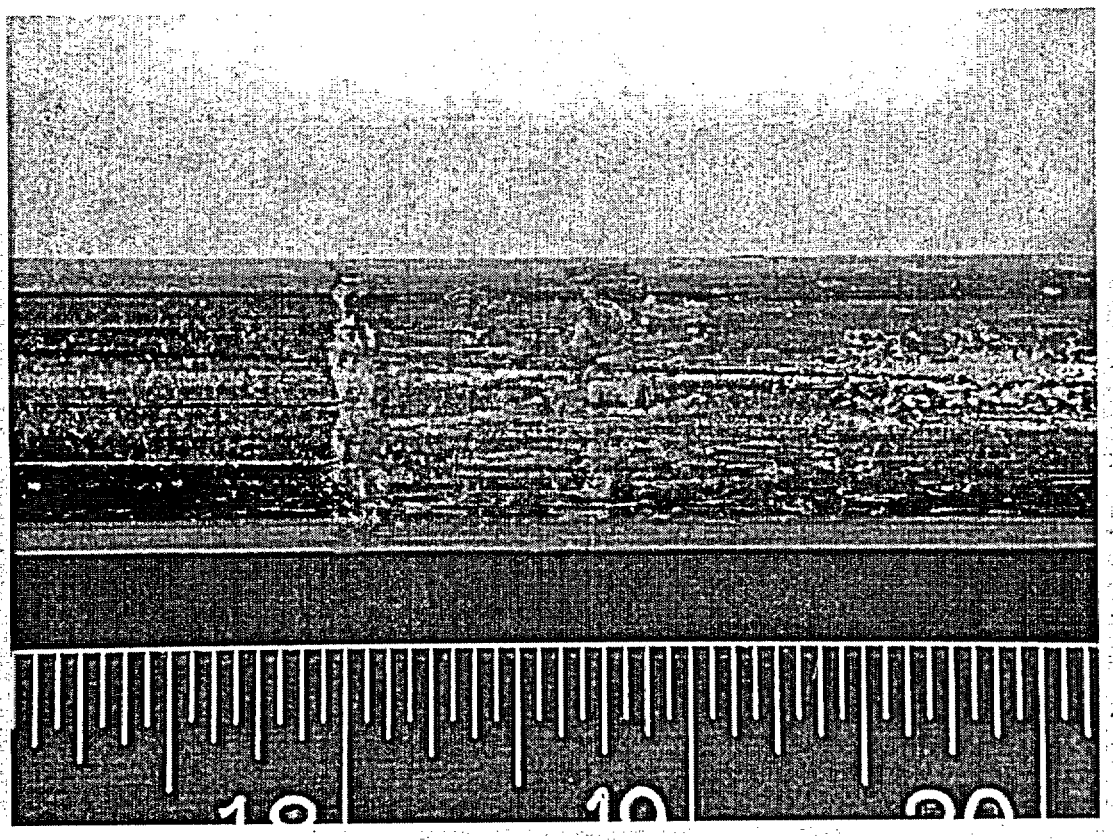

Figure 18. R35C57-8B at 315° 1.9X

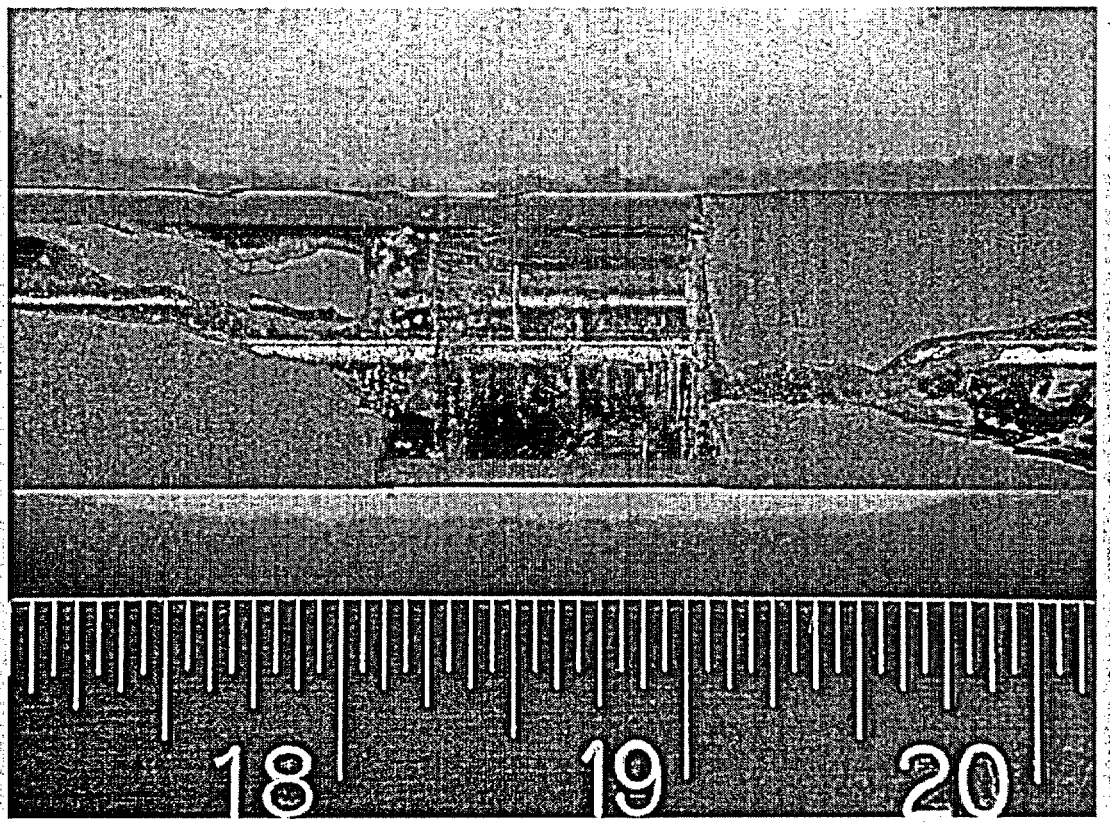

Figure 19. R44C45-13A at 0° 1.9X

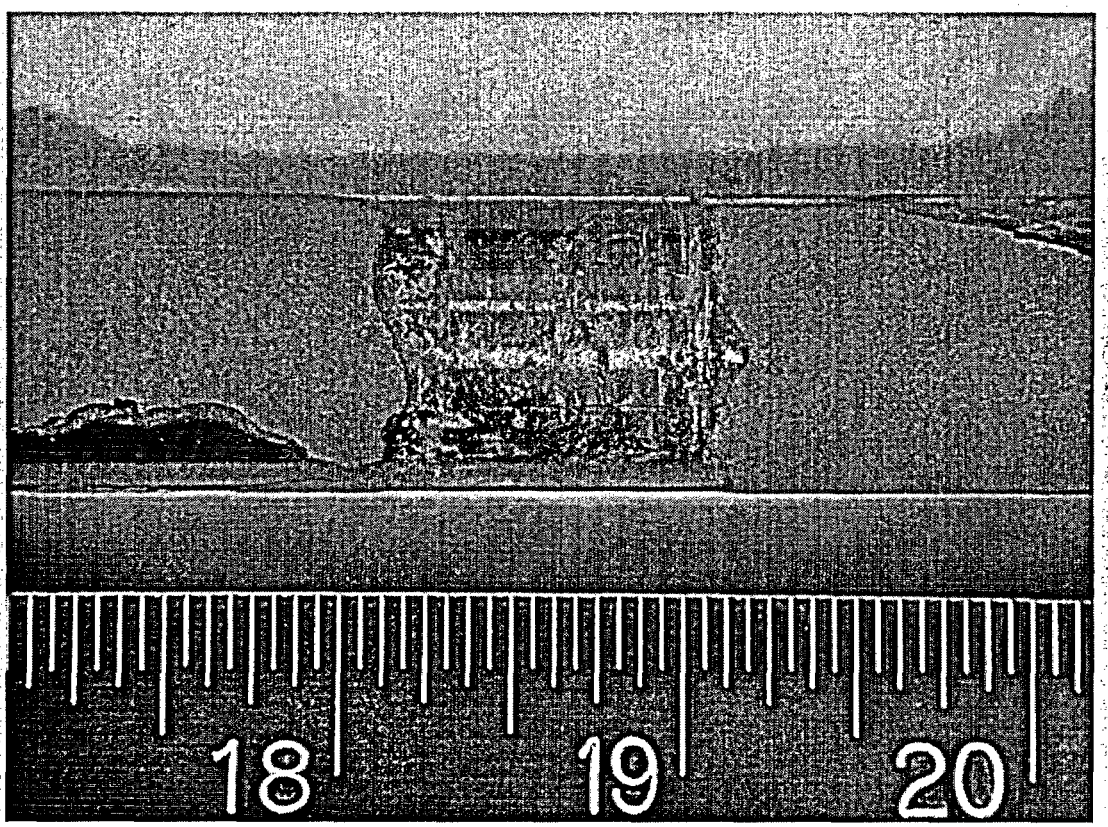

Figure 20. R44C45-13A at 45° 1.9X

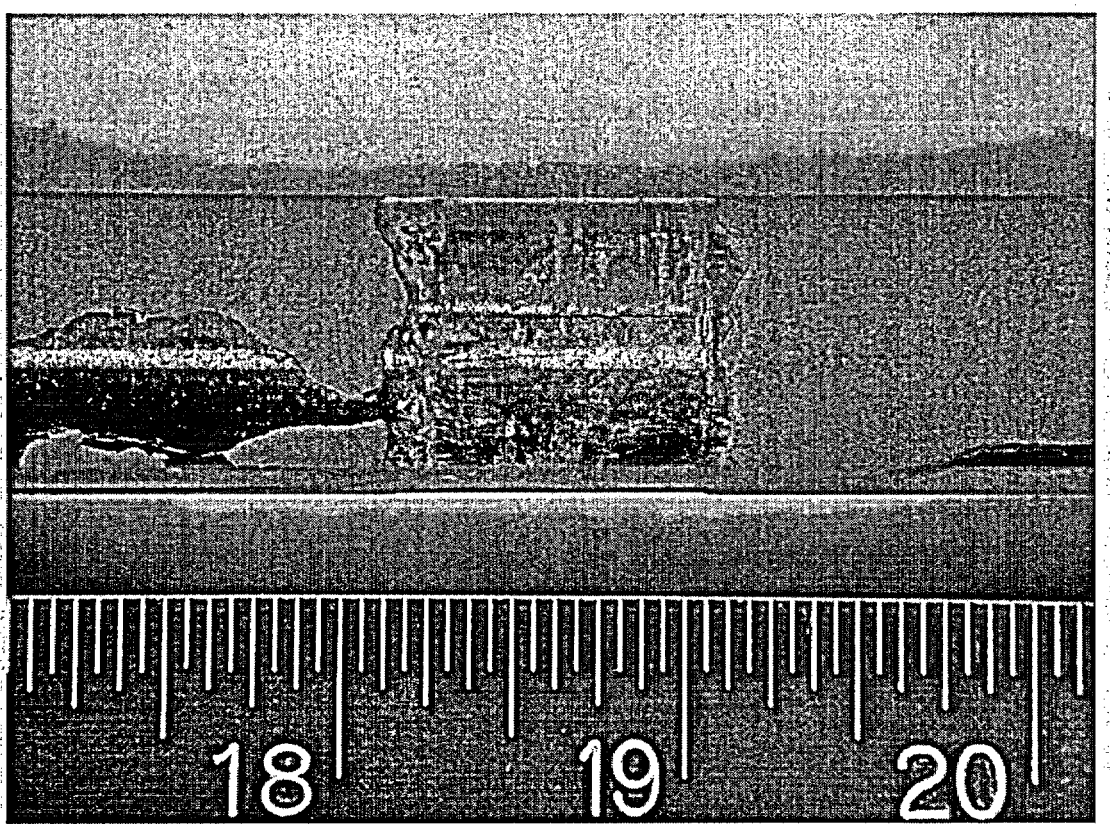

Figure 21. R44C45-13A at 90° 1.9X

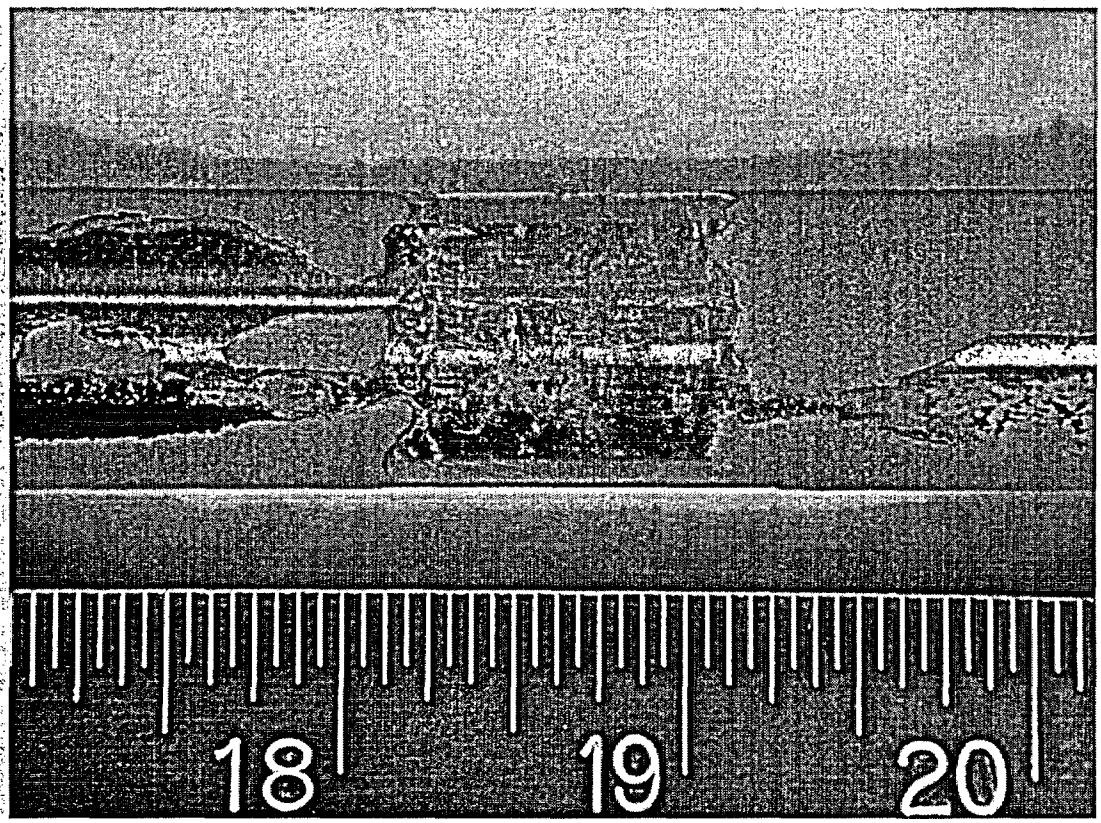

Figure 22. R44C45-13A at 135° 1.9X

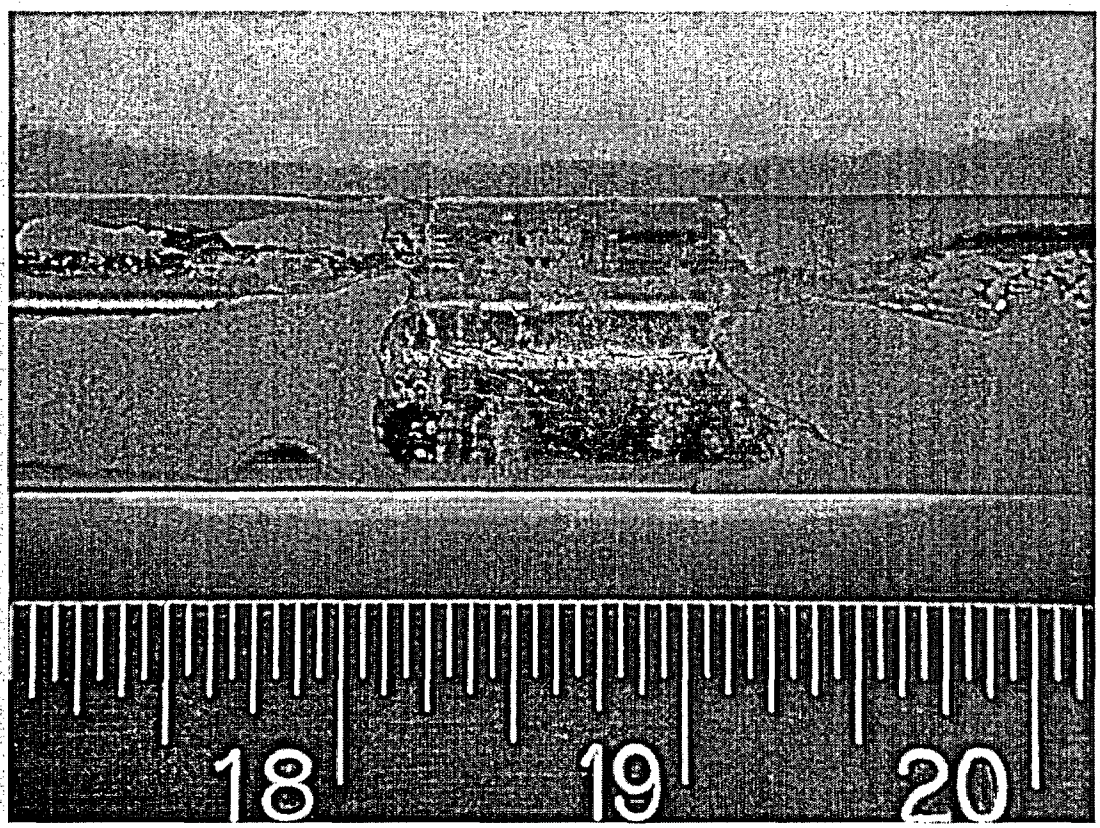

Figure 23. R44C45-13A at 180° 1.9X

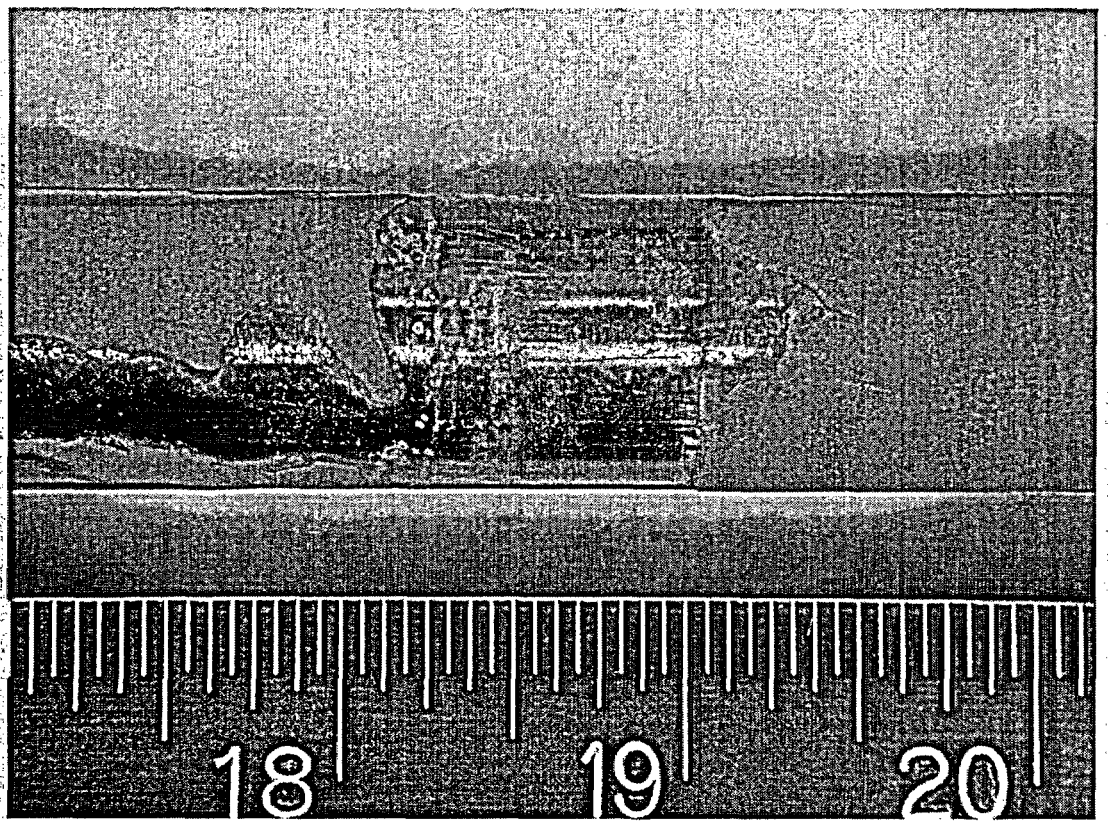

Figure 24. R44C45-13A at 225° 1.9X

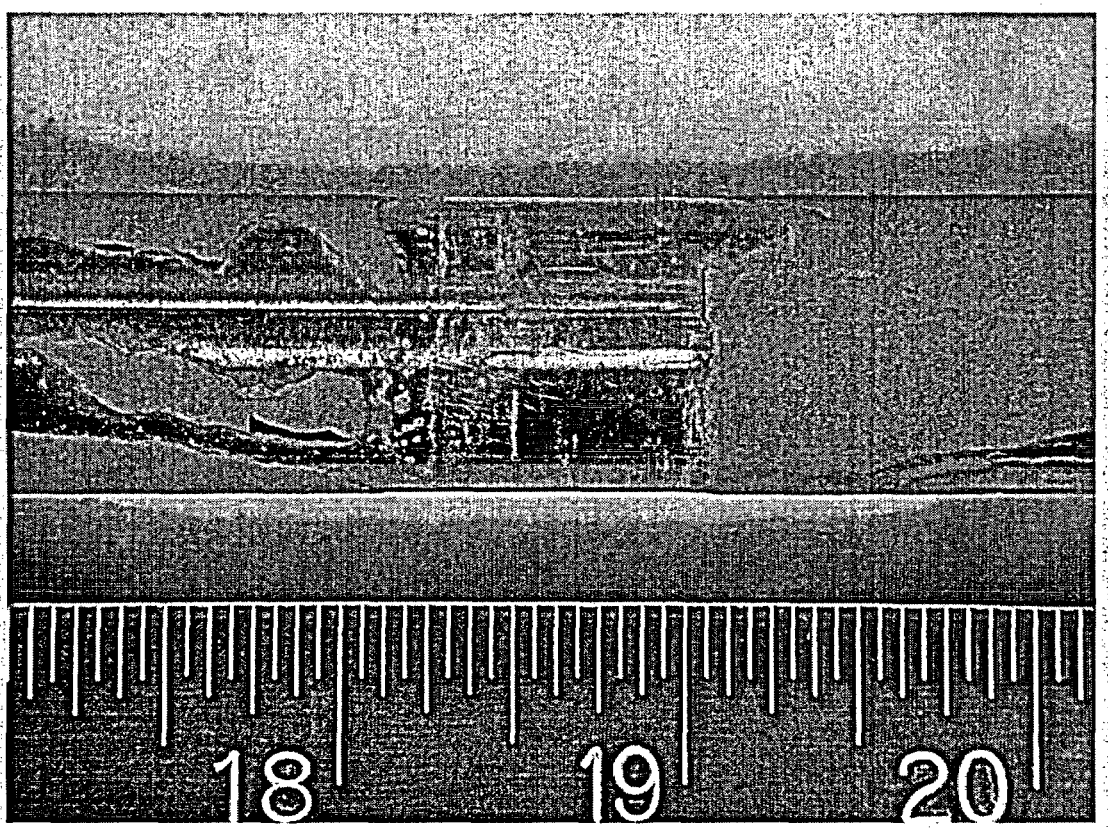

Figure 25. R44C45-13A at 270° 1.9X

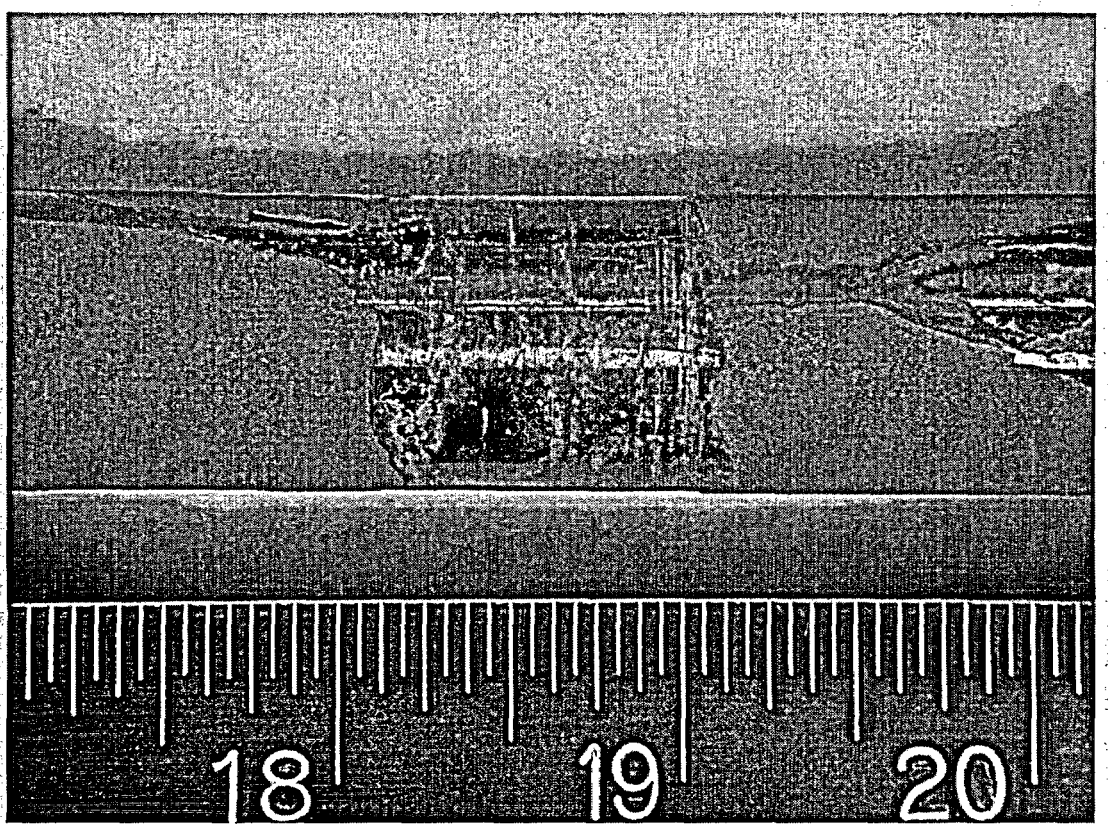

Figure 26. R44C45-13A at 315° 1.9X

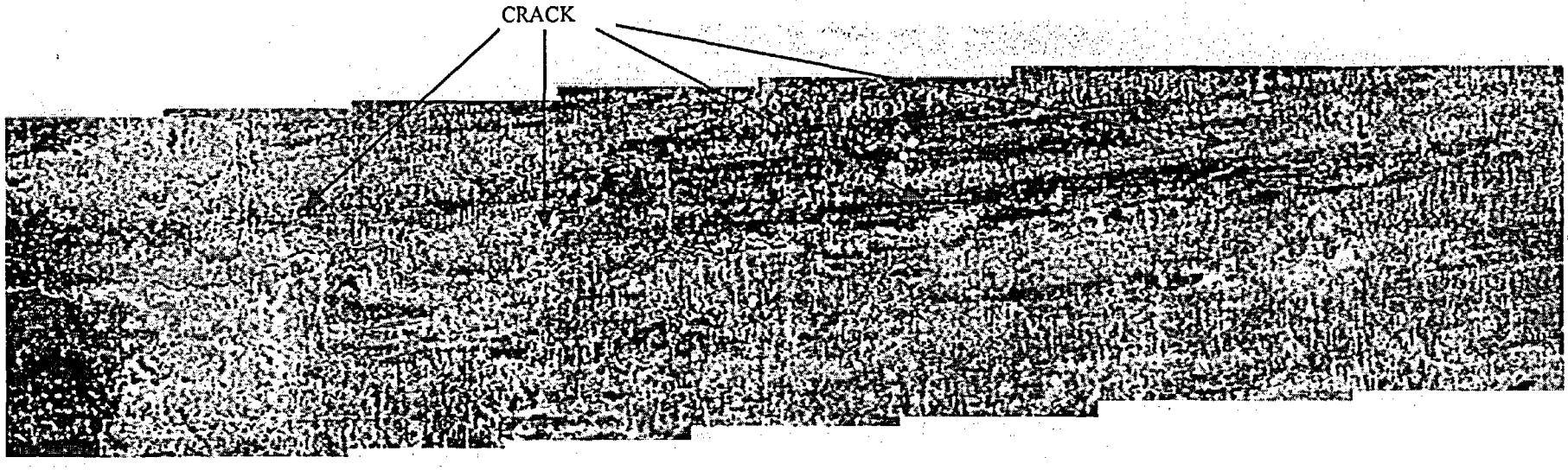

Figure 27. Axial crack In O2H TSP region of R35C57-8B at 170°. 24X

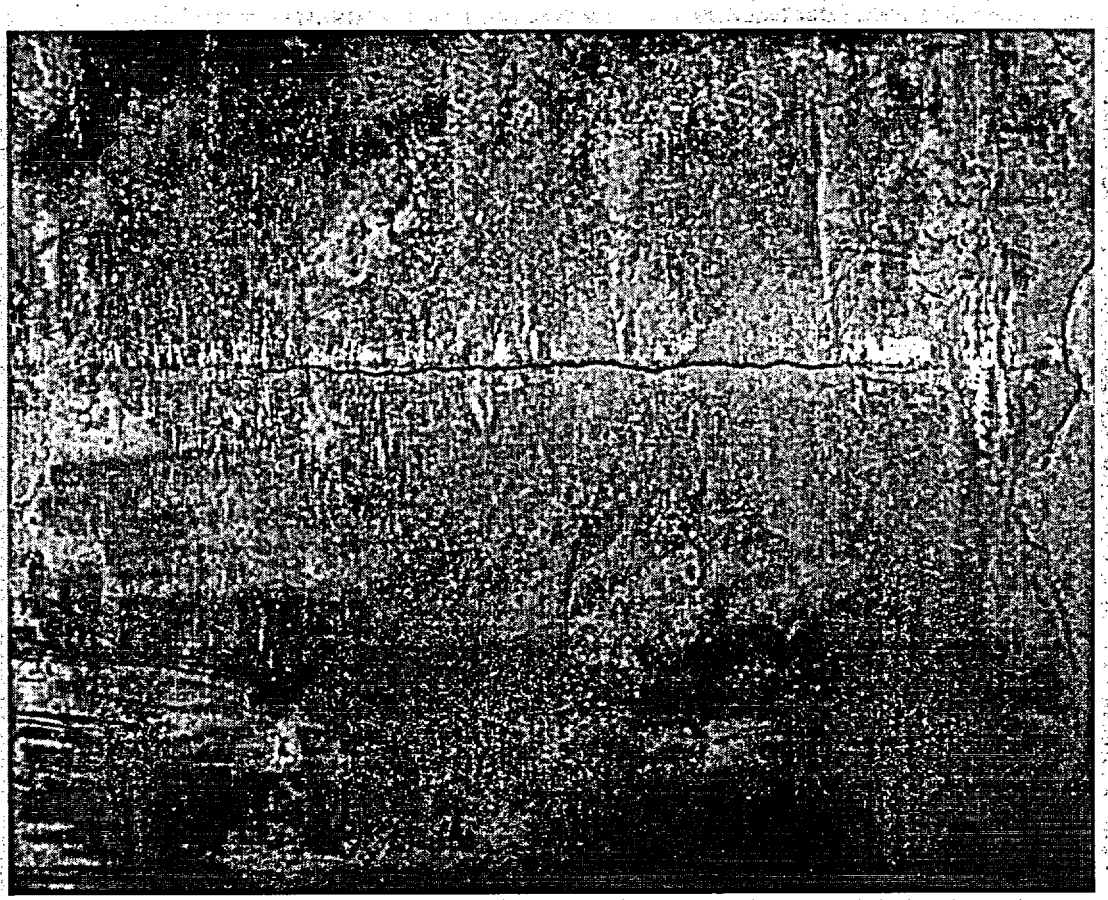

Figure 28. Axial crack in 02H TSP region of R44C45-13A at 90°. 6X

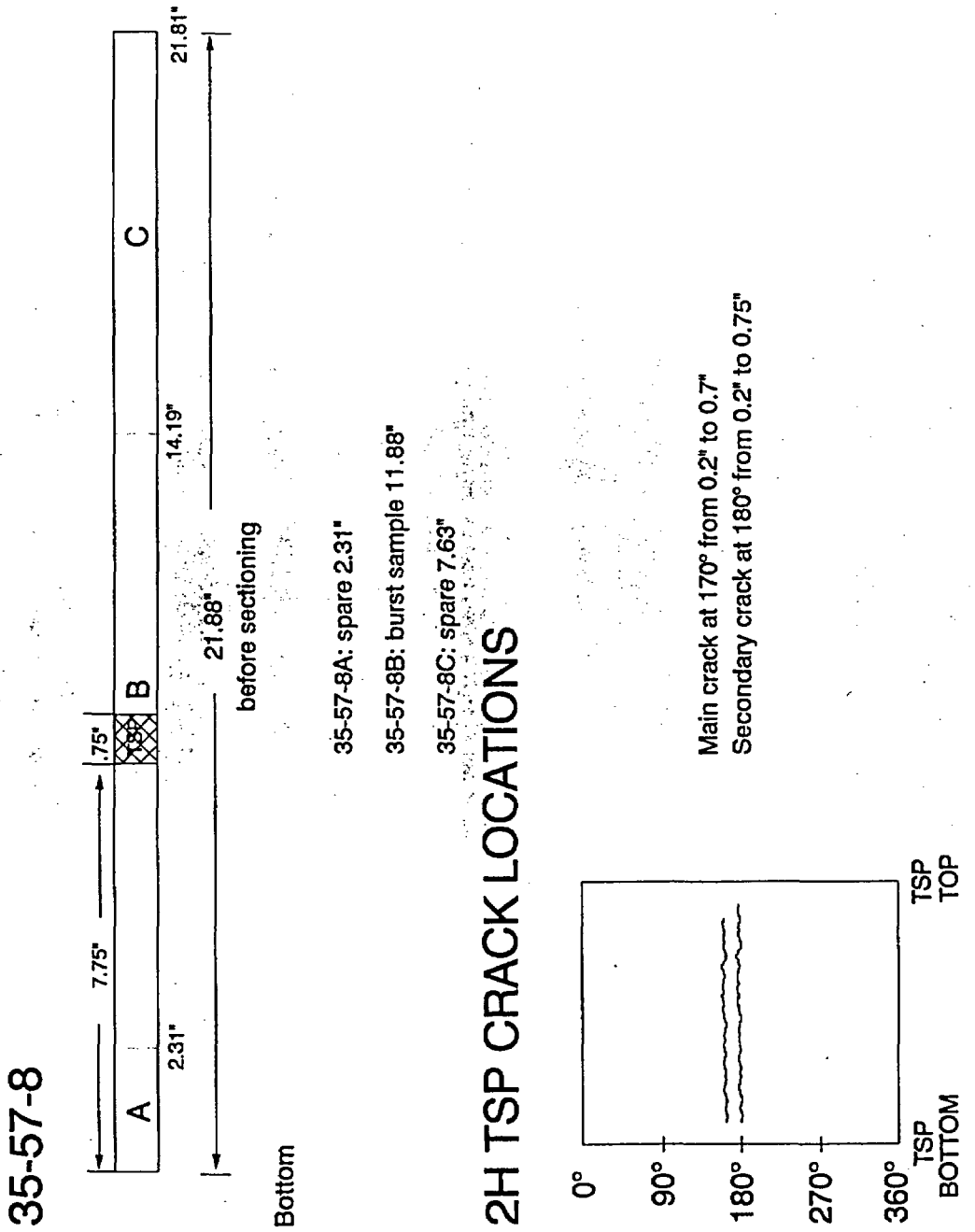

Figure 29. 2H TSP crack locations and initial sectioning of R35C57-8

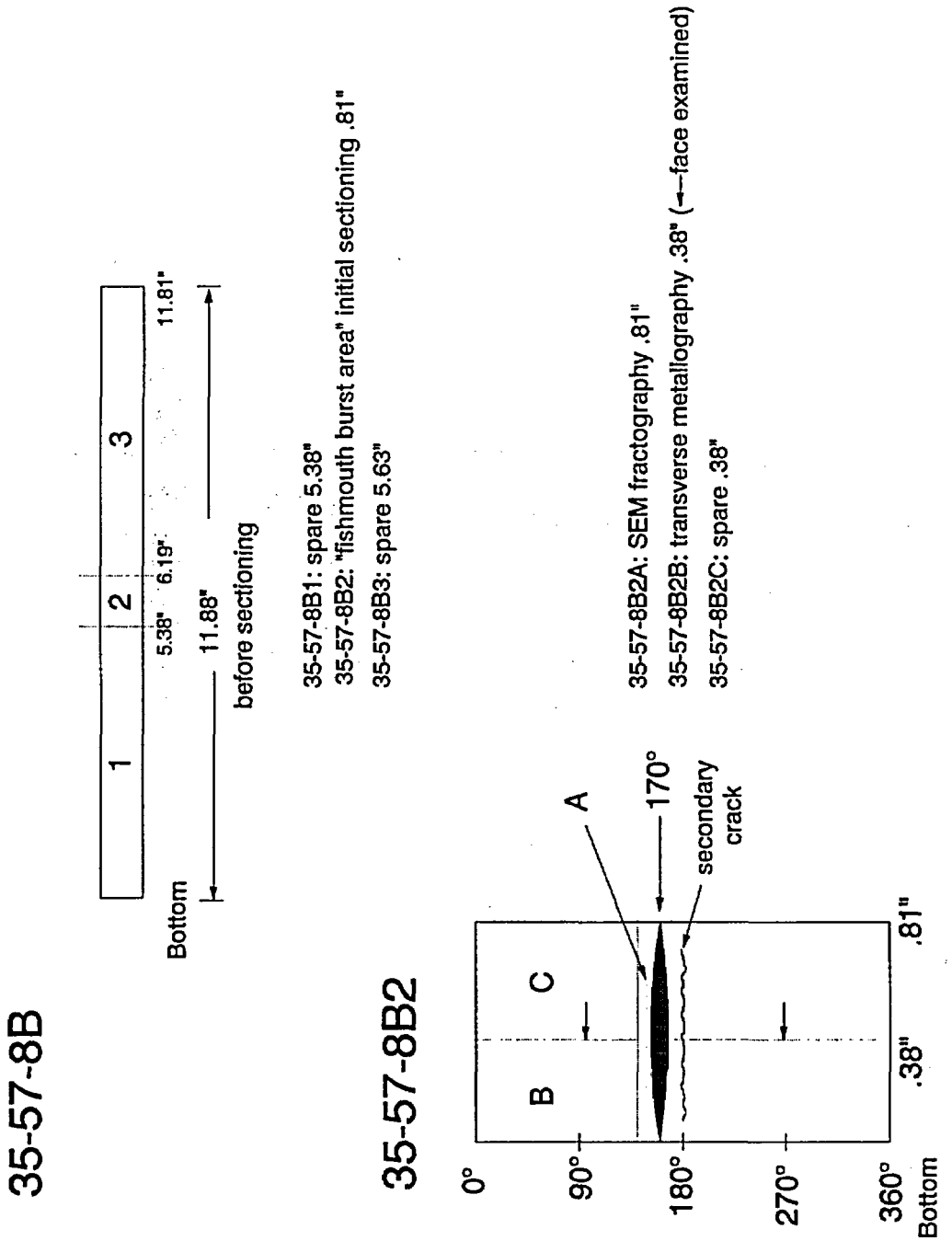

Figure 30. Sectioning of R35C57-8B

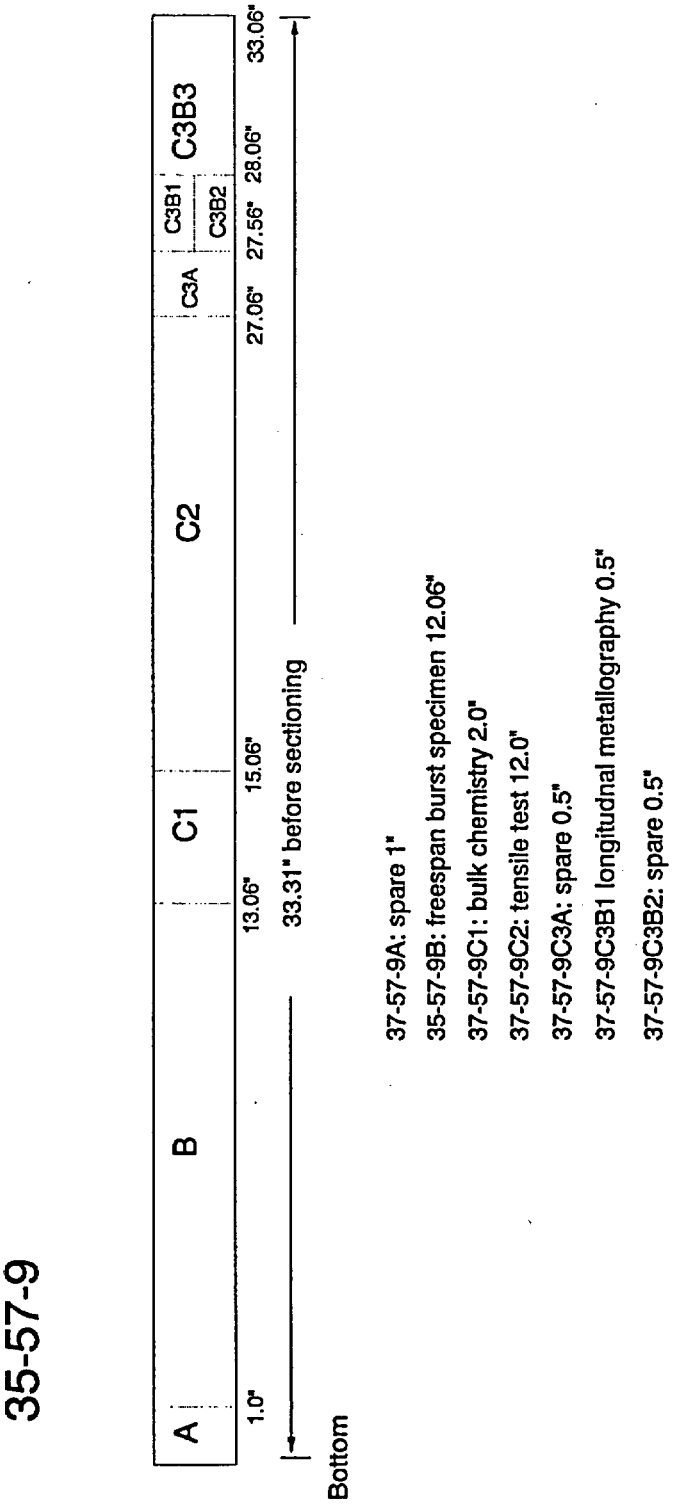

Figure 31. Initial sectioning of R35C57-9

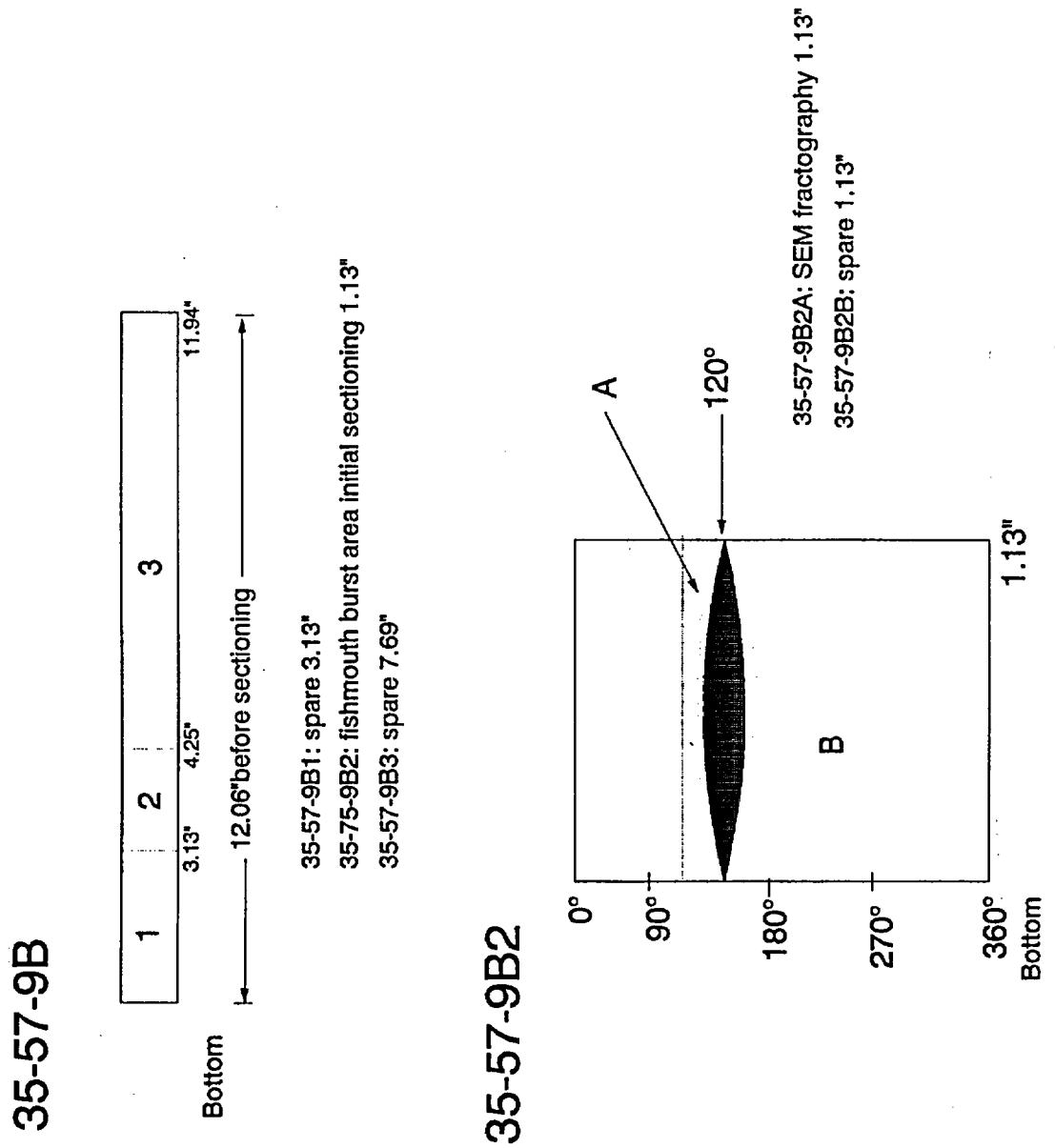

Figure 32. Sectioning of R35C57-9B

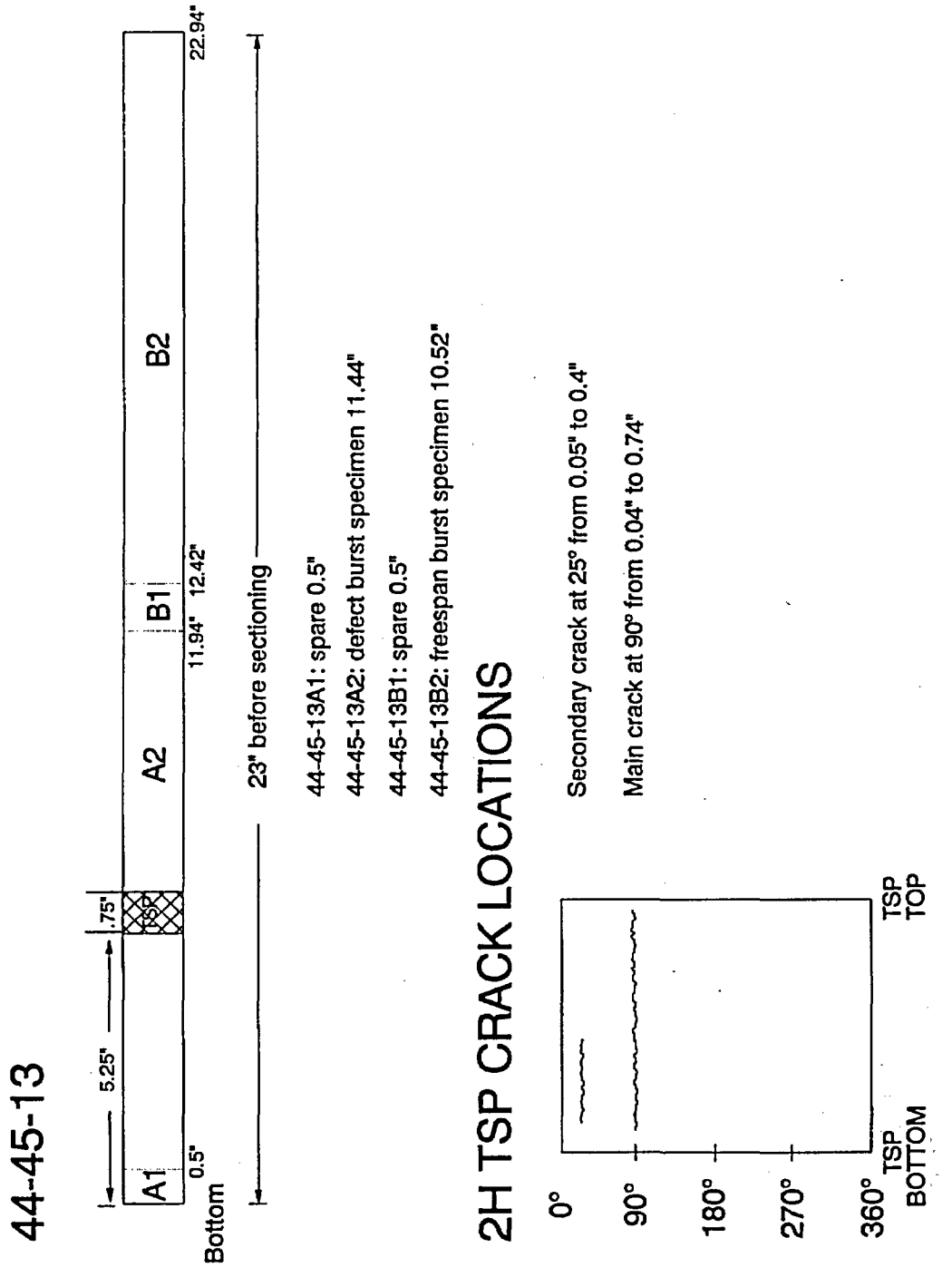

Figure 33. 2H TSP crack locations and initial sectioning of R44C45-13

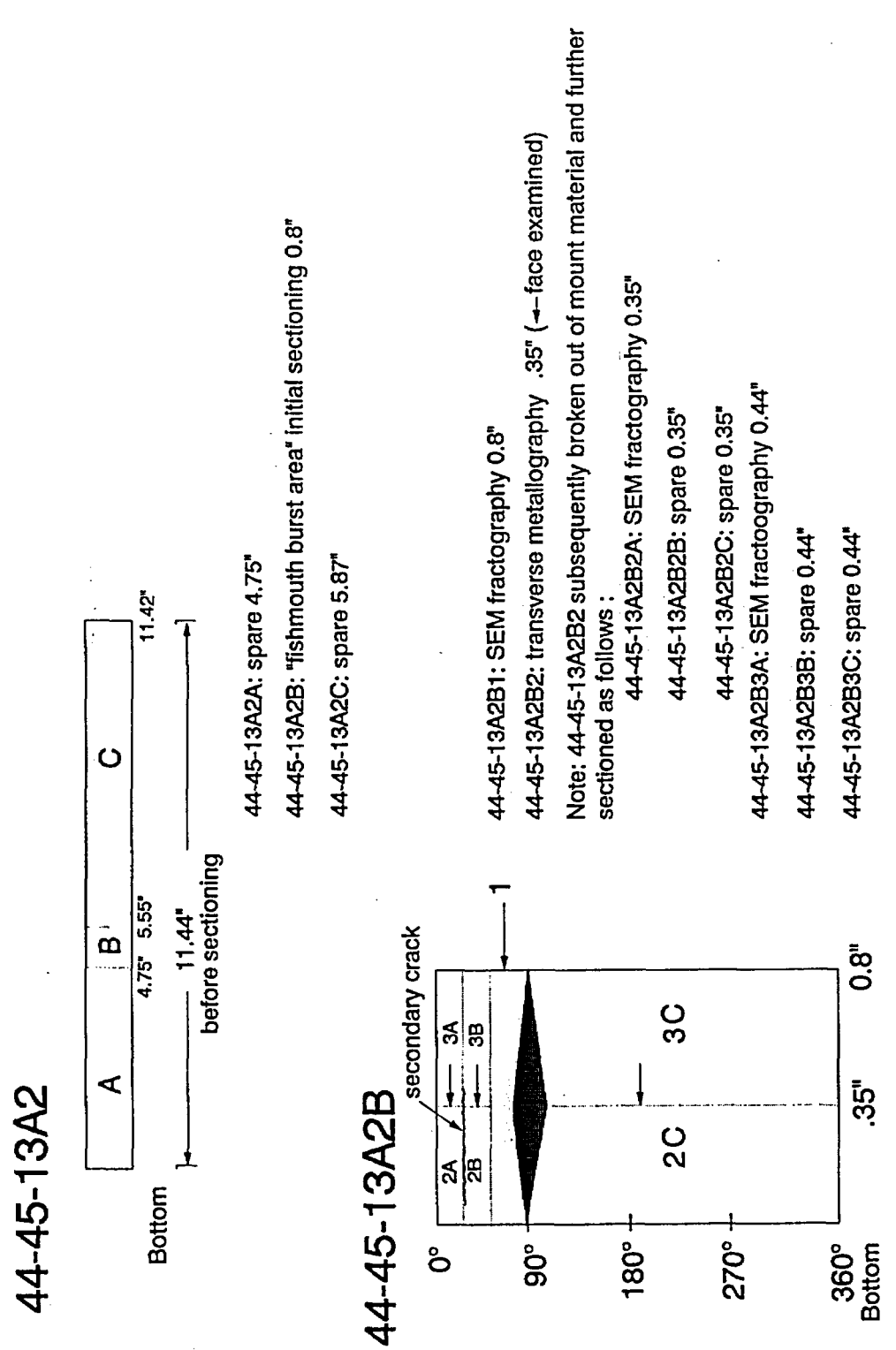

Figure 34. Sectioning of R44C45-13A2

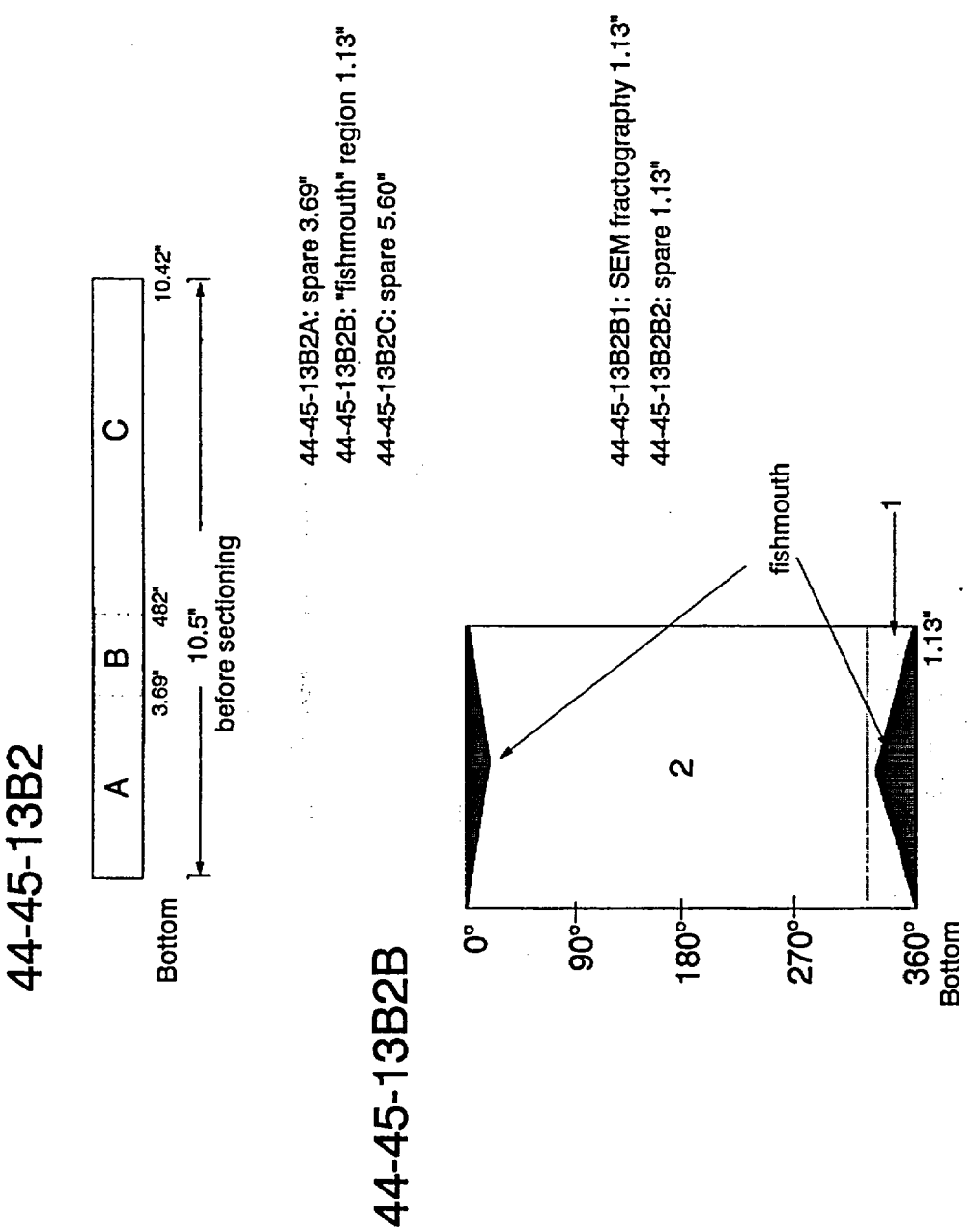

Figure 35. Sectioning of R44C45-13B2

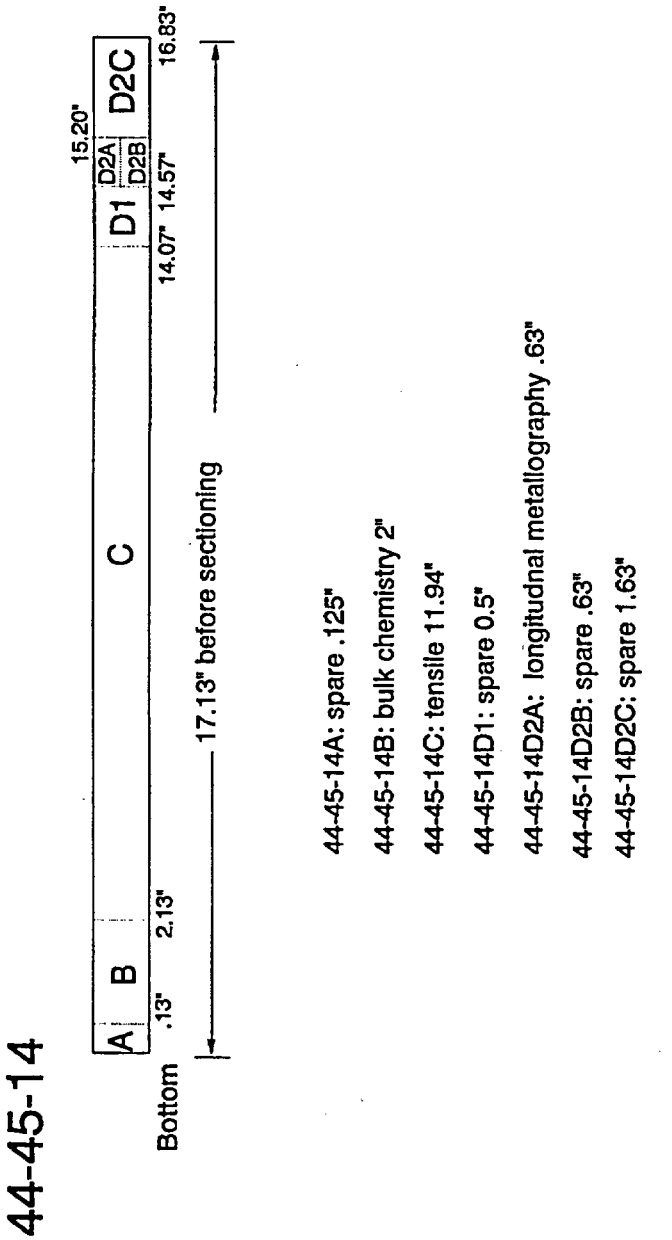

Figure 36. Initial sectioning of R44C45-14

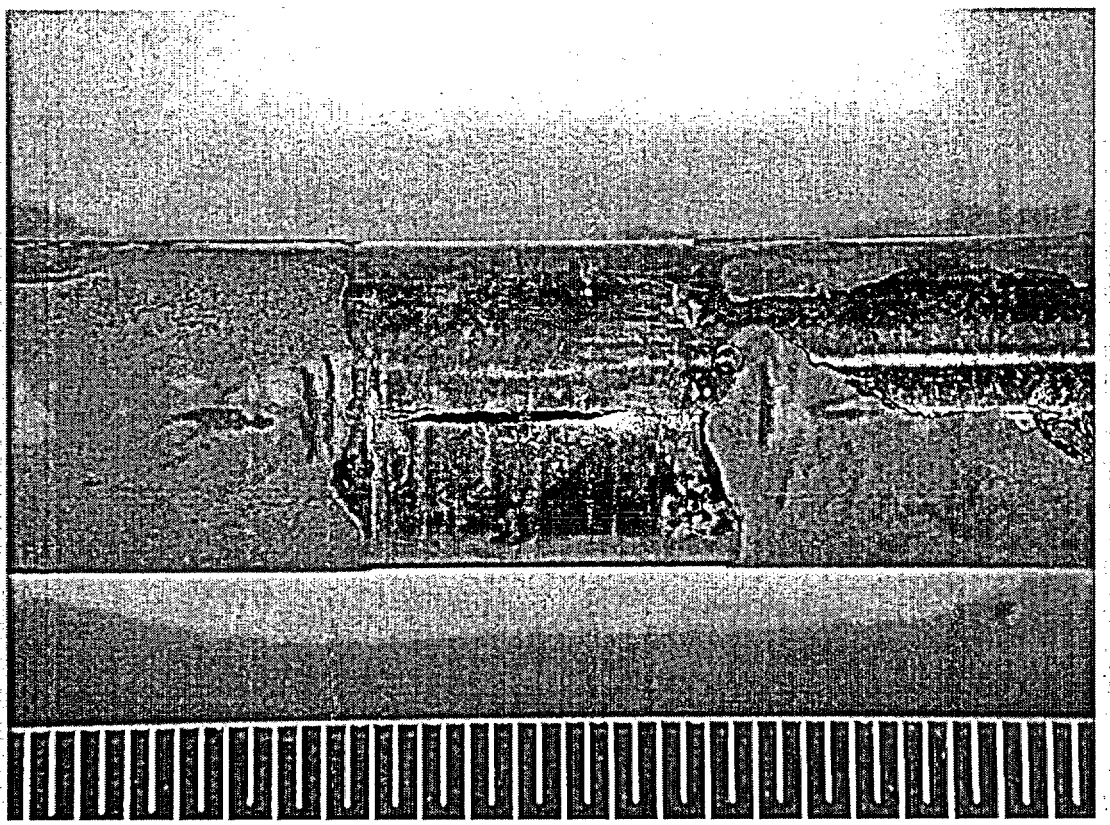

Figure 37. Crack opening on R44C45-13A2 after initial pressurization to 3,403 psi (shim slipped). Later burst tested to 4,226 psi. 2.1X

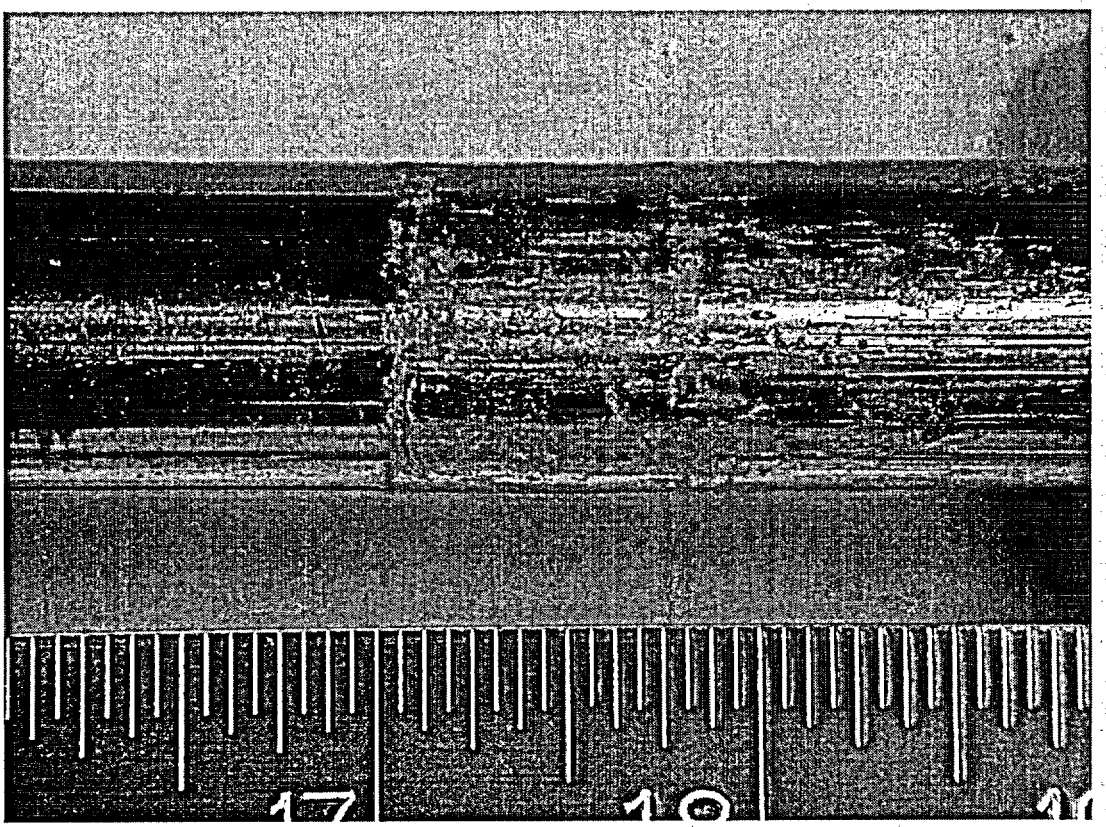

Figure 38. R35C57-8B at 0° after burst testing. 2.1X

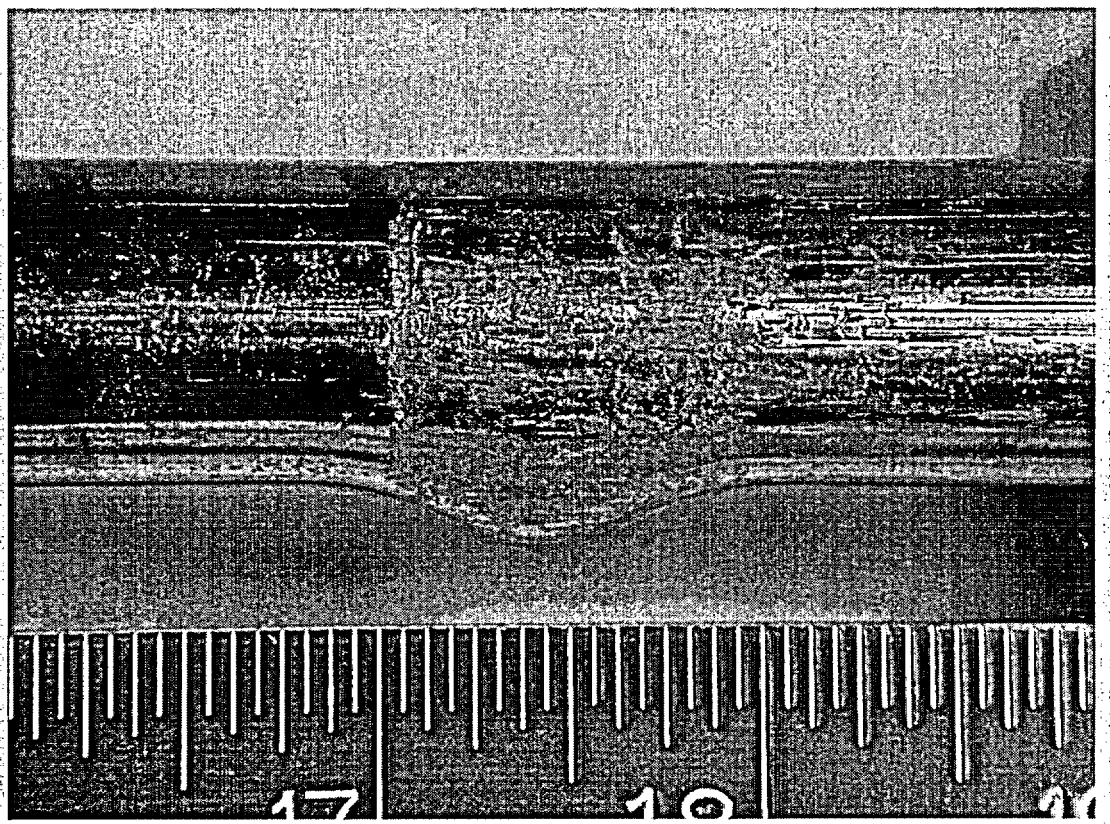

Figure 39. R35C57-8B at 45° after burst testing. 2.1X

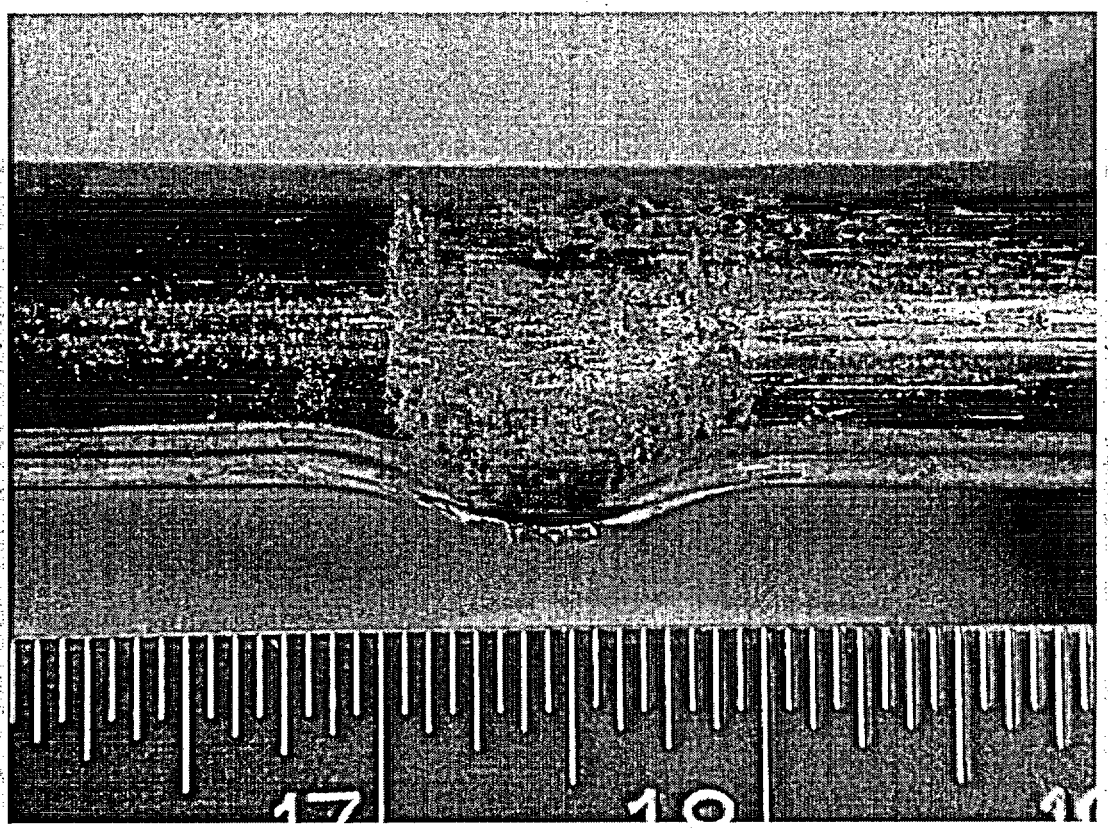

Figure 40. R35C57-8B at 90° after burst testing. 2.1X

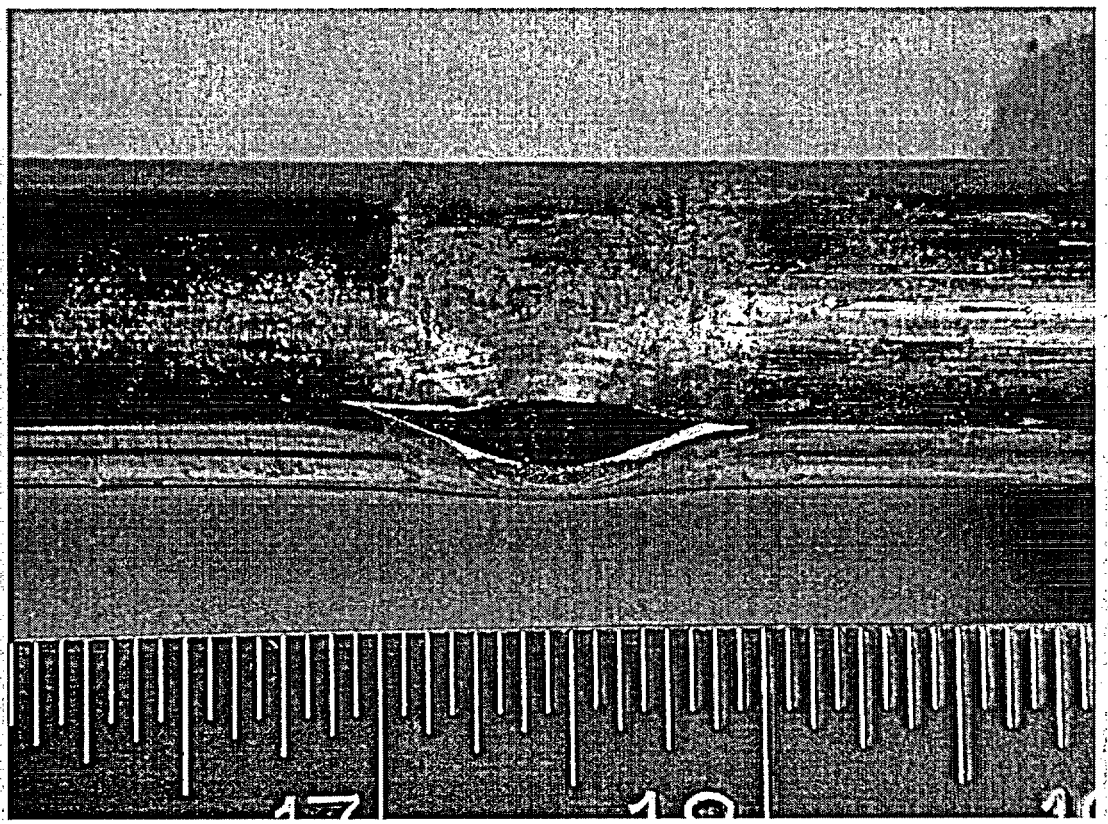

Figure 41. R35C57-8B at 135° after burst testing. 2.1X

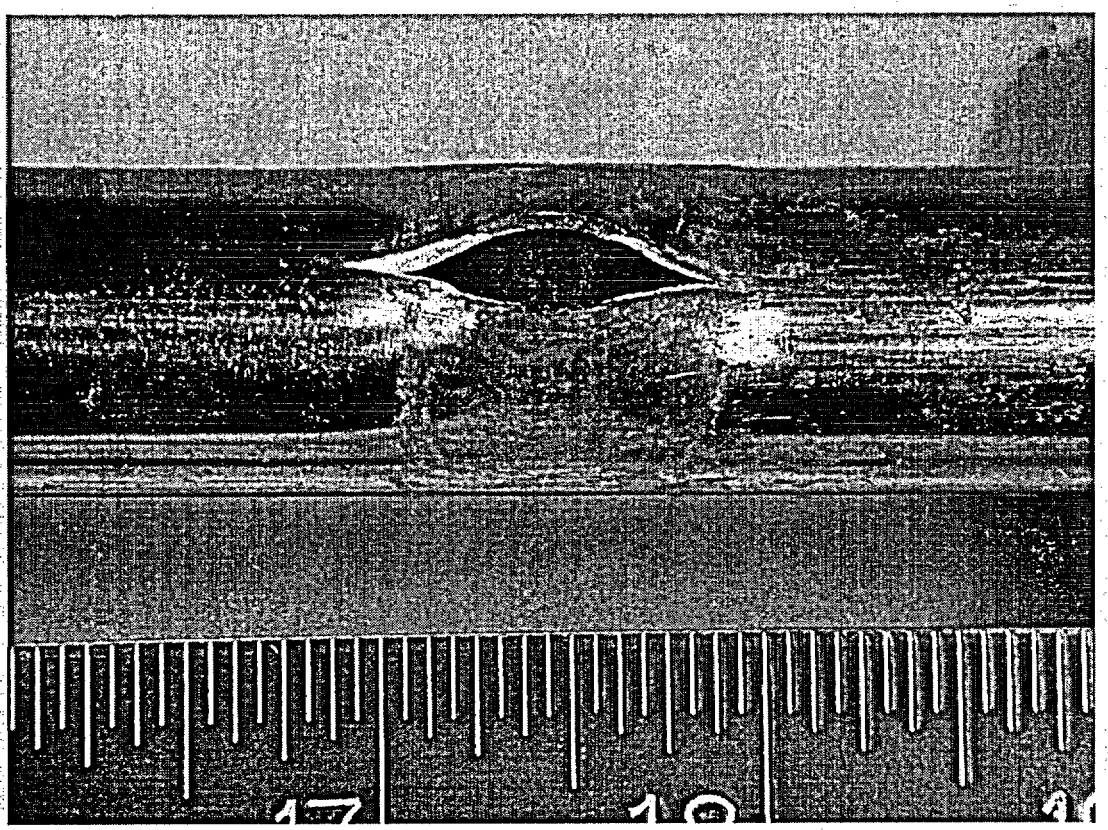

Figure 42. R35C57-8B at 180° after burst testing. 2.1X

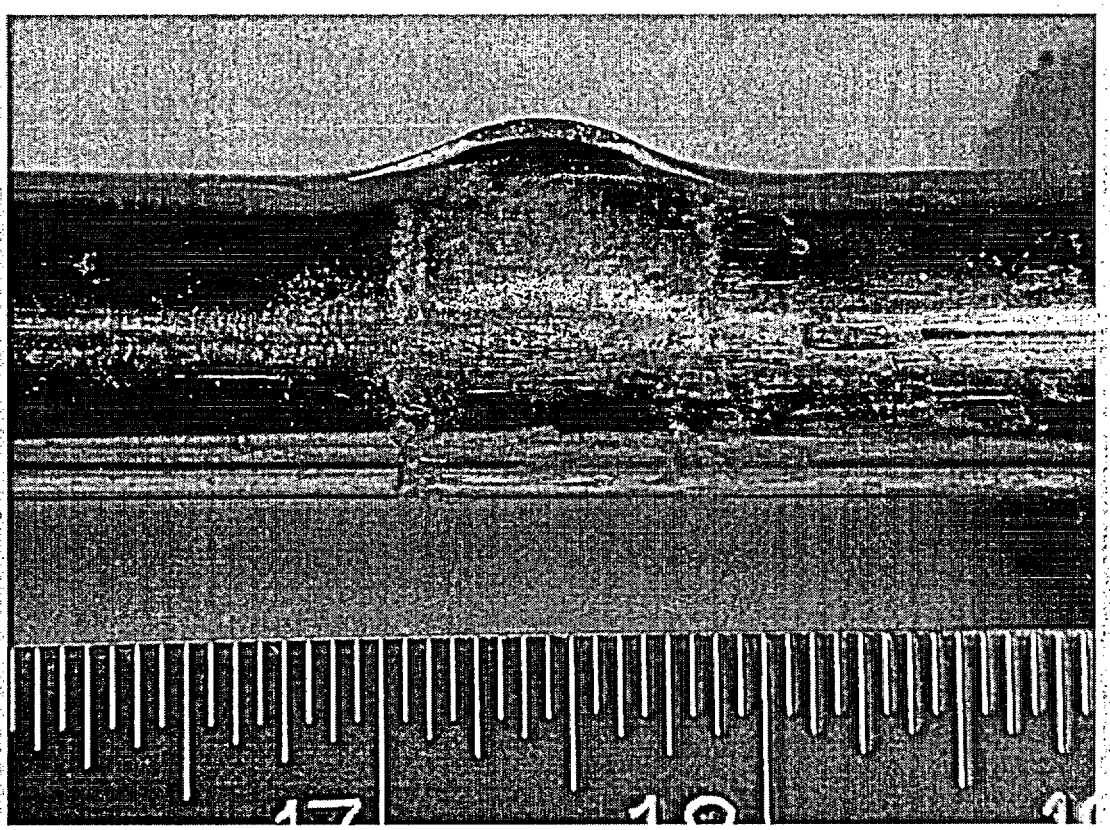

Figure 43. R35C57-8B at 225° after burst testing. 2.1X

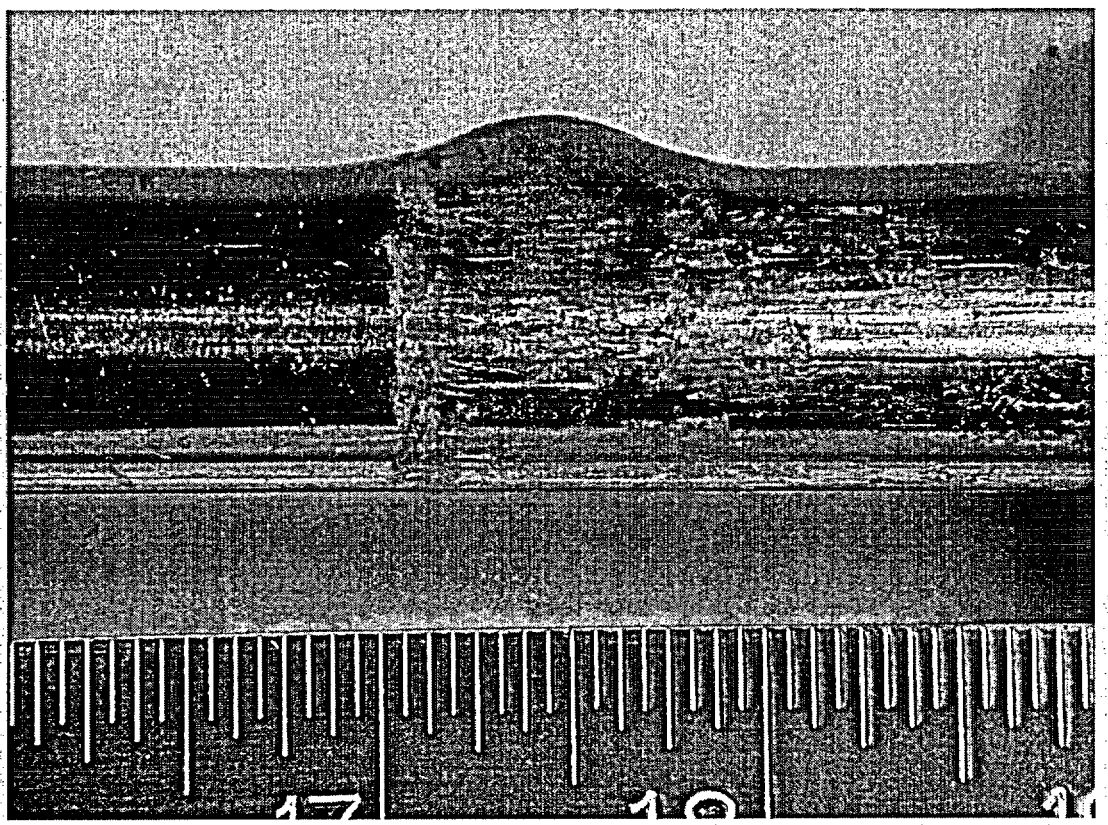

Figure 44. R35C57-8B at 270° after burst testing. 2.1X

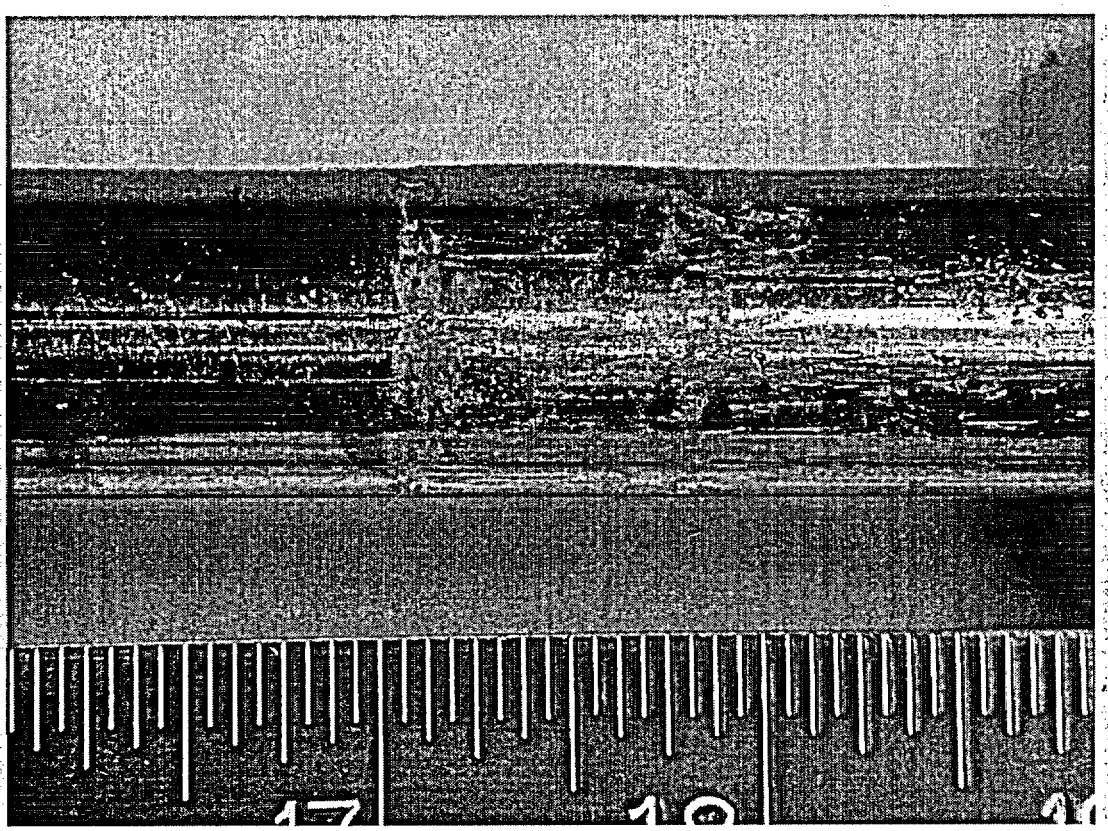

Figure 45. R35C57-8B at 315° after burst testing. 2.1X

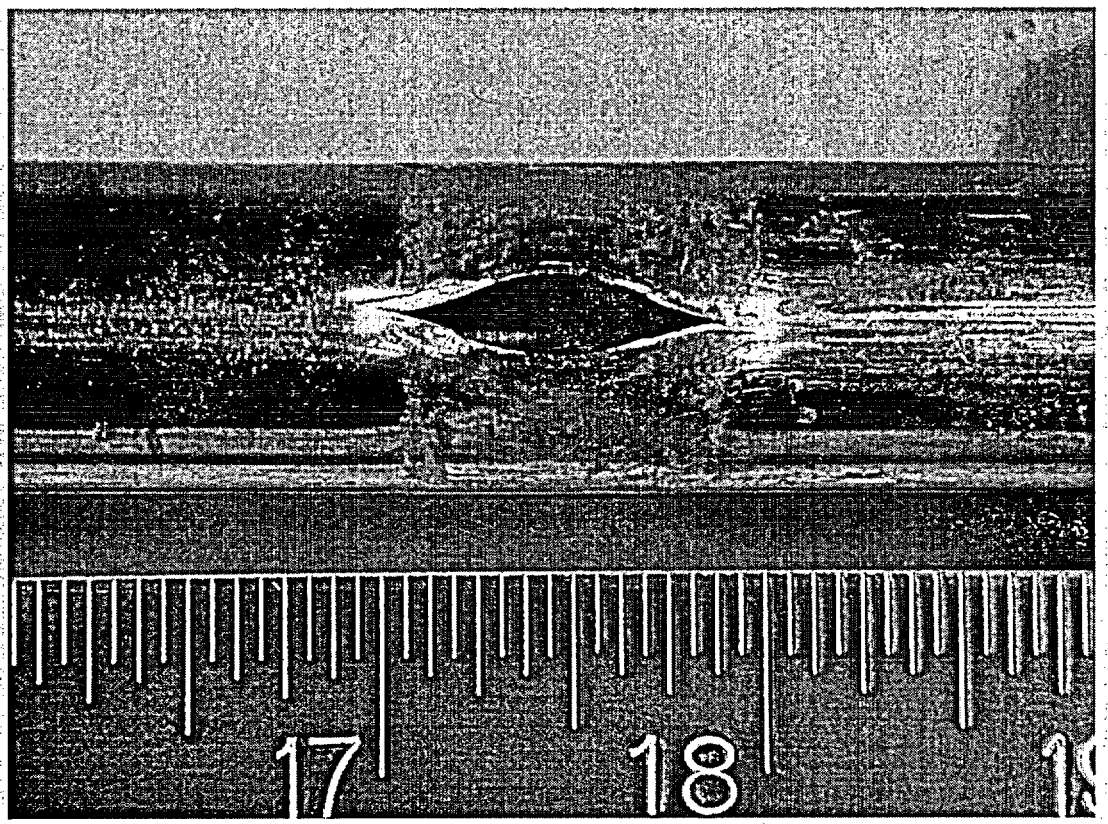

Figure 46. R35C57-8B at fish mouth opening at 170° after burst testing. 2.1X

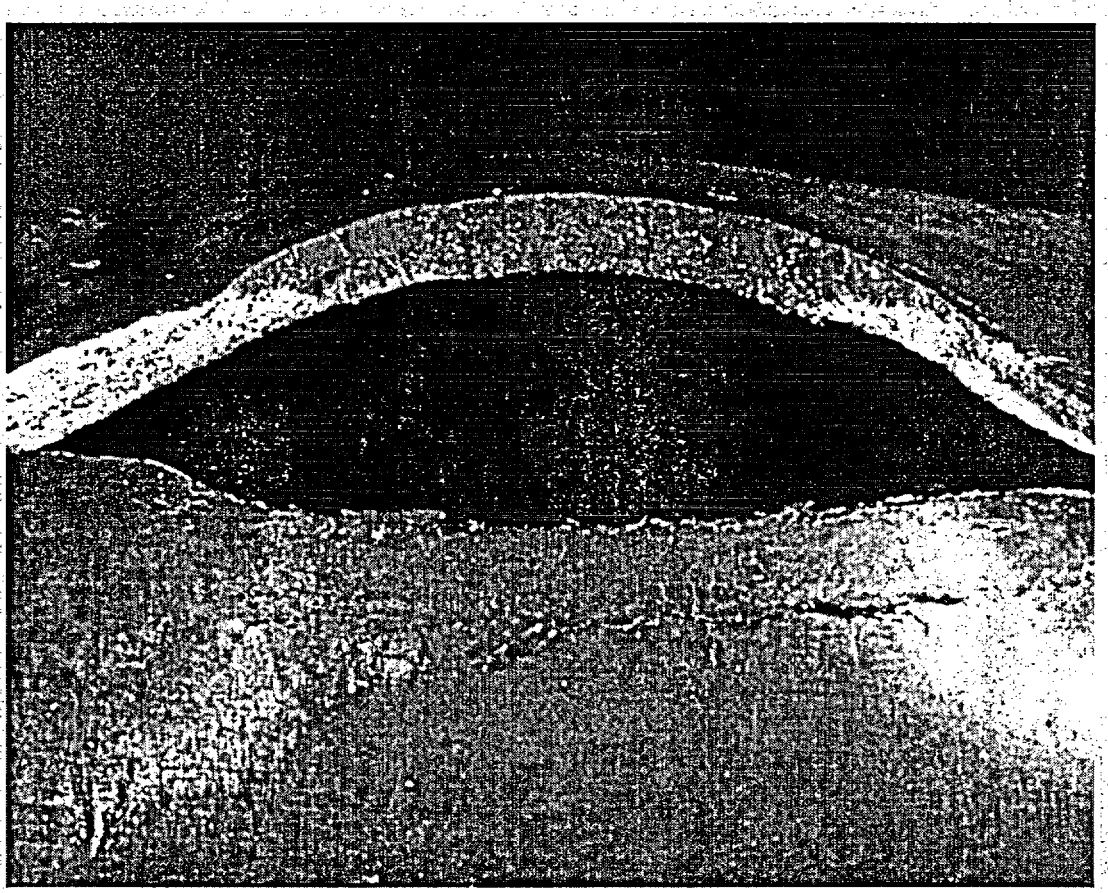

Figure 47. Oxidized CCW rupture surface on R35C57-8B along with secondary fissure. 8X

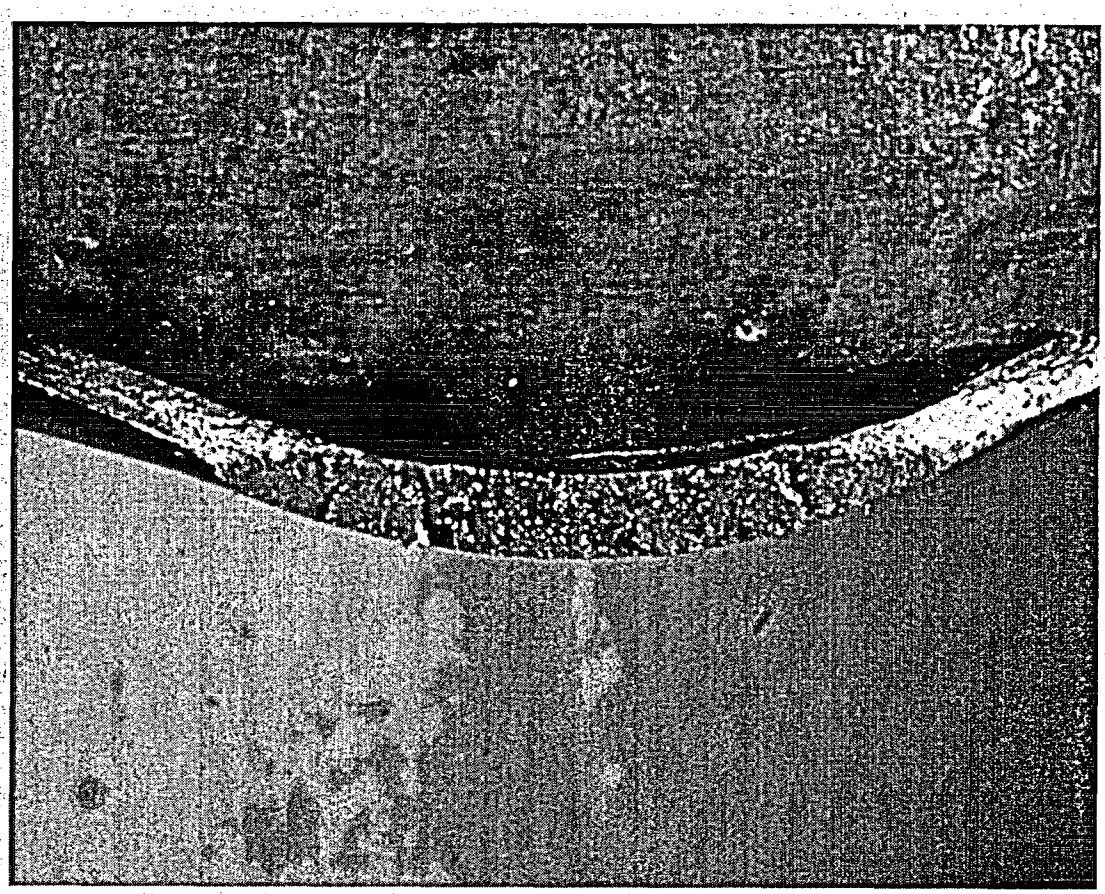

Figure 48. Oxidized CW rupture surface on R35C57-8B. 8X

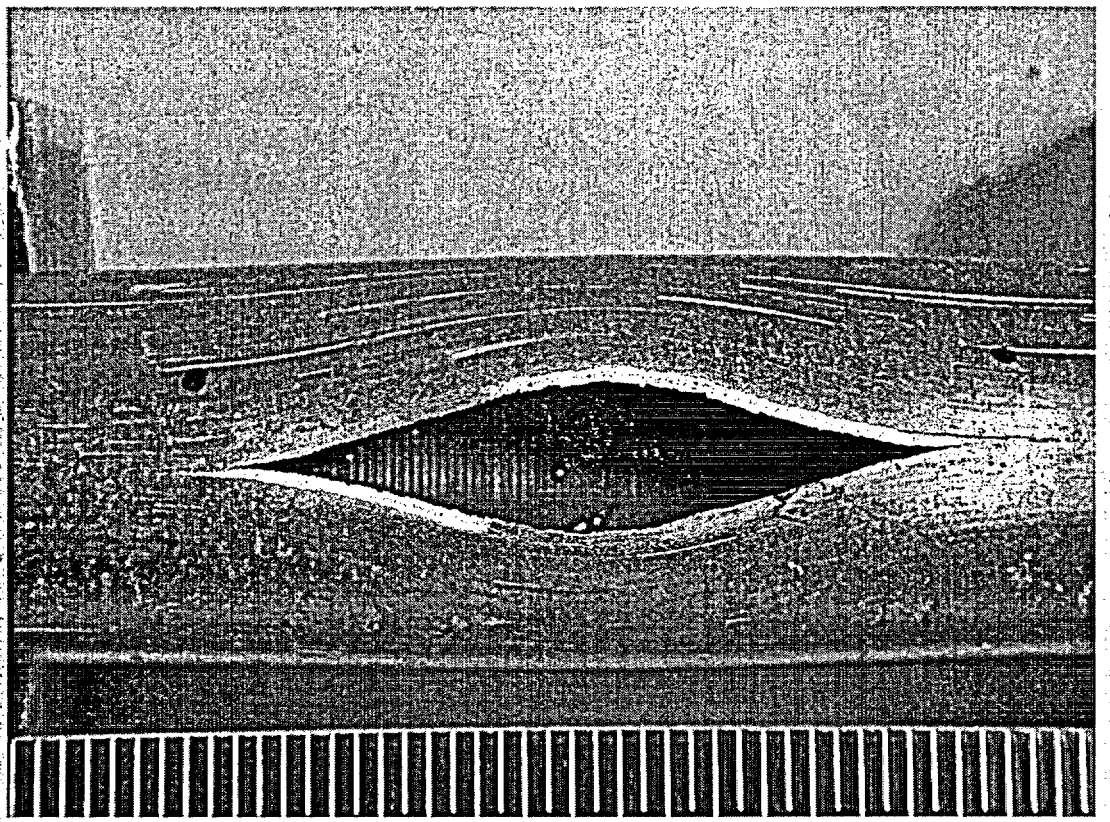

Figure 49. Free span burst region on R35C57-9B. 2.1X

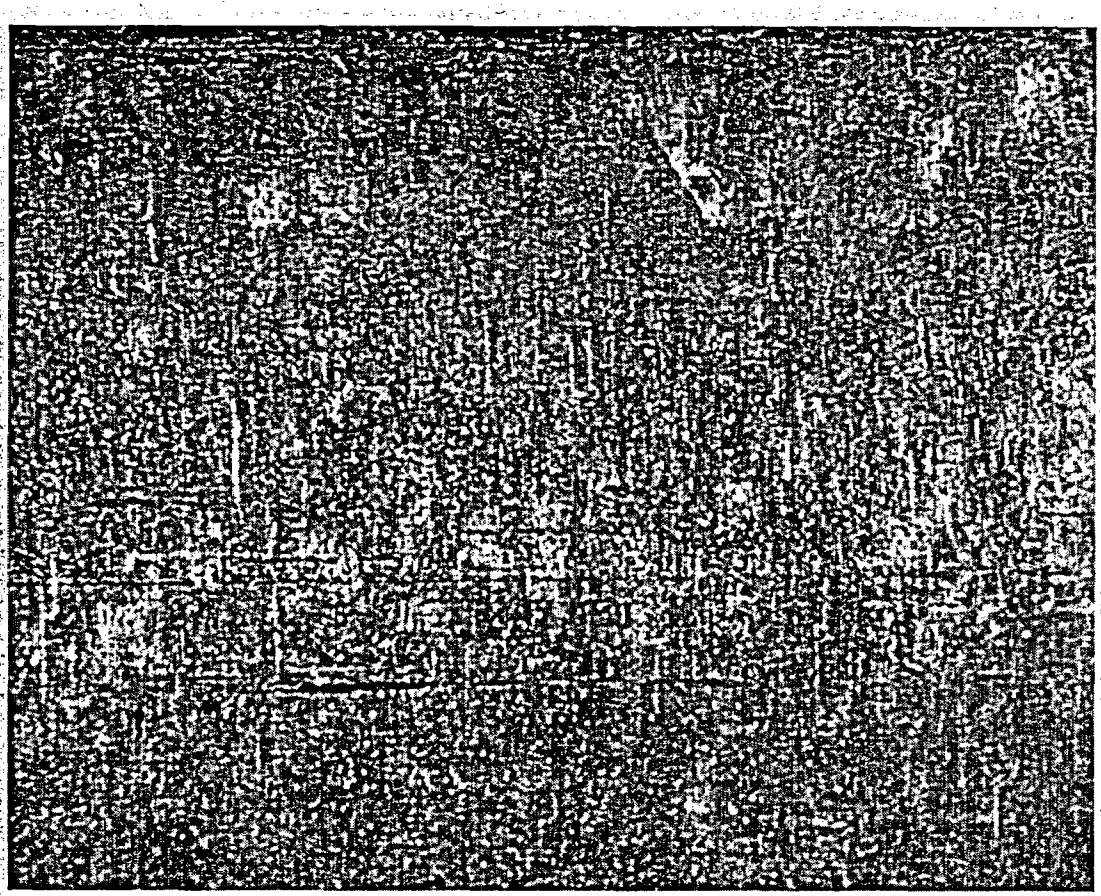

Figure 50. Typical mottled deposits on R35C57-9B after burst testing. 12X

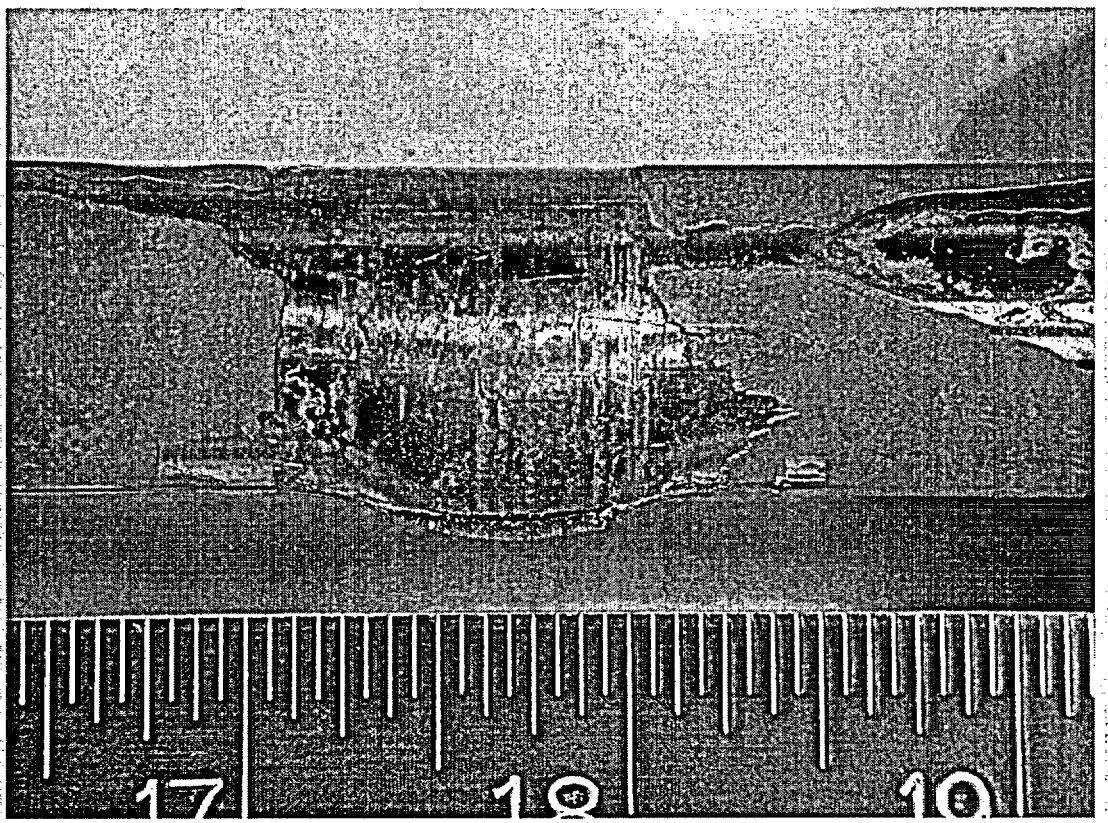

Figure 51. R44C45-13A2B1 at 0° after burst testing. 2.1X

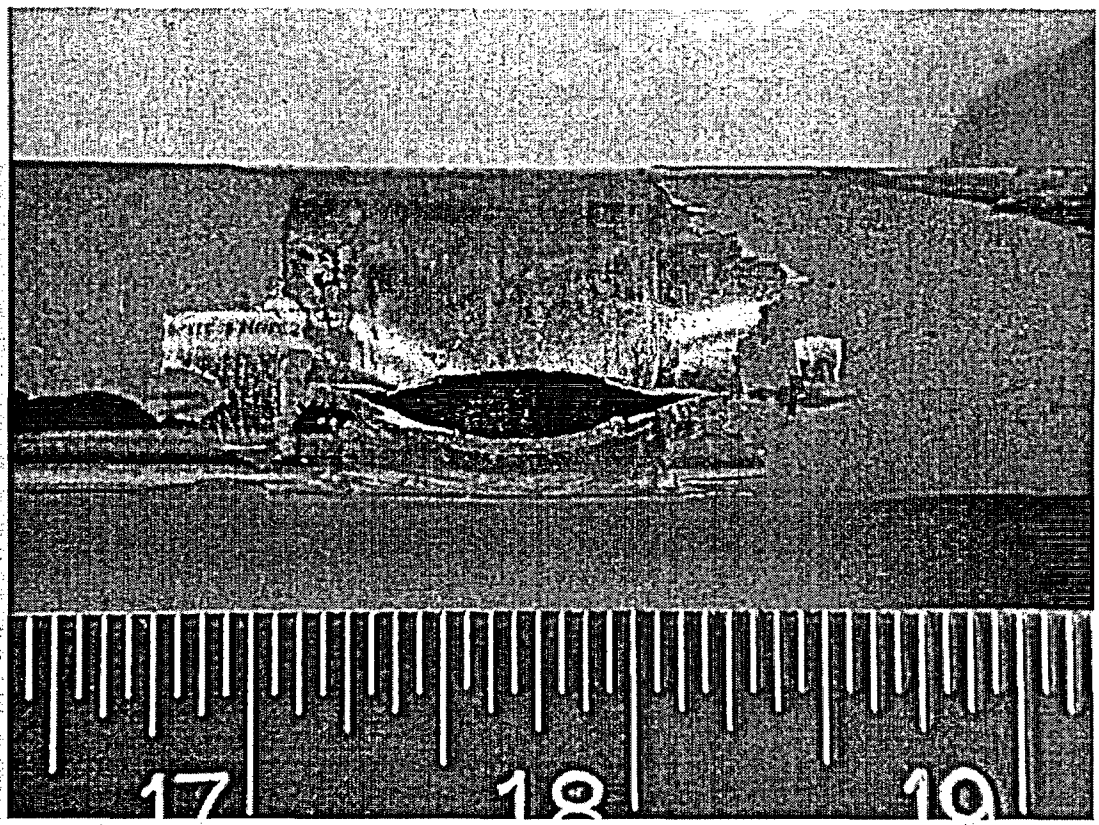

Figure 52. R44C45-13A2B1 at 45° after burst testing. 2.1X

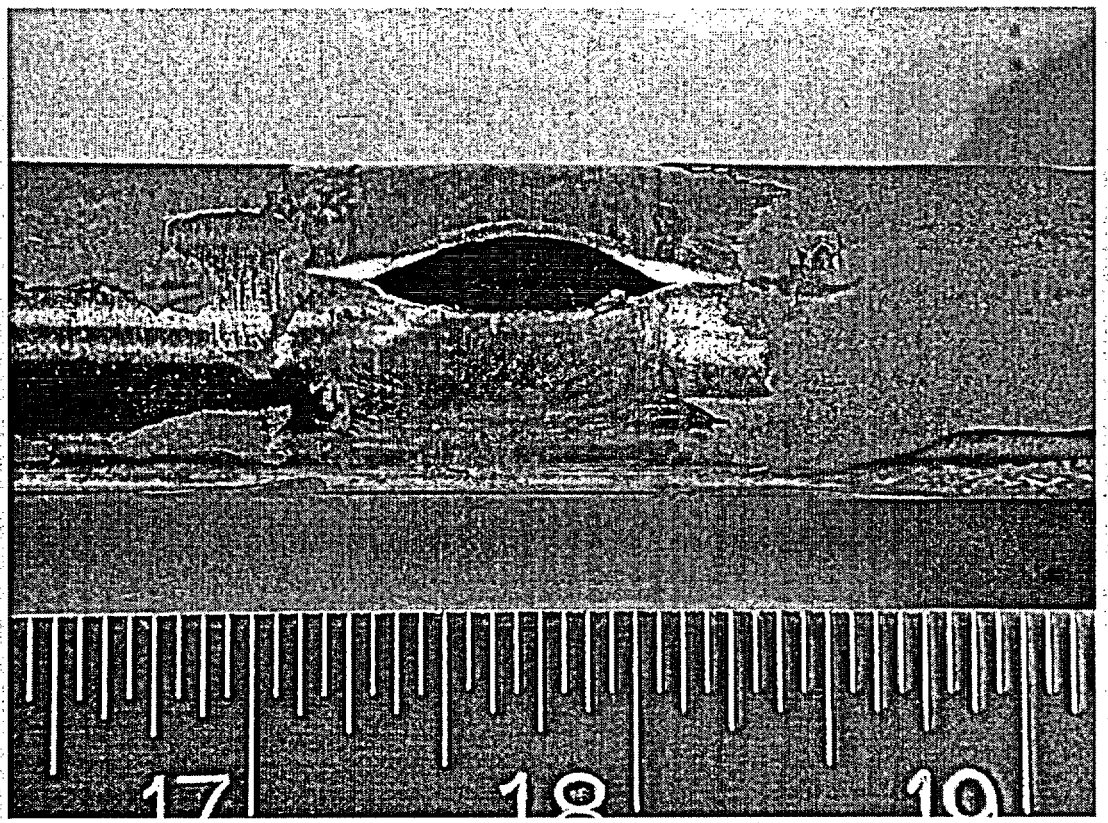

Figure 53. R44C45-13A2B1 at 90° after burst testing. 2.1X

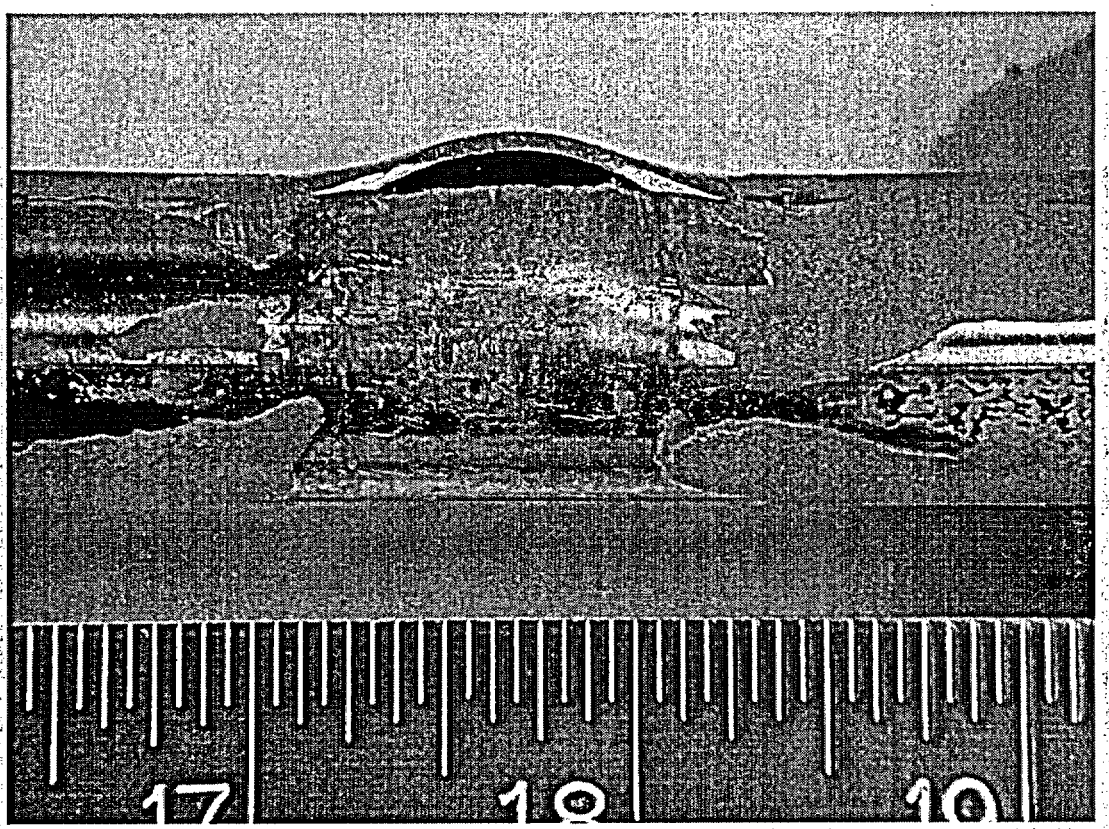

Figure 54. R44C45-13A2B1 at 135° after burst testing. 2.1X

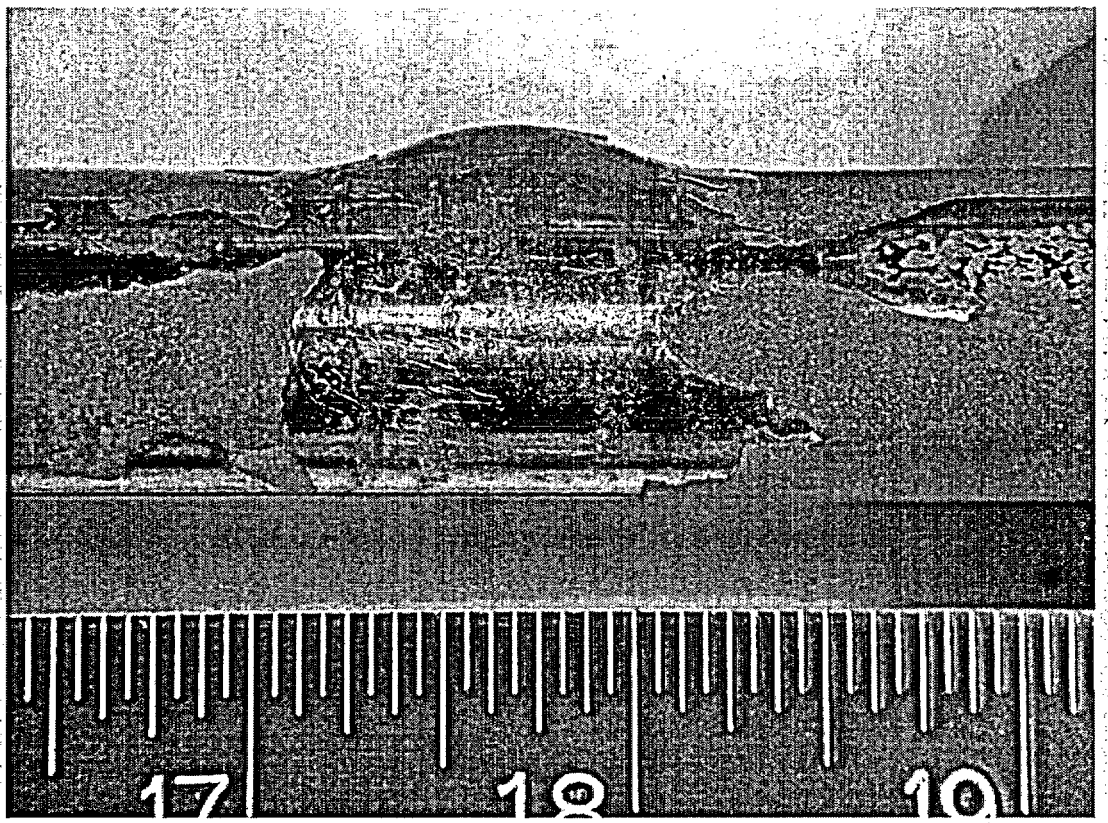

Figure 55. R44C45-13A2B1 at 180° after burst testing. 2.1X

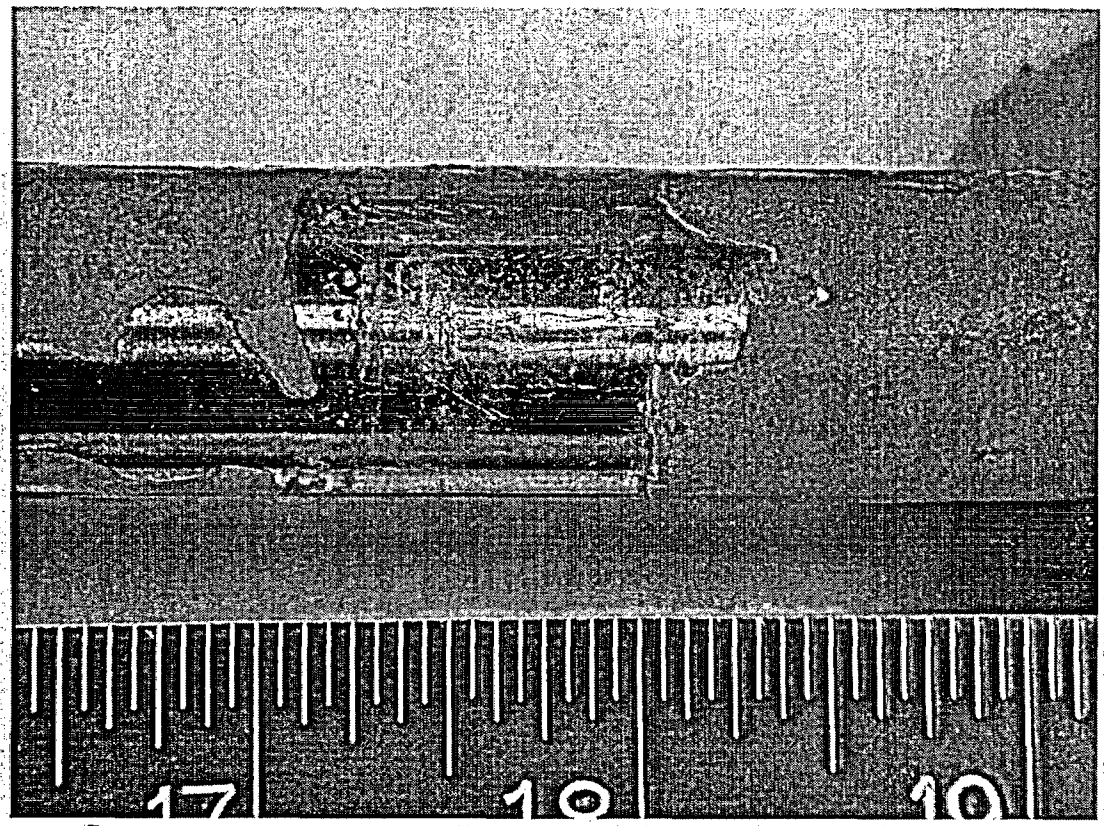

Figure 56. R44C45-13A2B1 at 225° after burst testing. 2.1X

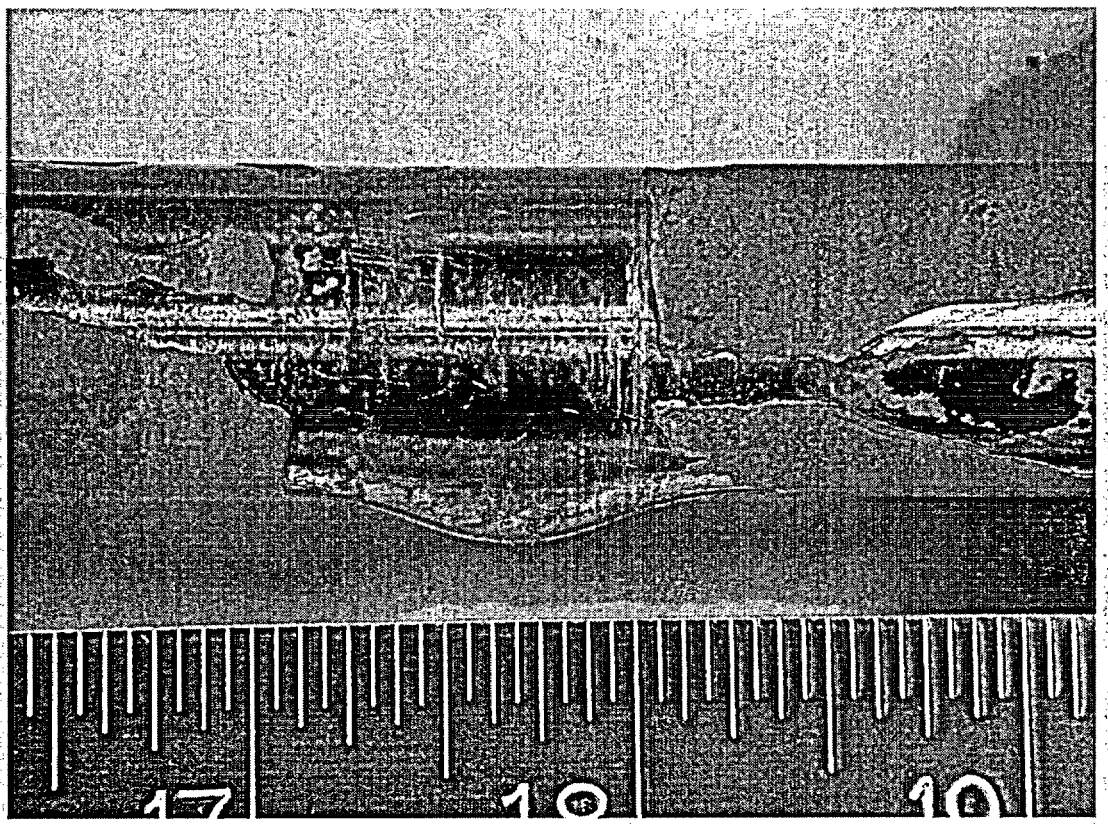

Figure 57. R44C45-13A2B1 at 270° after burst testing. 2.1X

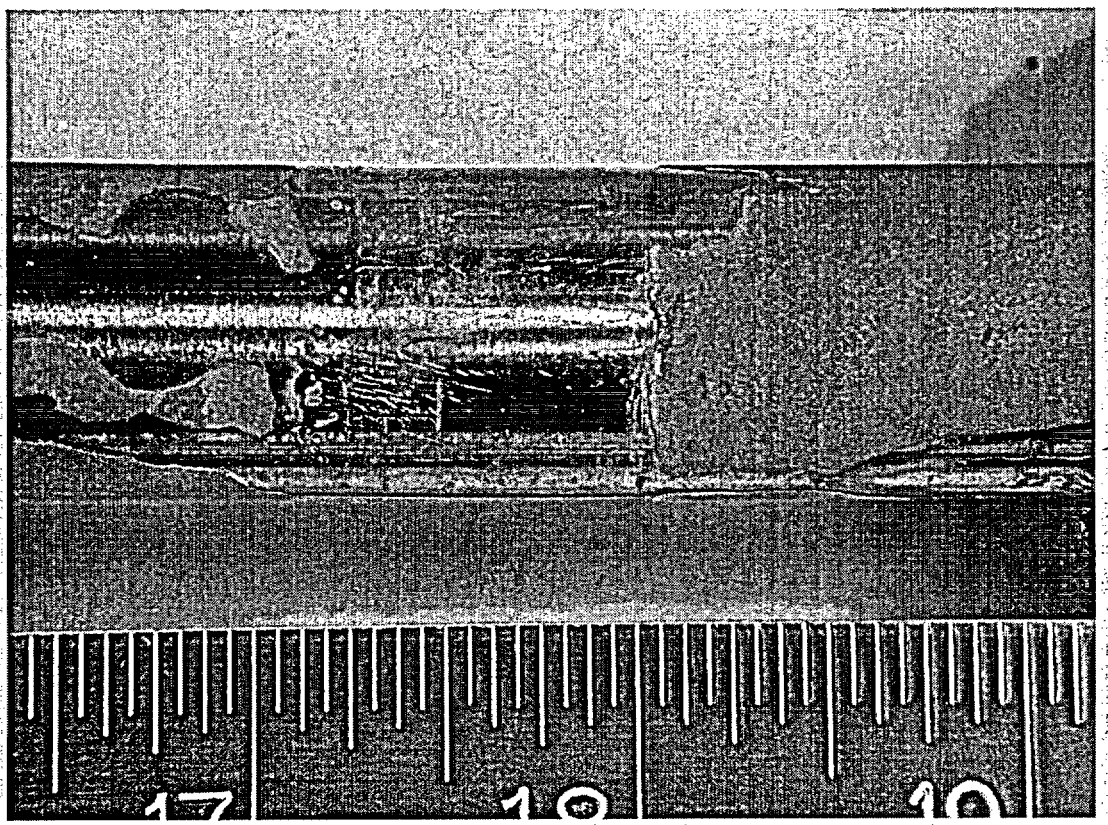

Figure 58. R44C45-13A2B1 at 315° after burst testing. 2.1X

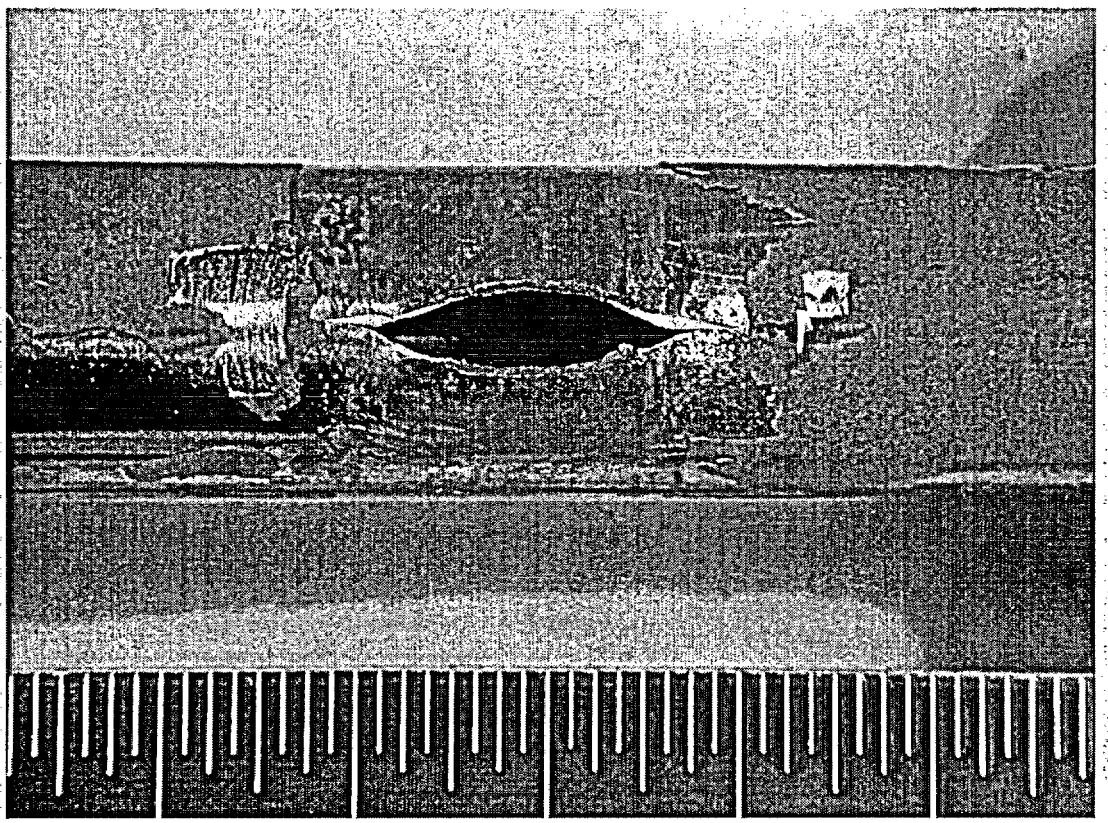

Figure 59. R44C45-13A2B1 at fish mouth opening at 90° after burst testing. 2.1X

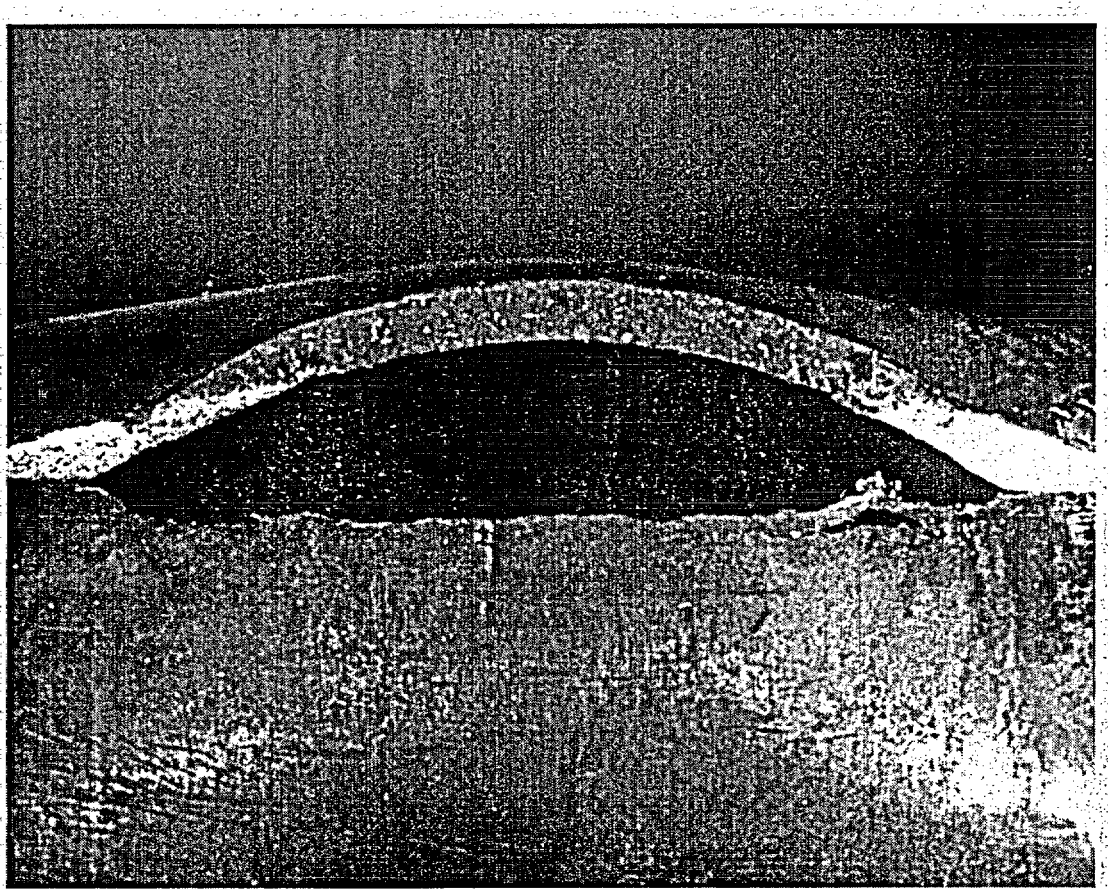

Figure 60. Oxidized CCW rupture surface on R44C45-13A2B1. 6X

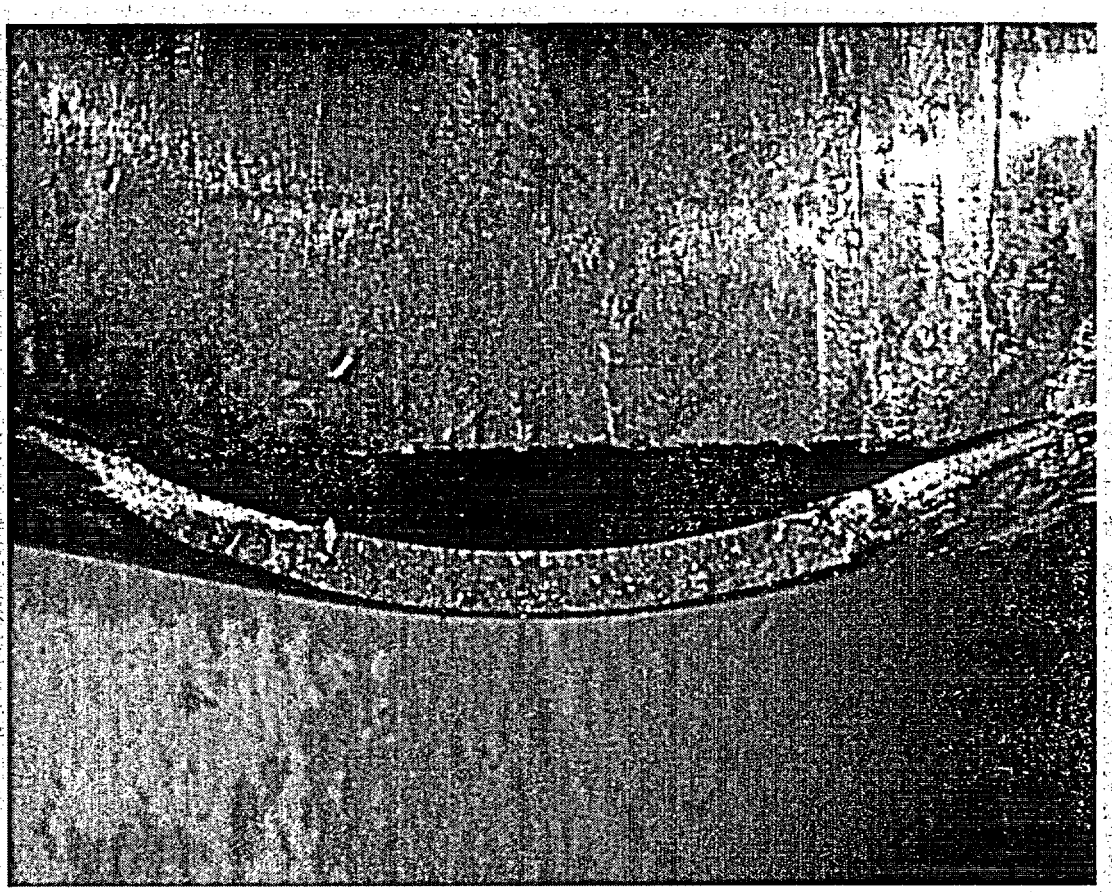

Figure 61. Oxidized CW rupture surface on R44C45-13A2B1. 6X

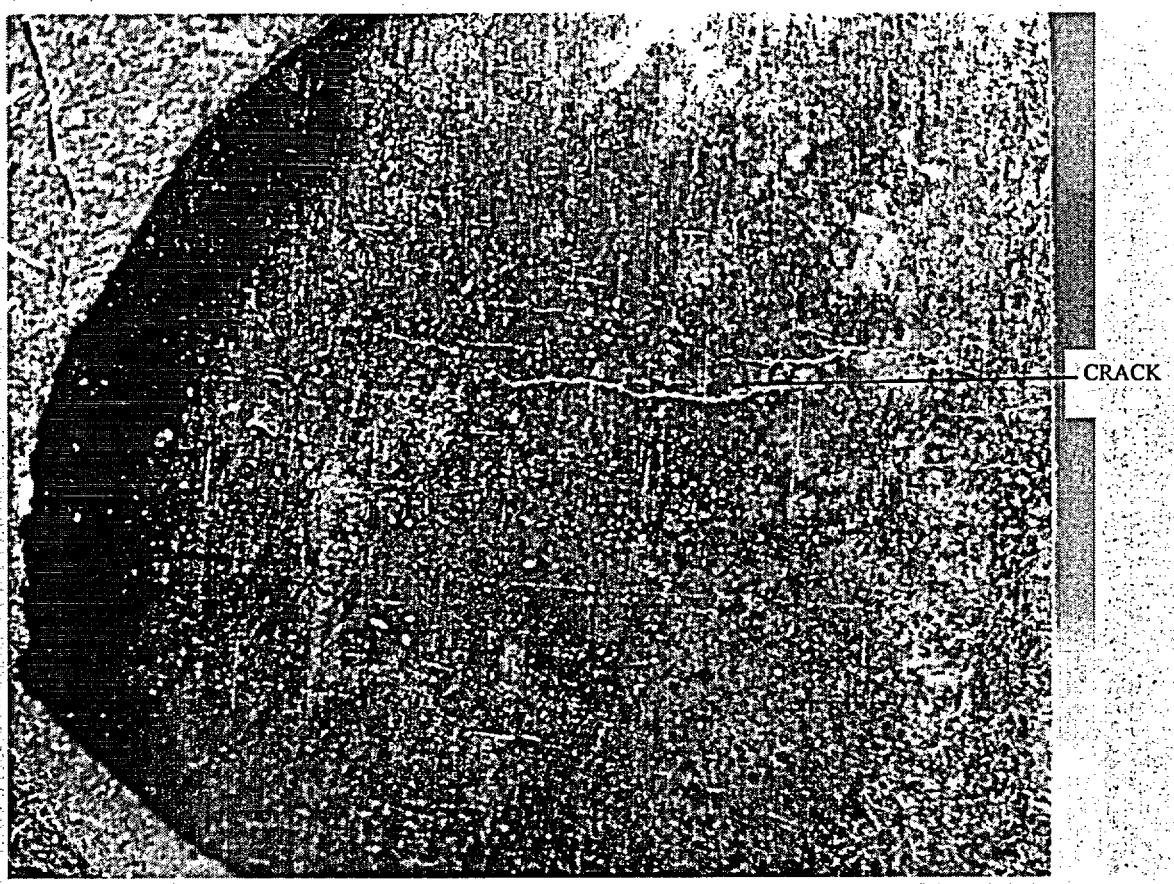

Figure 62. Secondary crack near 25° on R44C45-13A2B2 (broken out of metallographic mount). 15X

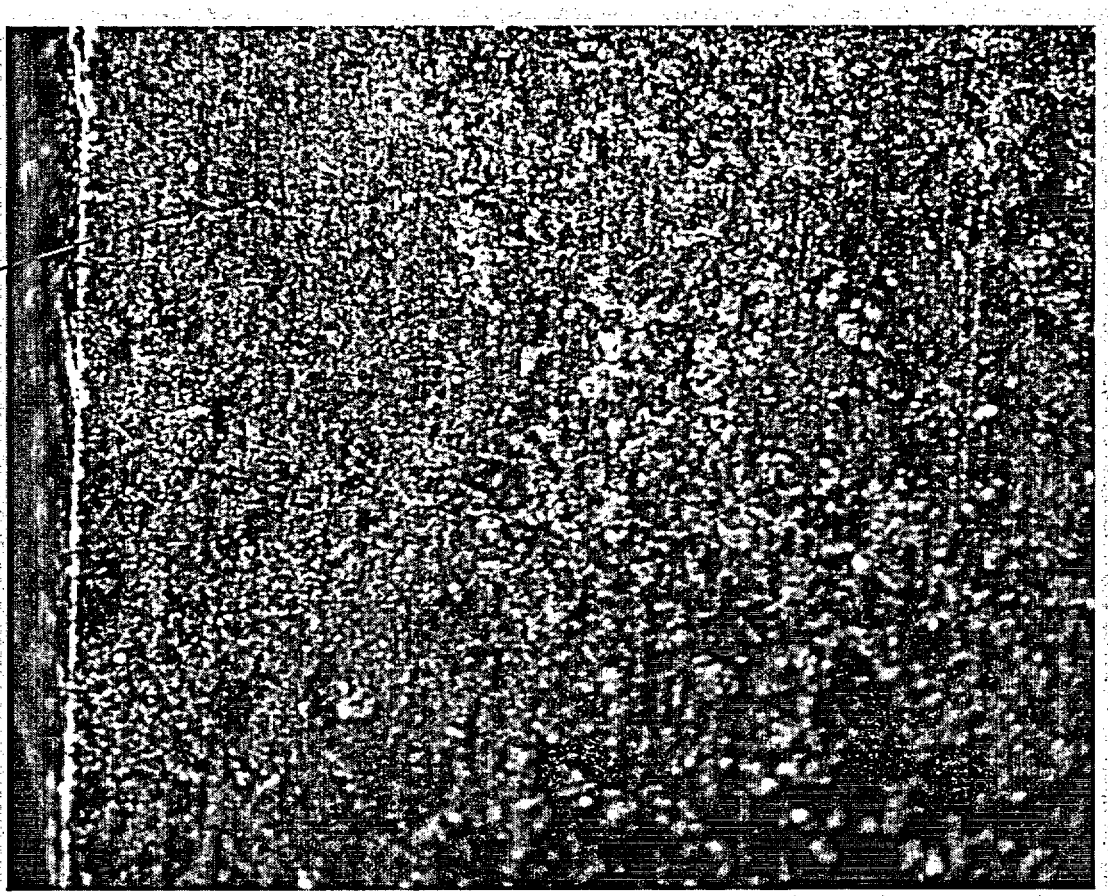

Figure 63. Other half of secondary crack near 25° on R44C45-13A2B3. 83X

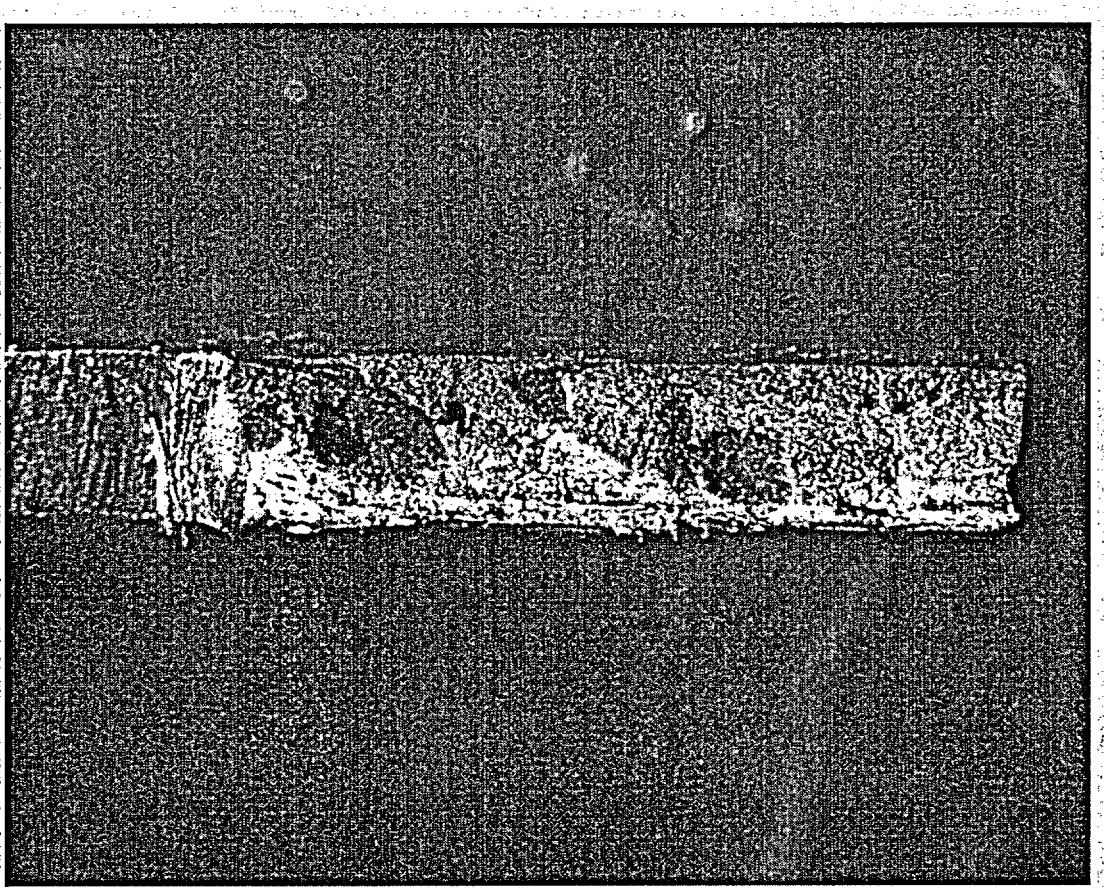

Figure 64. CCW fracture surface of lower half of section through crack at 25° on R44C45 in 2H TSP. 16.6X

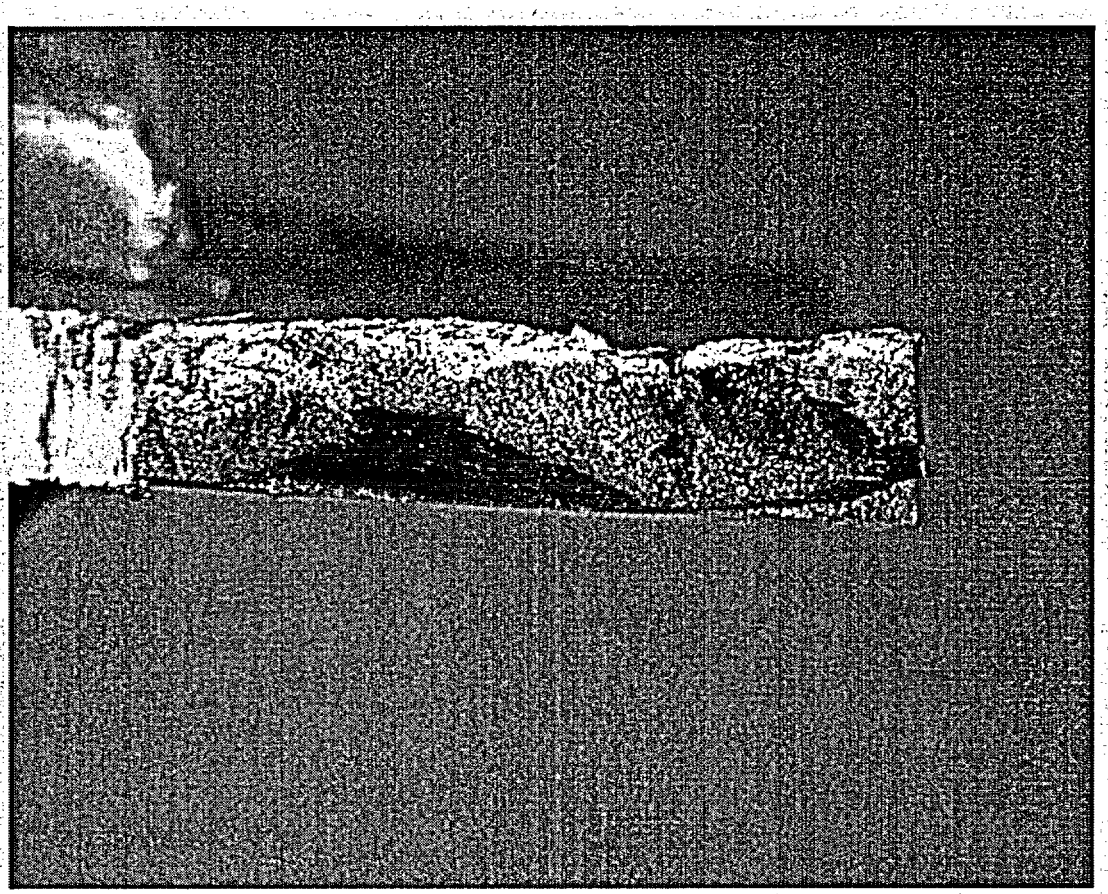

Figure 65. CW fracture surface of lower half of section through crack at 25° on R44C45 in 2H TSP. 16.6X

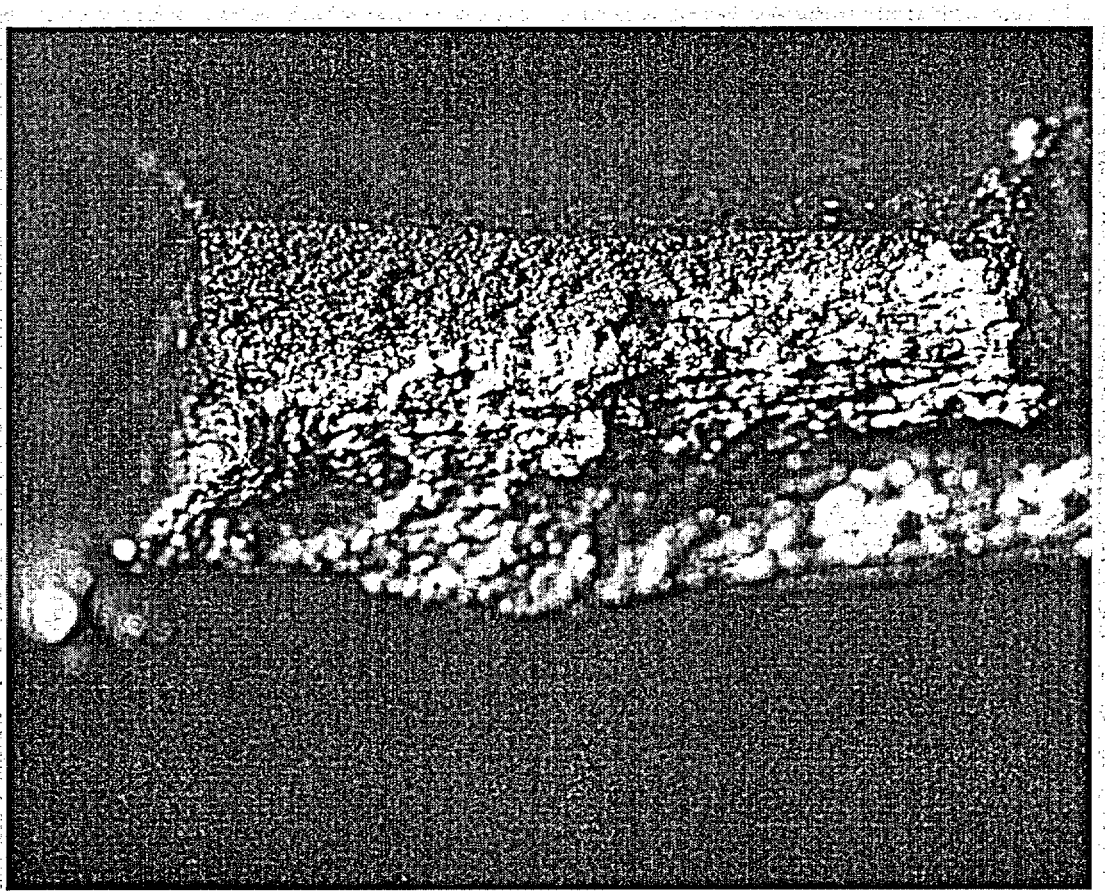

Figure 66. CCW fracture surface of upper half of section through crack at 25° on R44C45 in 2H TSP.

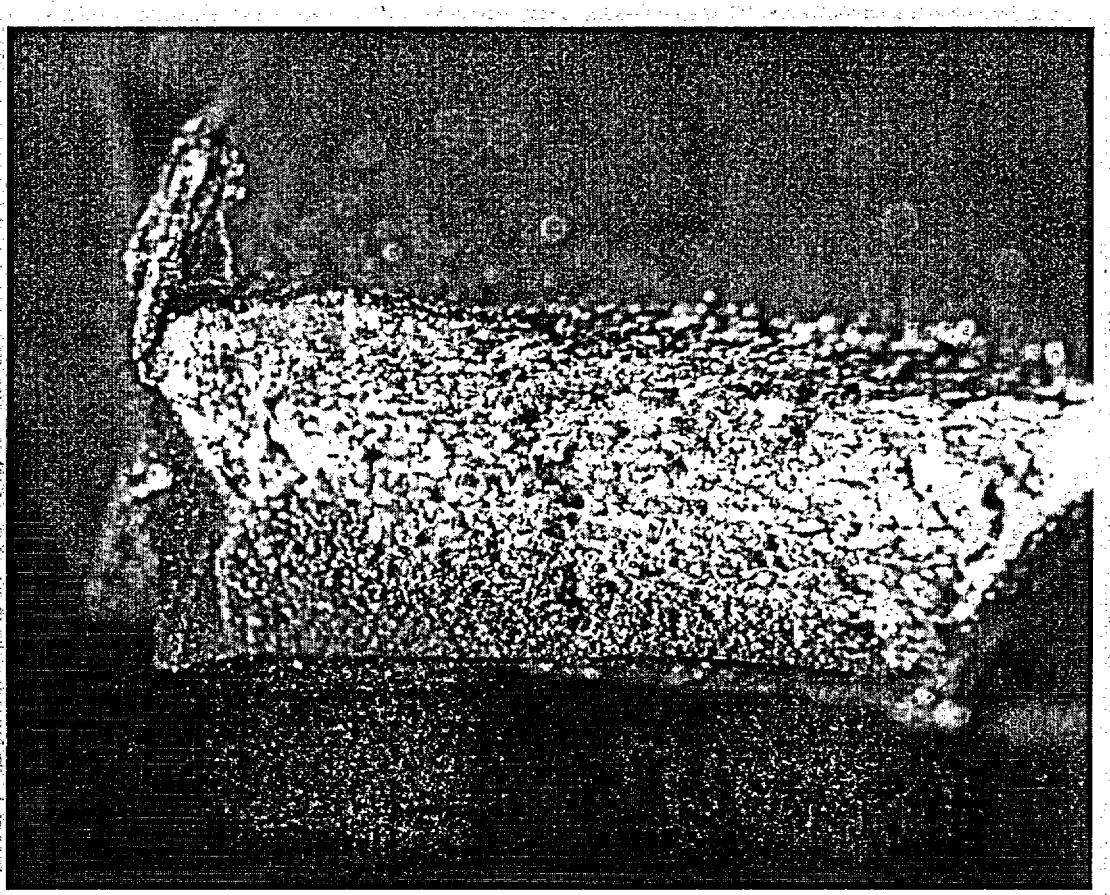

Figure 67. CW fracture surface of upper half of section through crack at 25° on R44C45 in 2H TSP.

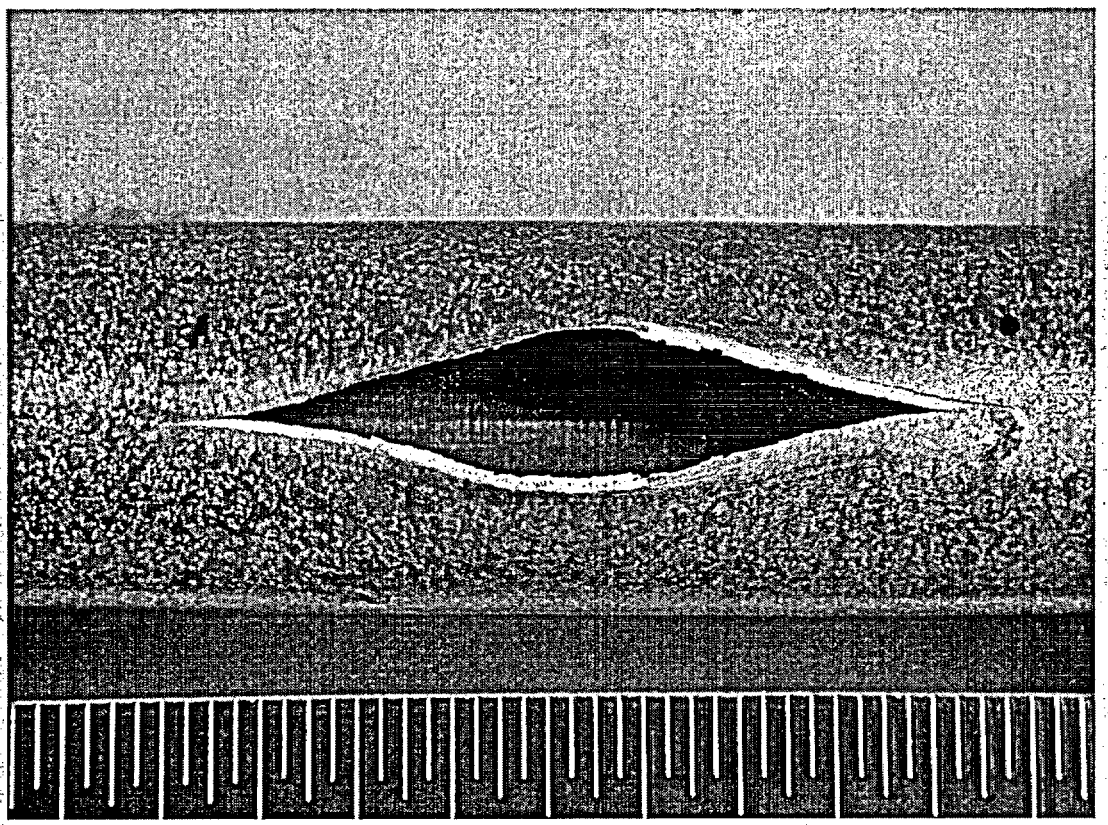

Figure 68. Free span burst region on R44C45-13B2. 2.1X

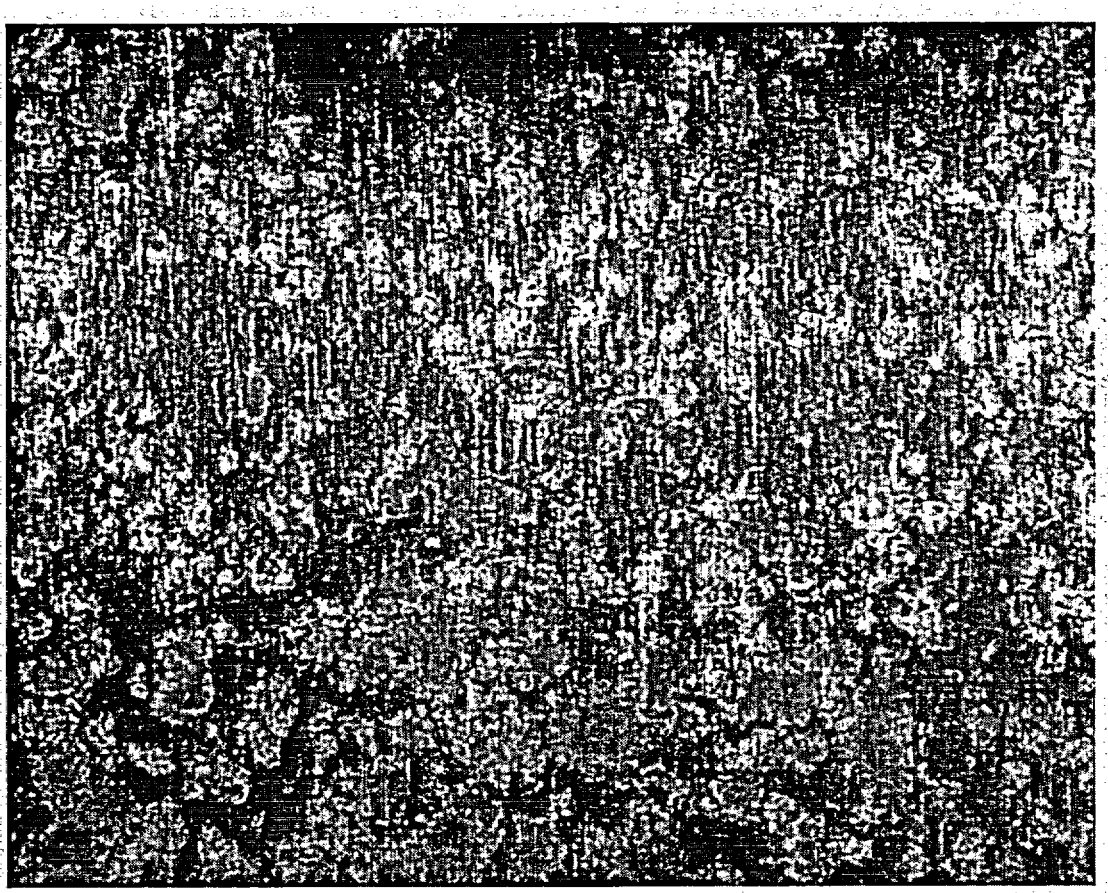

Figure 69. Typical mottled deposits on R44C45-13B2 after burst testing. 12X

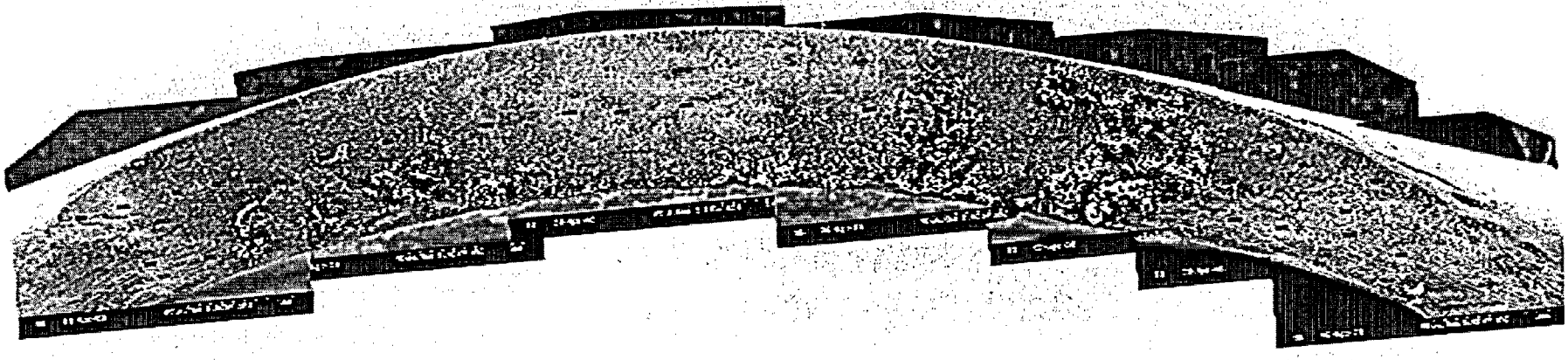

Bottom

Figure 70. Overall mosaic of R35C57-8B2B. SE 20X

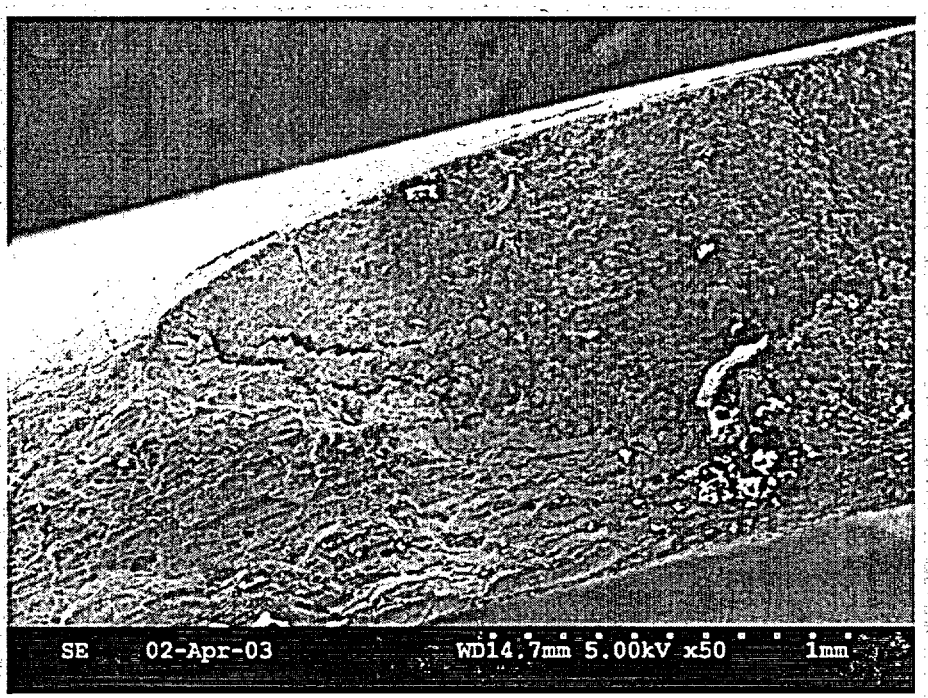

Figure 71. Bottom edge of IGSCC region on R35C57-8B2B.

SE 50X

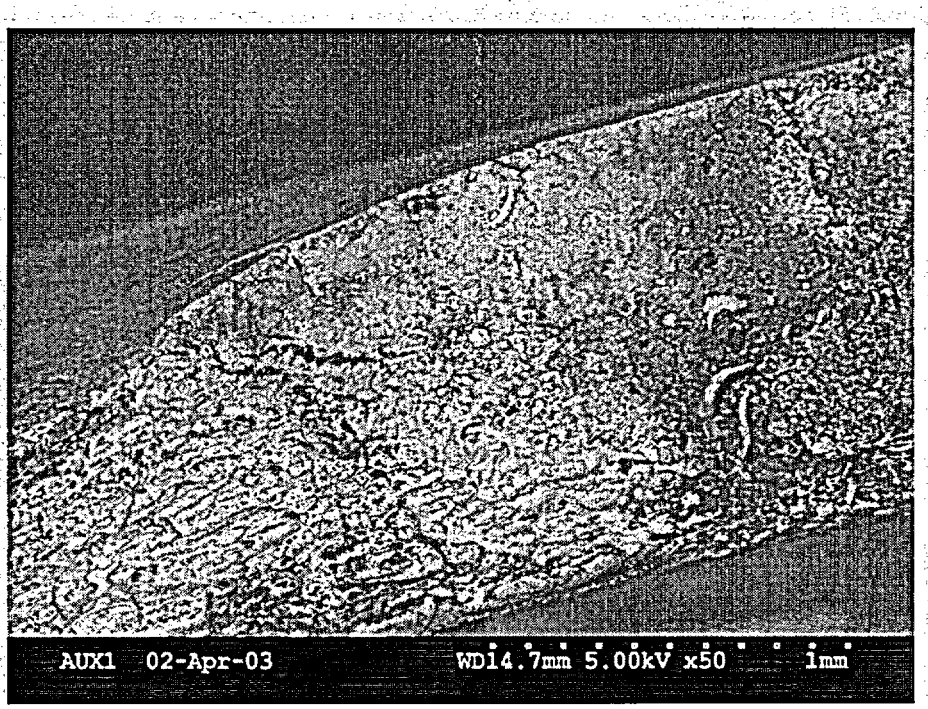

Figure 72. Bottom edge of IGSCC region on R35C57-8B2B.

BSE 50X

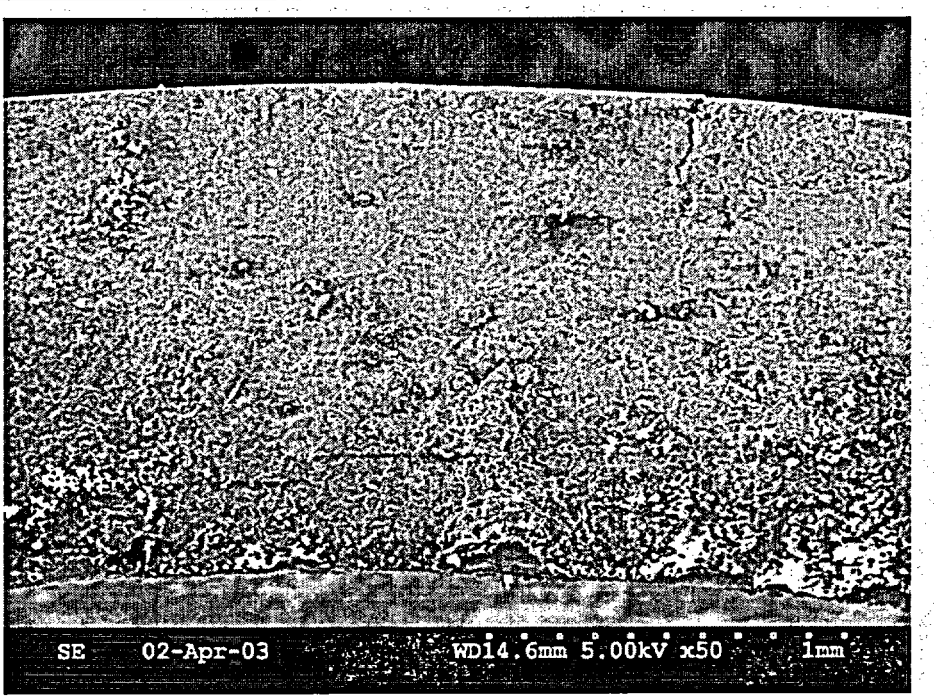

Figure 73. Near center of IGSCC region on R35C57-8B2B.

SE 50X

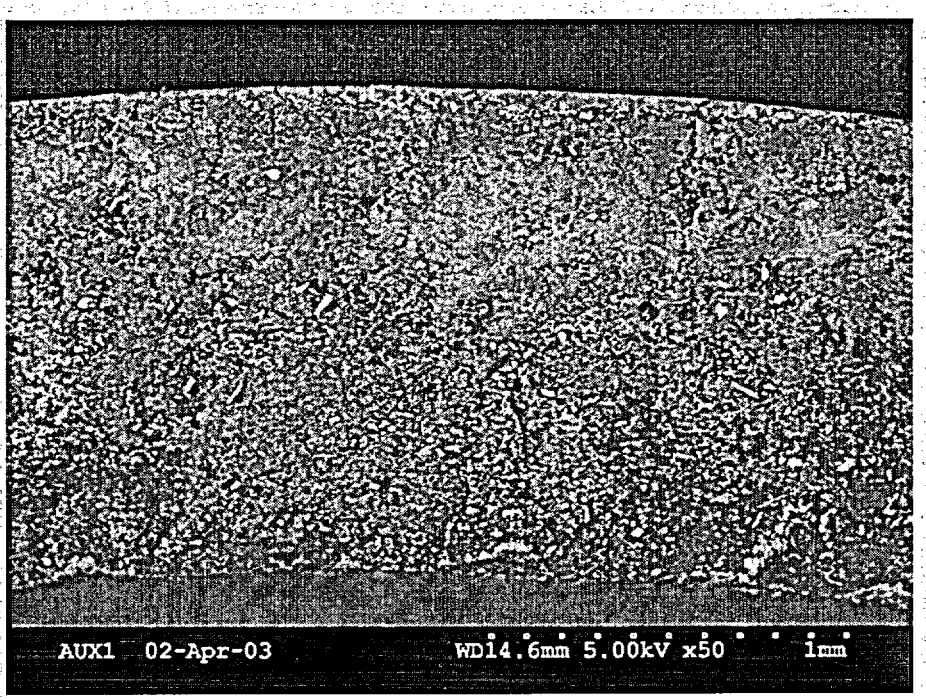

Figure 74. Near center of IGSCC region on R35C57-8B2B.

BSE 50X

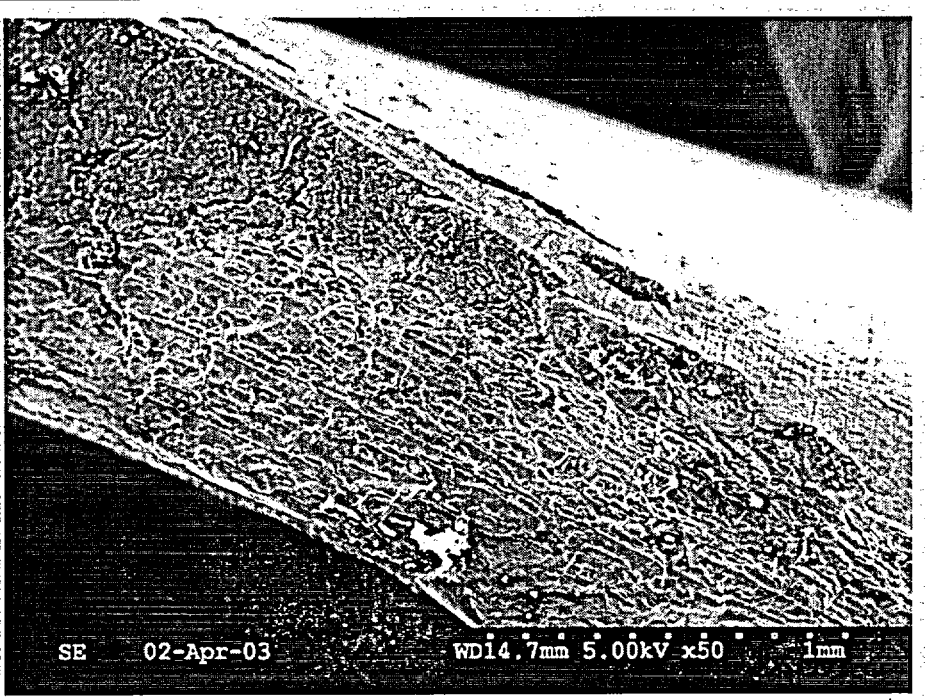

Figure 75. Near top edge of IGSCC region on R35C57-8B2B.

SE 50X

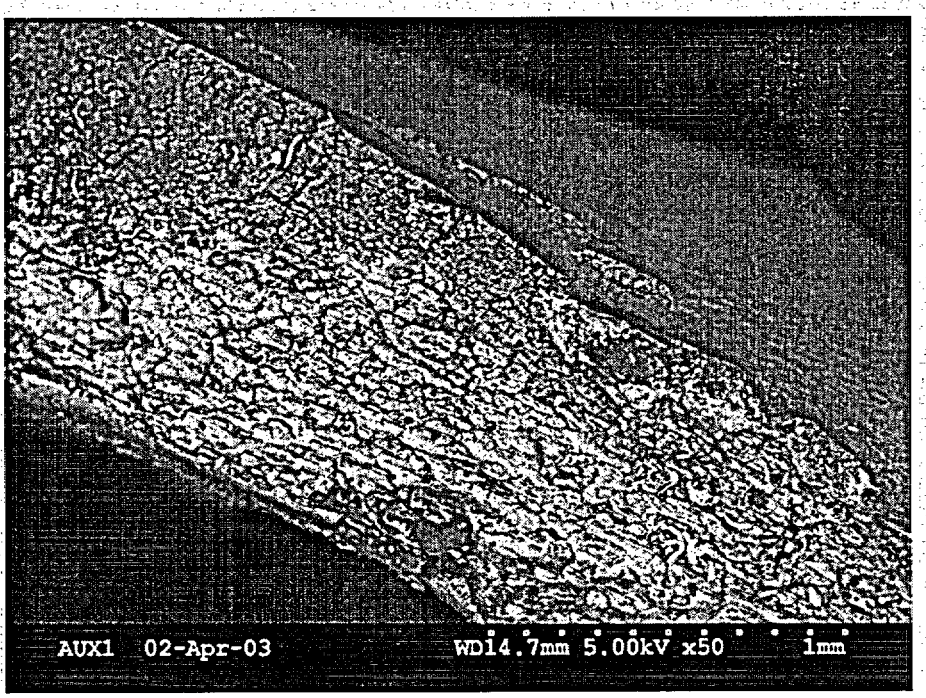

Figure 76. Near top edge of IGSCC region on R35C57-8B2B.

BSE 50X

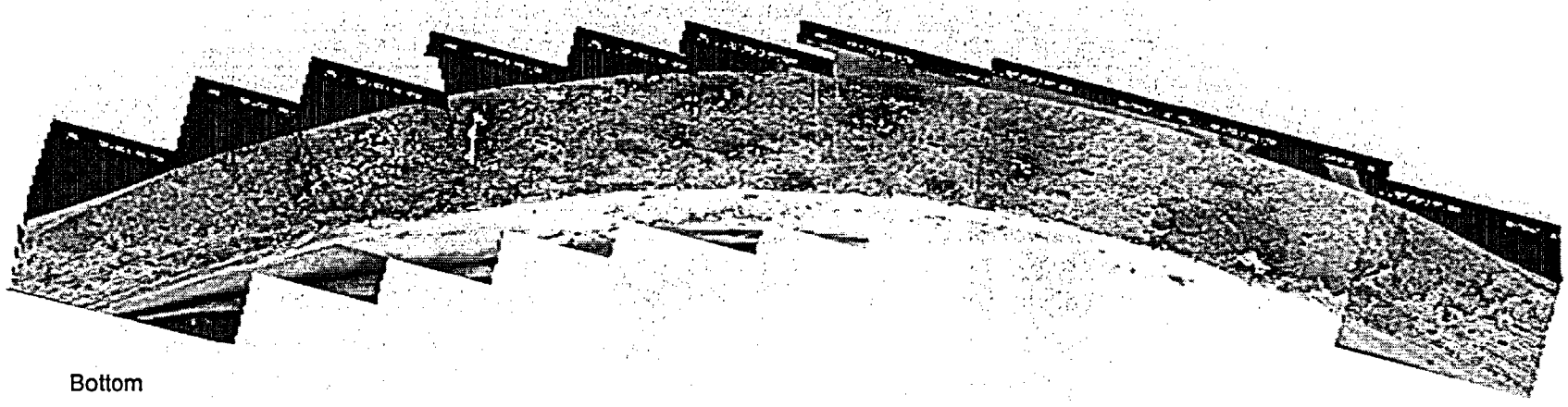

Figure 77. Overall mosaic of R44C45-13A2B1. SE 14X

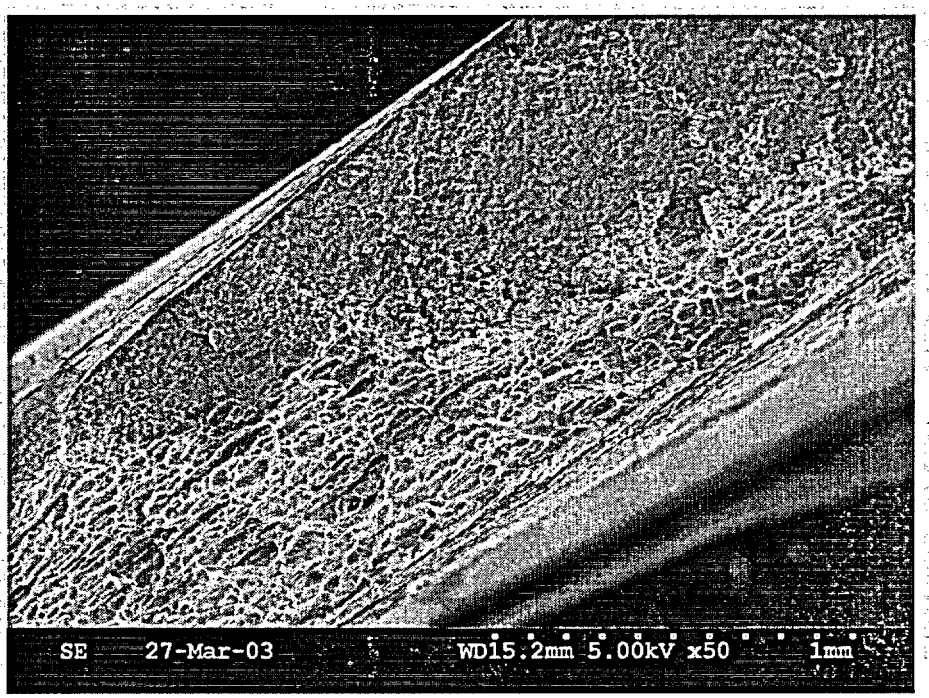

Figure 78. Bottom edge of IGSCC region on R44C45-13A2B1. SE 50X

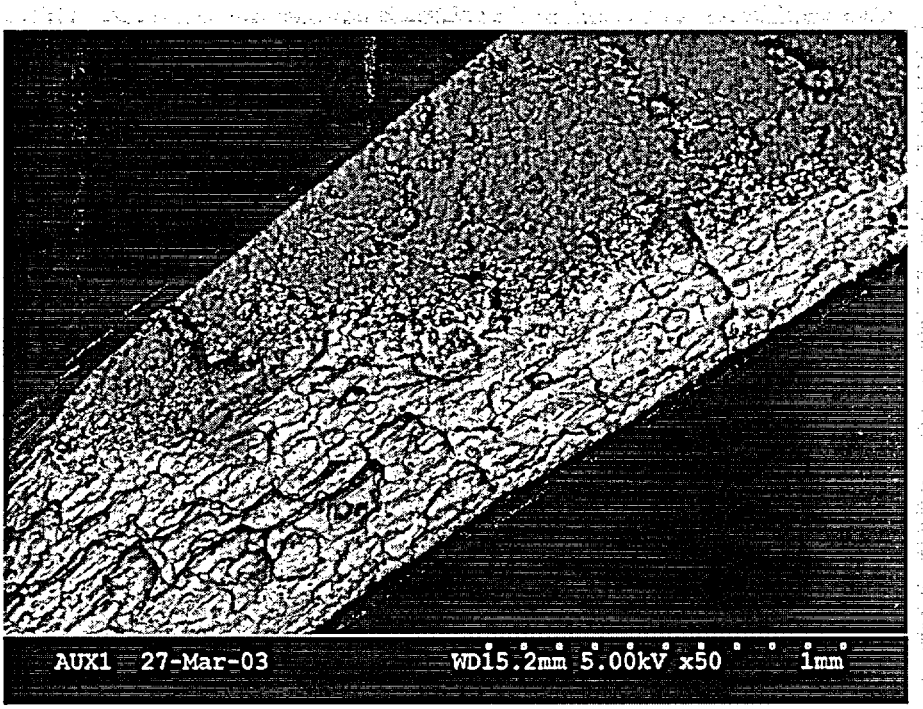

Figure 79. Bottom edge of IGSCC region on R44C45-13A2B1. BSE 50X

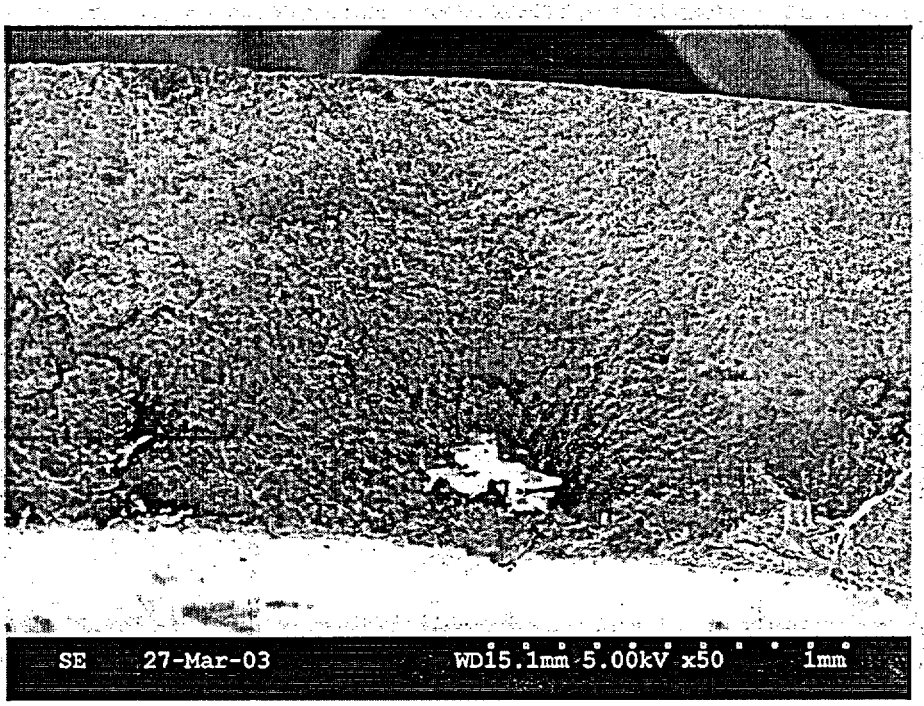

Figure 80. Near center of IGSCC region on R44C45-13A2B1.
SE 50X

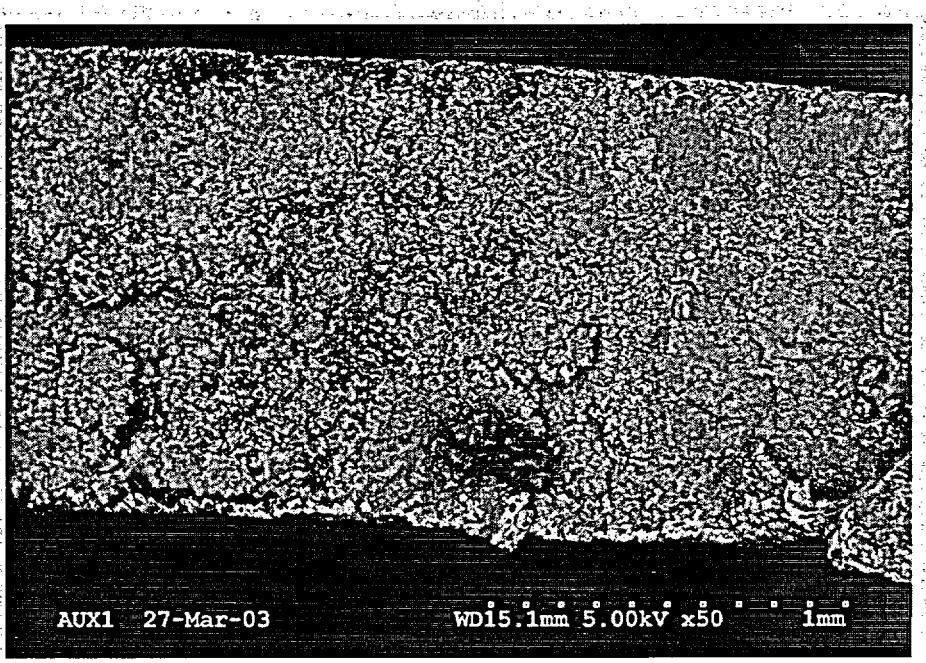

Figure 81. Near center of IGSCC region on R44C45-13A2B1.
BSE 50X

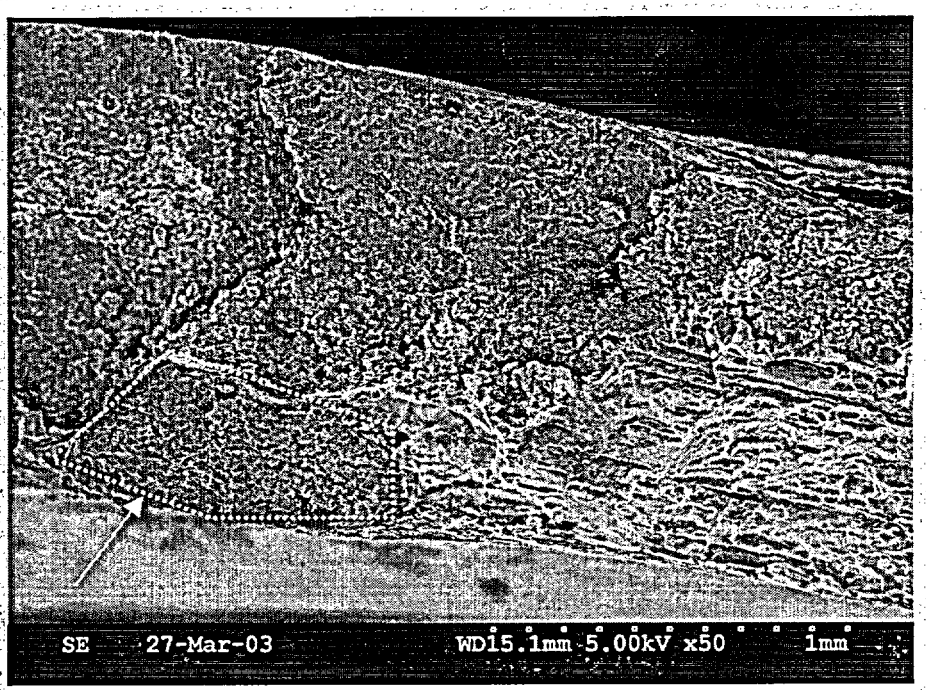

Figure 82. Near top edge of IGSCC region on R44C45-13A2B1. An out-of-plane small crack is indicated by the white arrow and boxed-in region.

SE 50X

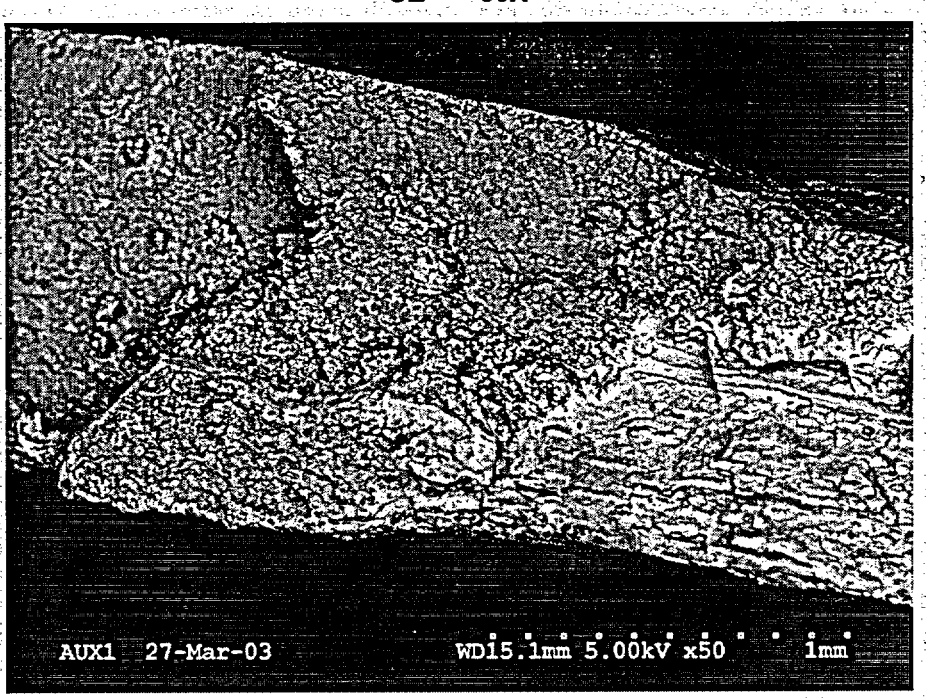

Figure 83. Near top edge of IGSCC region on R44C45-13A2B1.

BSE 50X

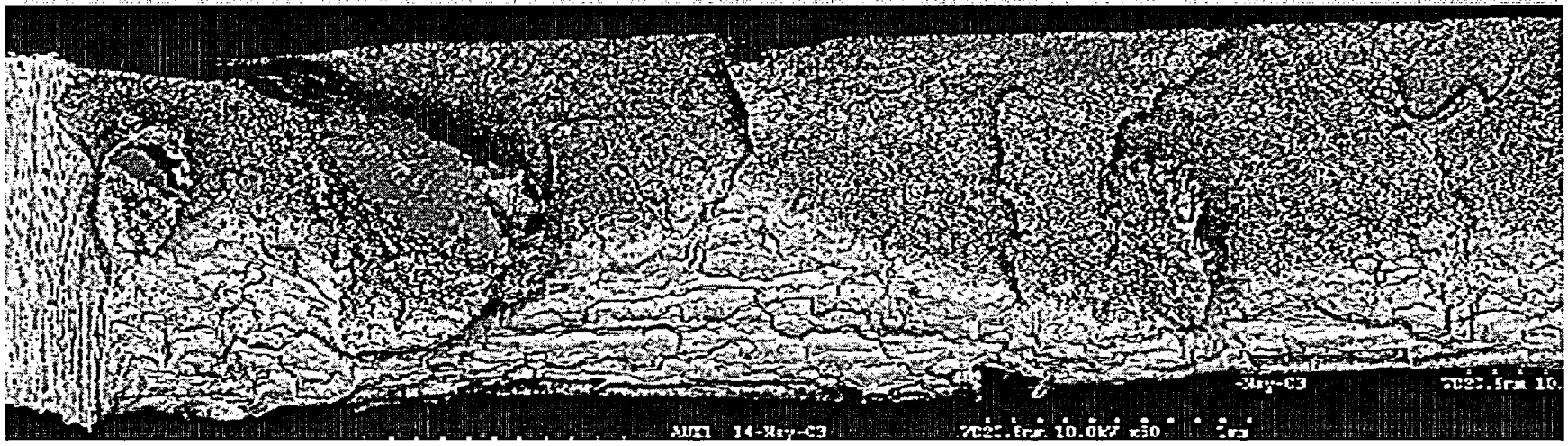

Figure 84a. Overall BSE mosaic of R44C45-13A2B2A (bottommost section). 36X

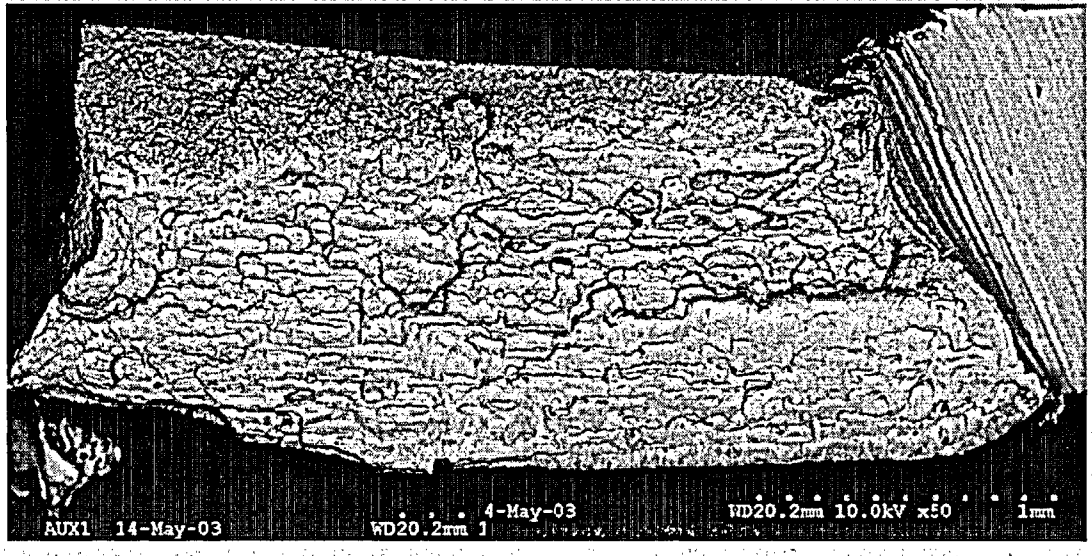

Figure 84b. Overall BSE mosaic of R44C45-13A2B3A (topmost section). 42X

Figure 84. Mosaics of two sections comprising crack at 25° on R44C45

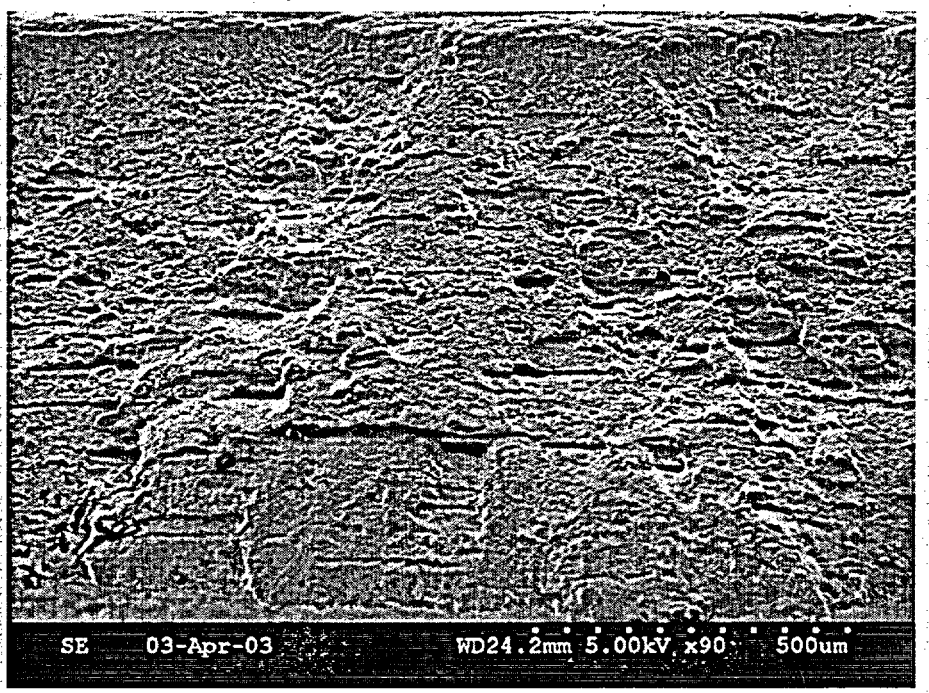

**Figure 85. Typical ductile region on R35C57-9B2A.
SE 90X**

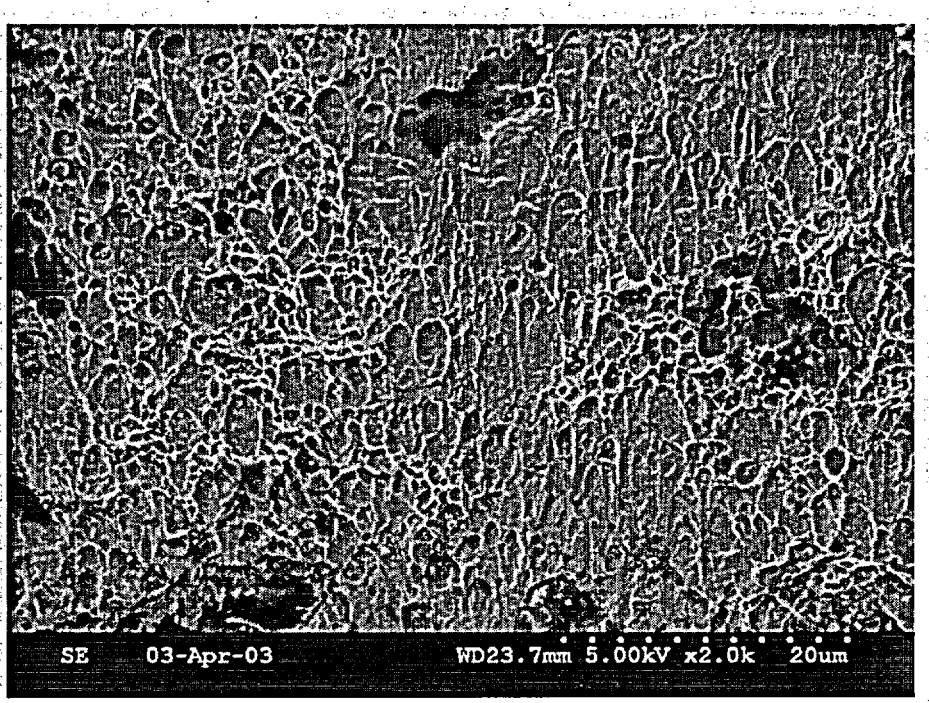

**Figure 86. Typical ductile region on R35C57-9B2A.
SE 2000X**

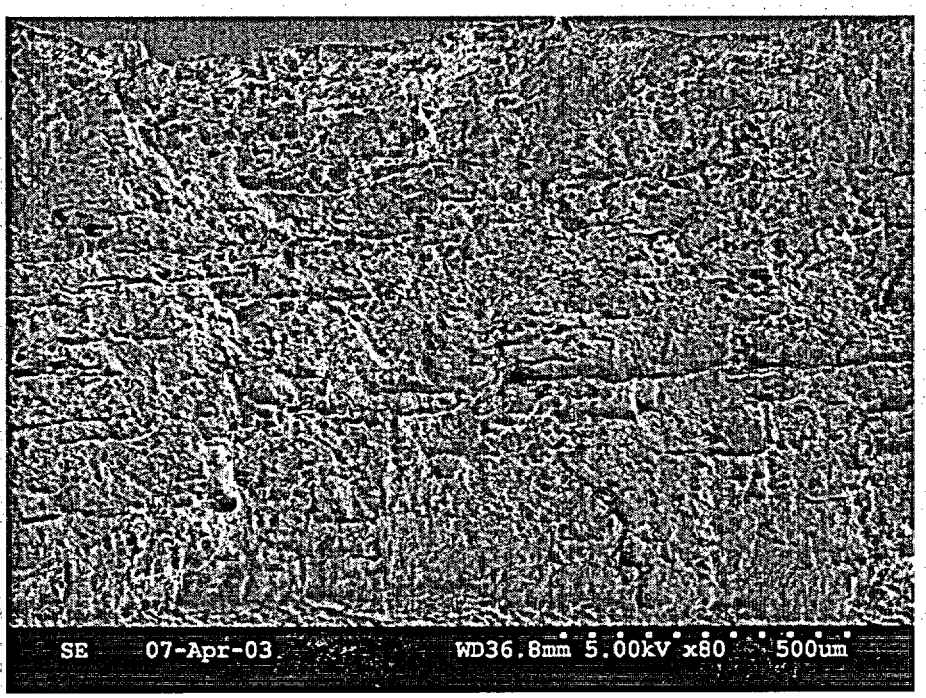

Figure 87. Typical ductile region on R44C45-13B2B1.
SE 80X

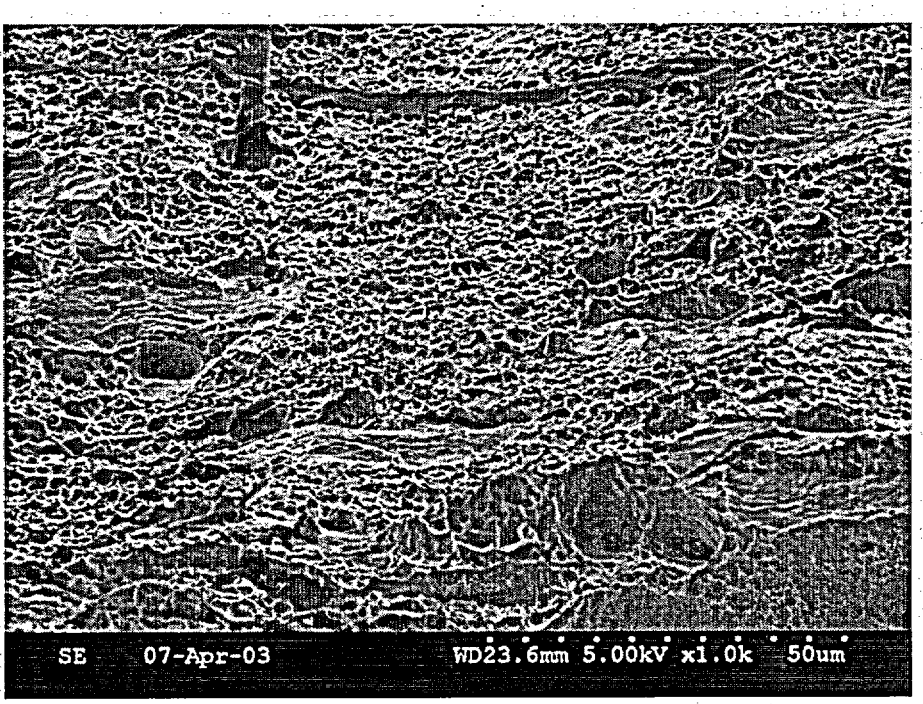

Figure 88. Typical ductile region on R44C45-13B2B1.
SE 1000X

Figure 89. Typical OD wall near burst rupture on R35C57-8B2B. WDS performed on Area 1. BSE 250X

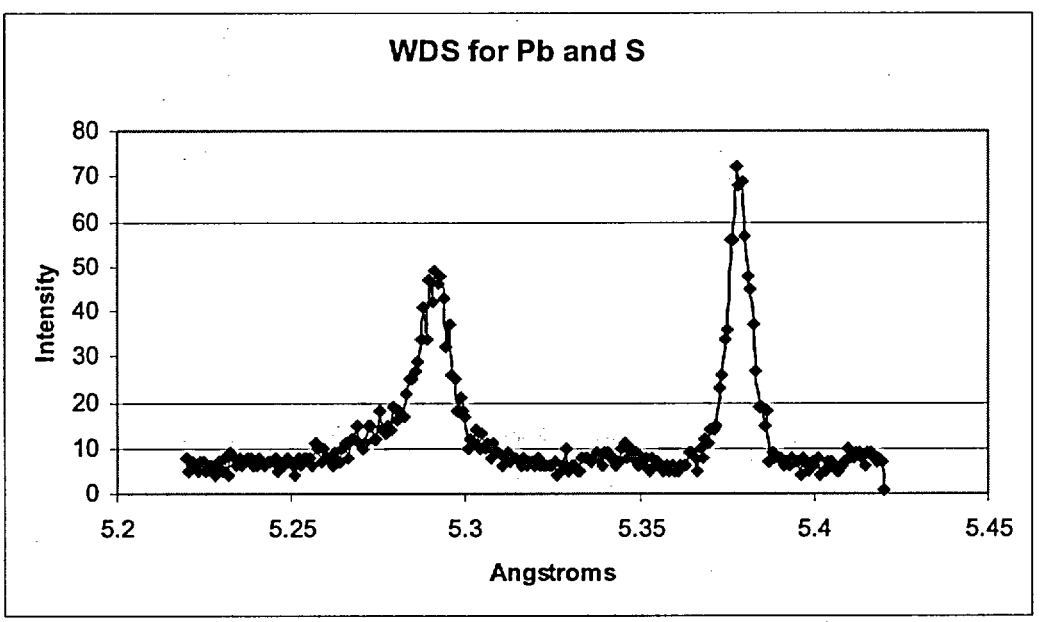

Figure 90. WDS of Area 1 in Figure 89. Main peak is sulphur (5.3722 A°) and secondary peak is lead (5.286 A°).

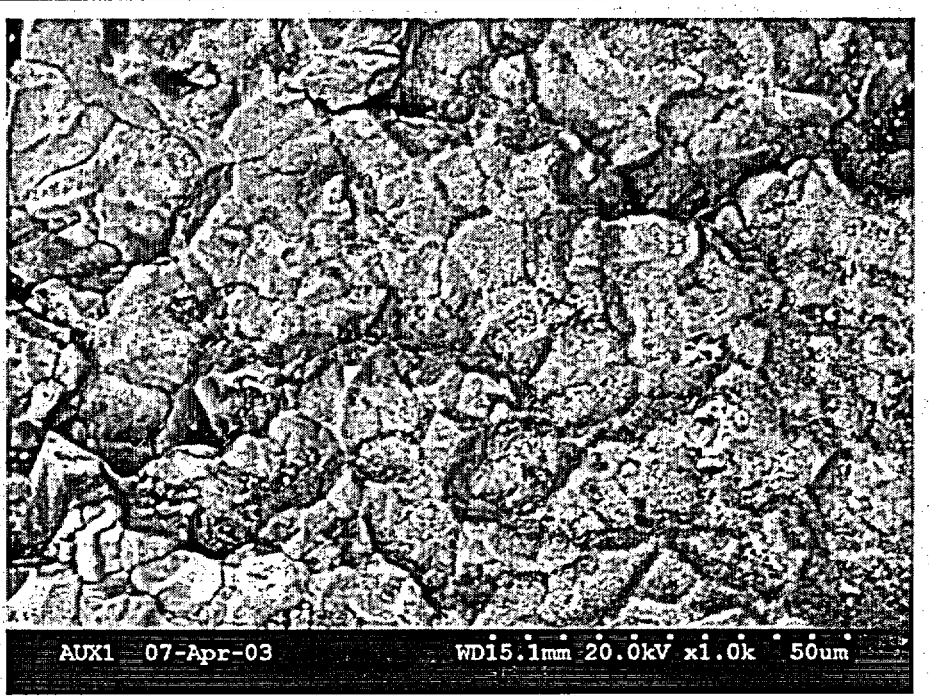

Figure 91. Typical IGSCC on R35C57-8B2B rupture surface. BSE 1000X

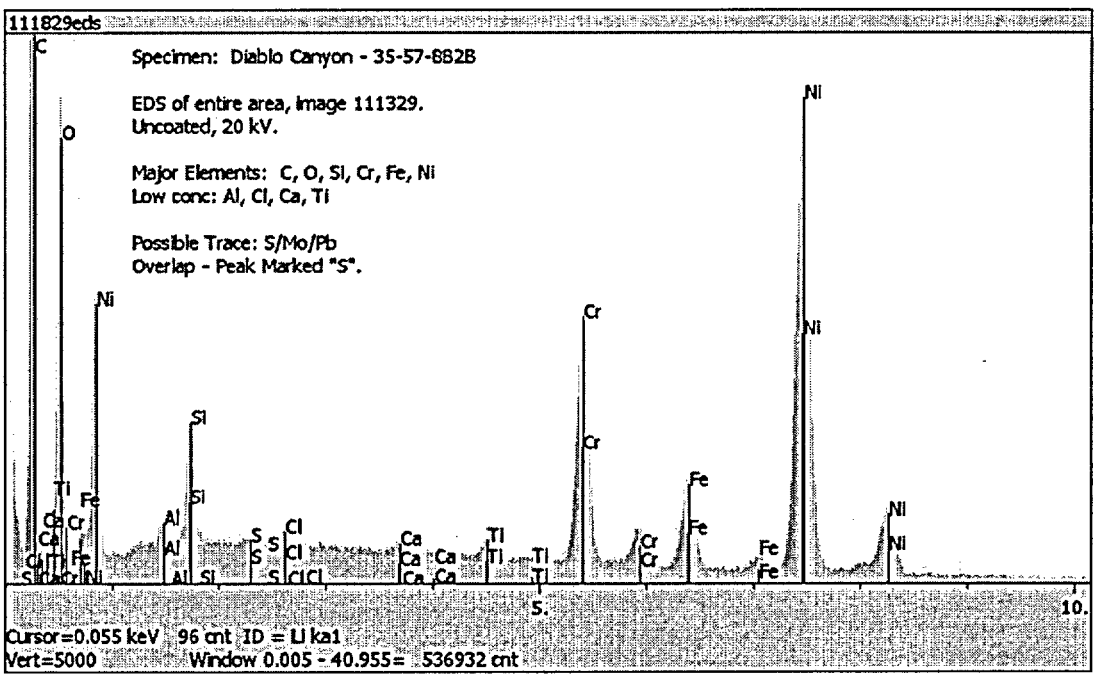

Figure 92. EDS of entire IGSCC area in Figure 91.

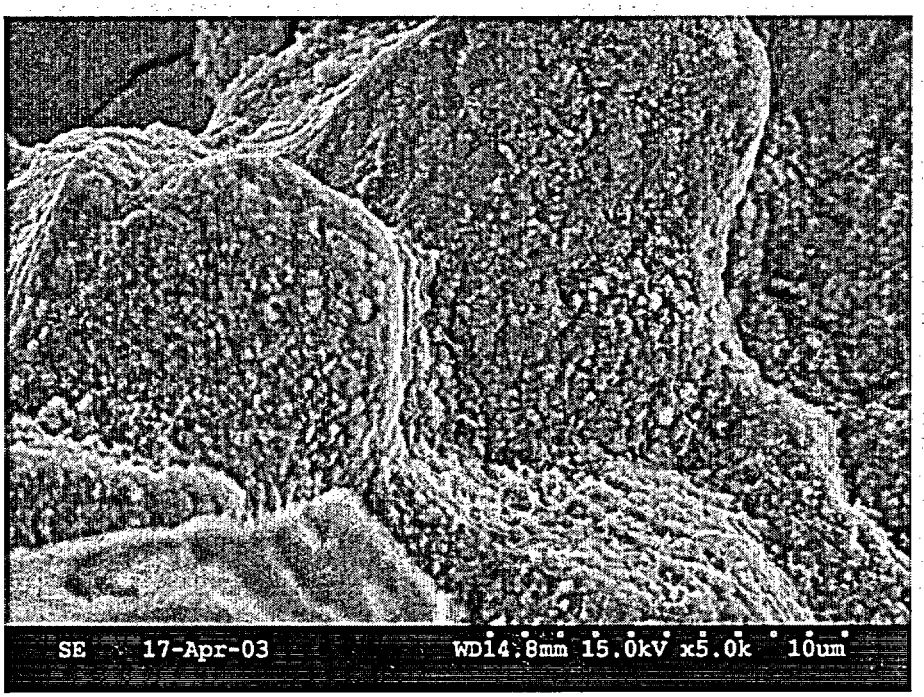

Figure 93. Area on rupture surface of R35C57-8B2B used for WDS analysis for lead and sulphur. SE 1000X

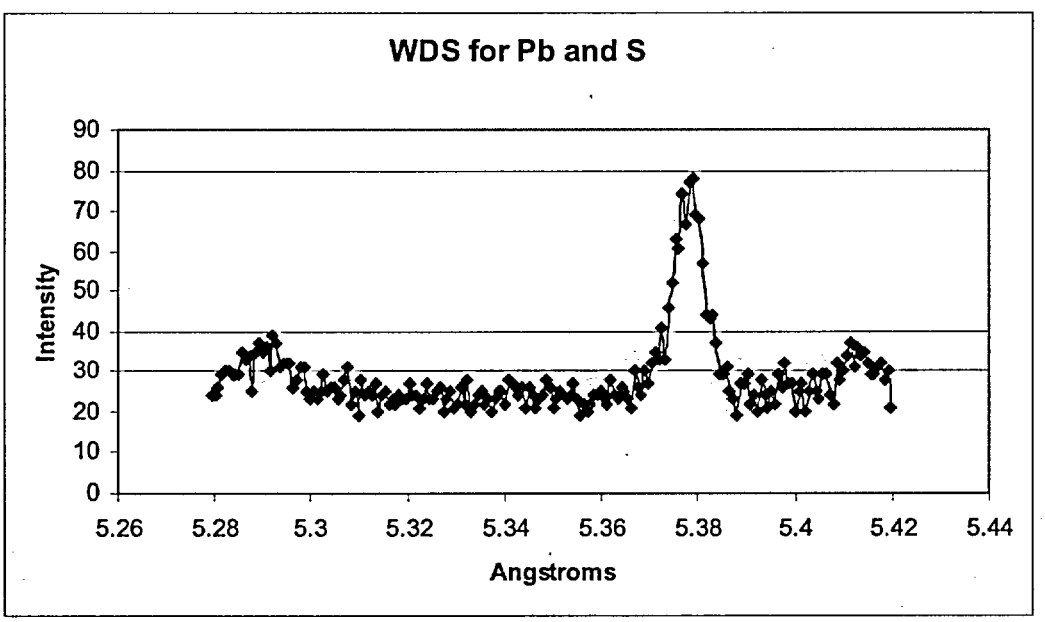

Figure 94. WDS of area in Figure 93. Main peak is sulphur (5.3722 A°) and secondary peak is lead (5.286 A°).

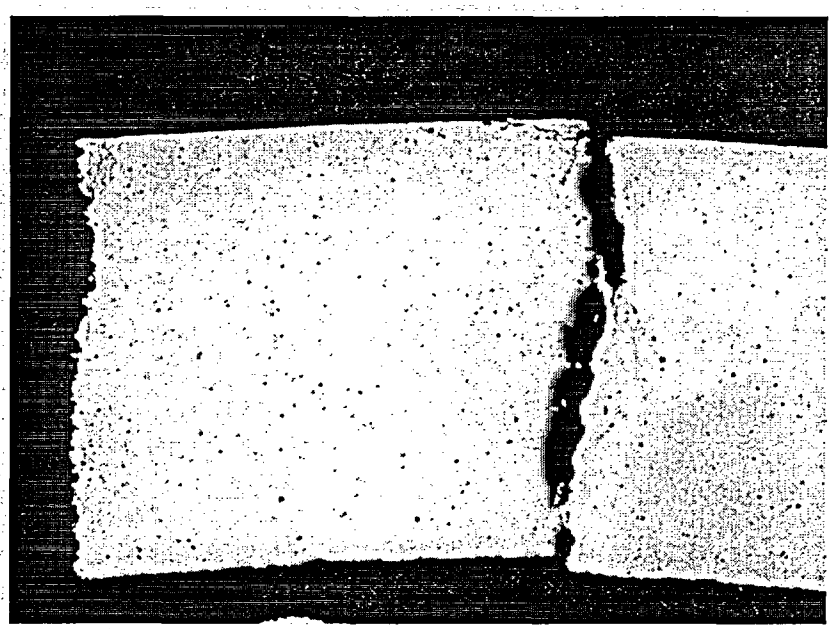

Figure 95. Rupture surface (170°) and secondary through wall crack (180°) on R35C57-8B2B. 46X

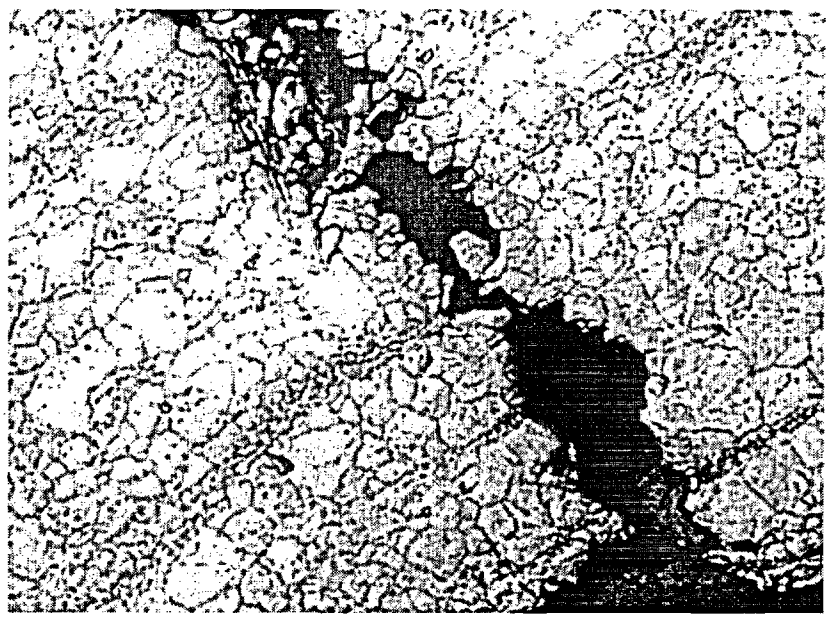

Figure 96. Etched microstructure of secondary crack on ID surface of R35C57-8B2B. 480X

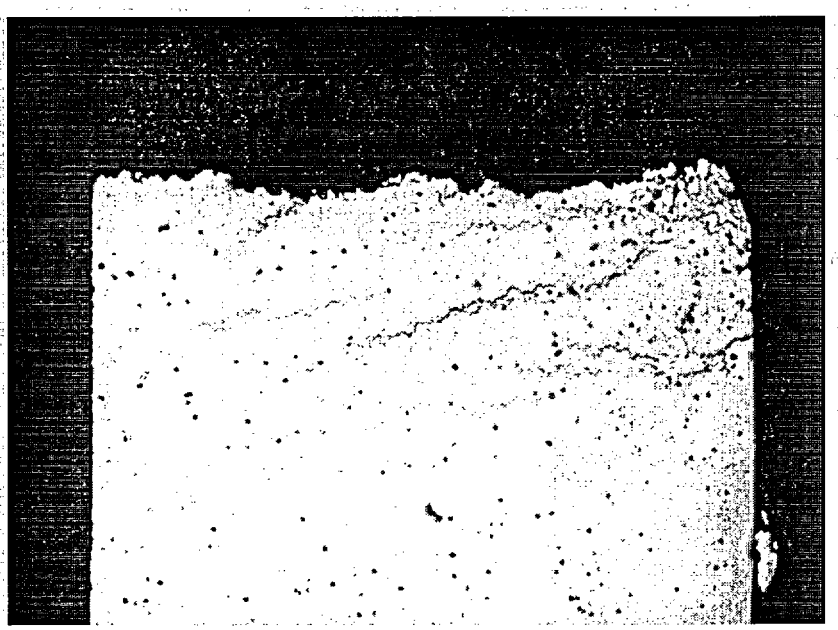

Figure 97. Secondary cracking near rupture surface of R44C45-13A2B2. 75X

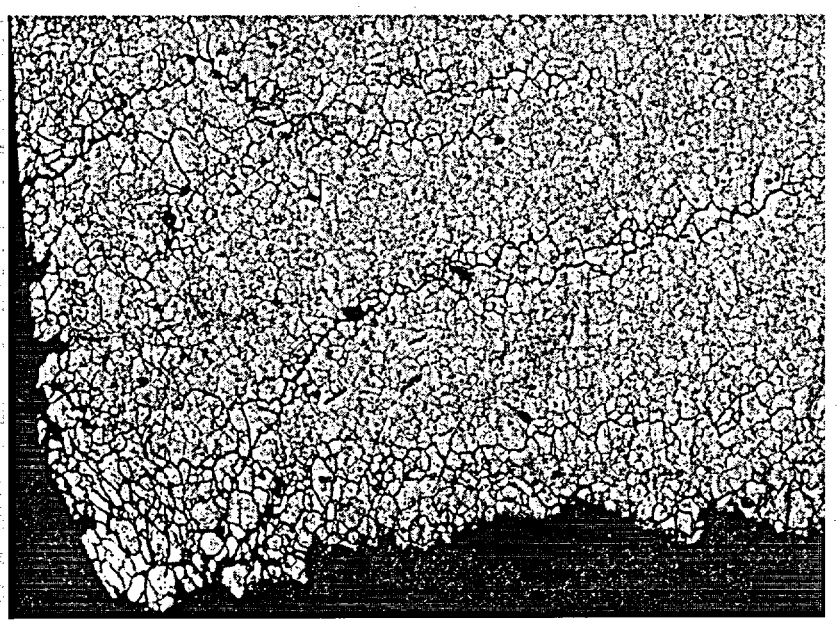

Figure 98. Etched microstructure near rupture surface on R44C45-13A2B2. 189X

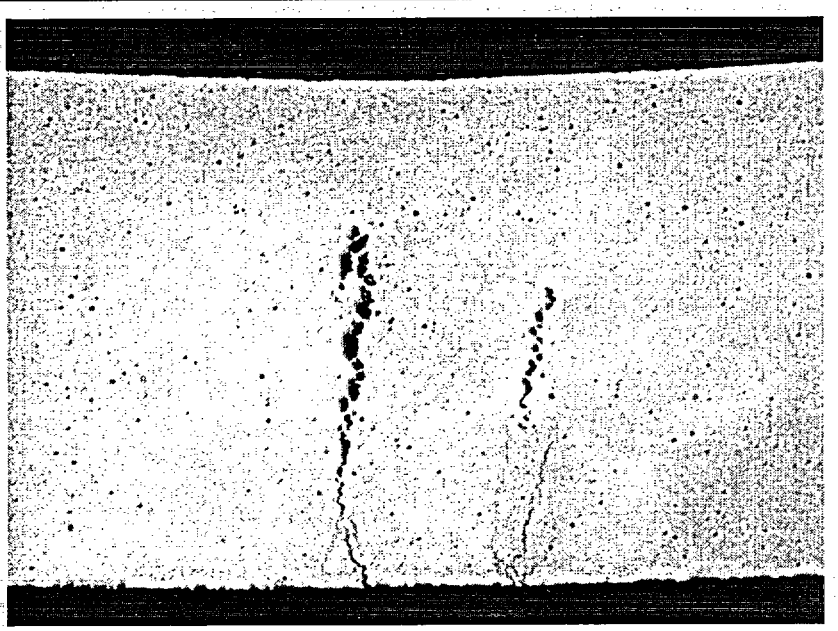

Figure 99. Secondary cracks on R44C45-13A2B2 near 25°. 58X

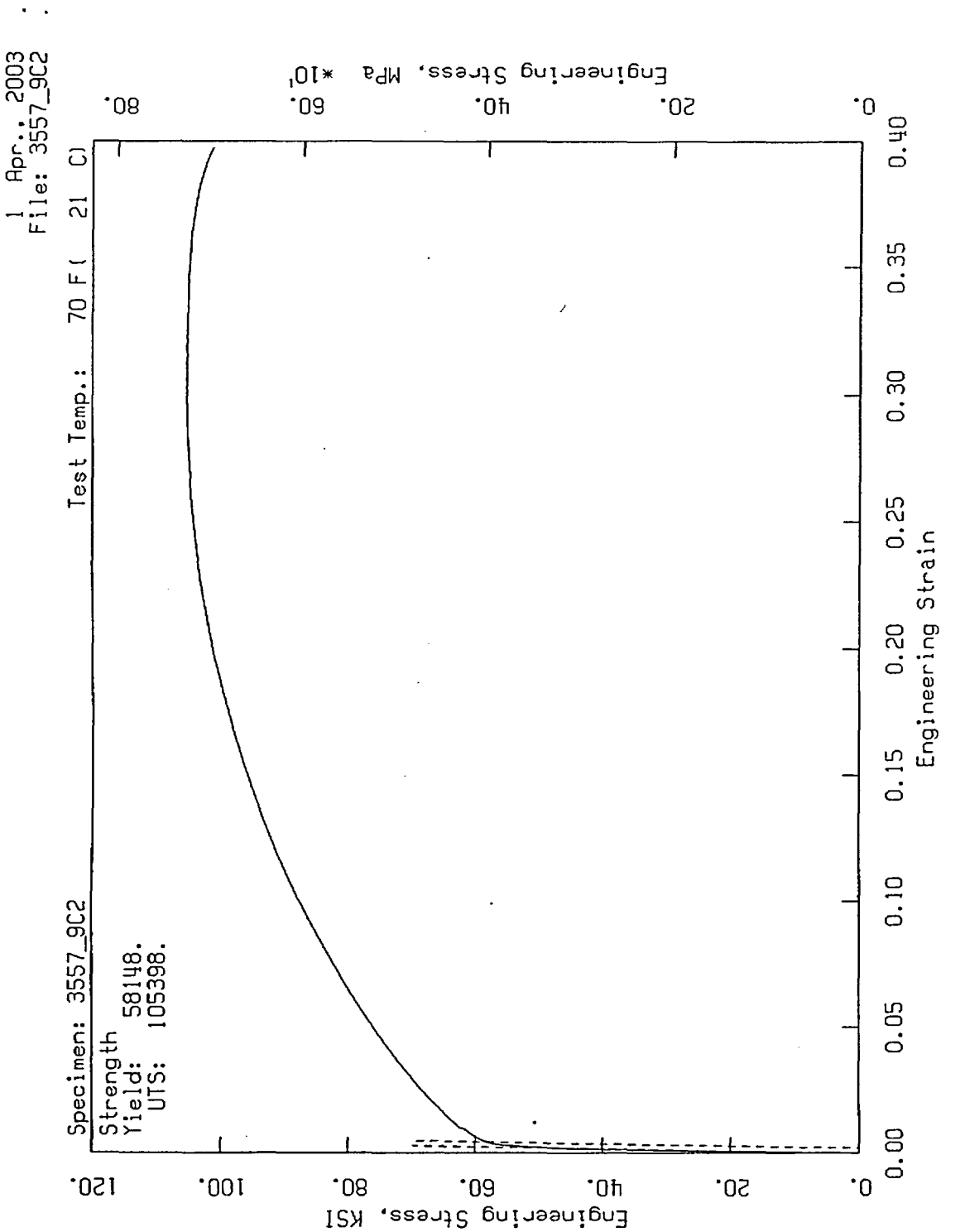

Figure 100. Engineering Stress/Strain Curve for R35C57-9C2

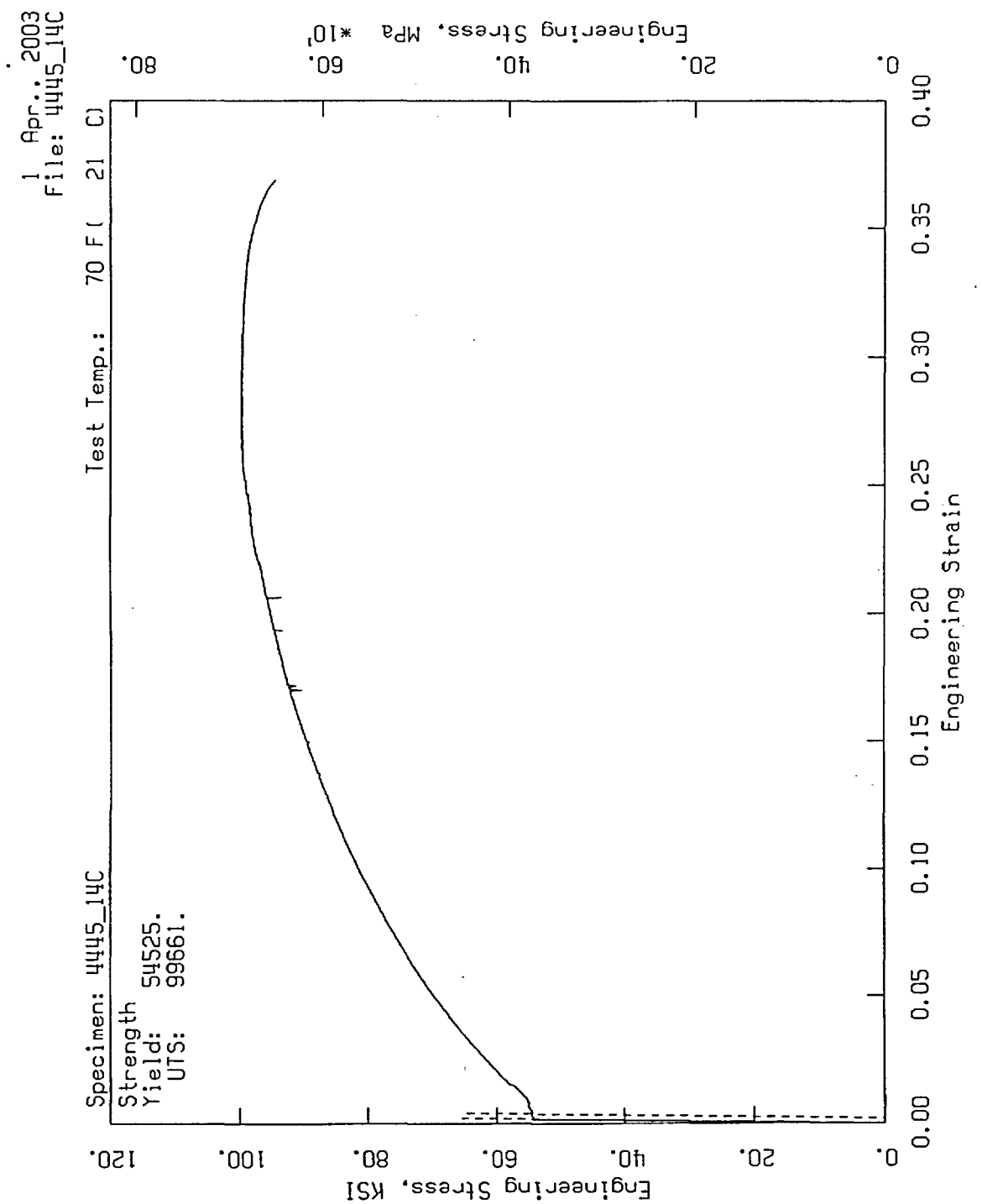

Figure 101. Engineering Stress/Strain Curve for R44C45-14C

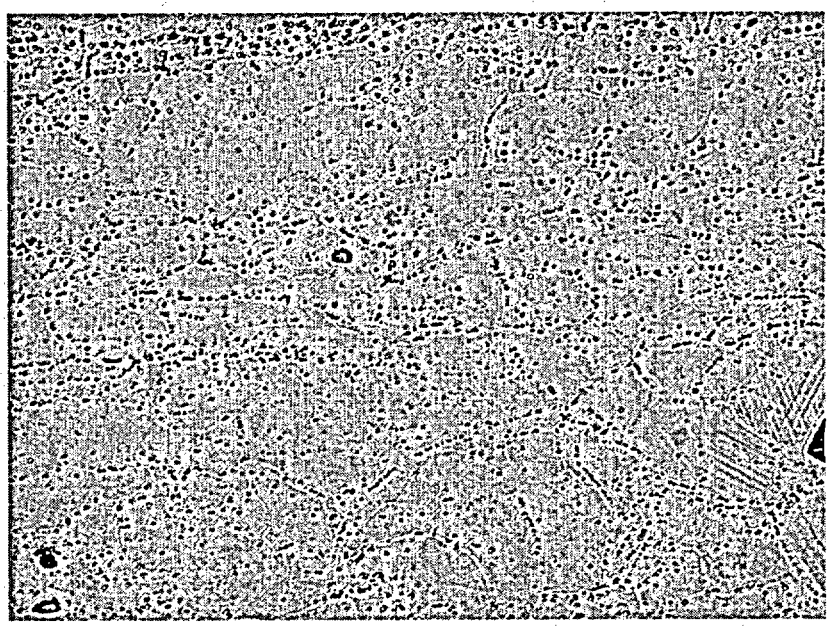

Figure 102. Carbide distribution in R35C57-9C3B1. 685X

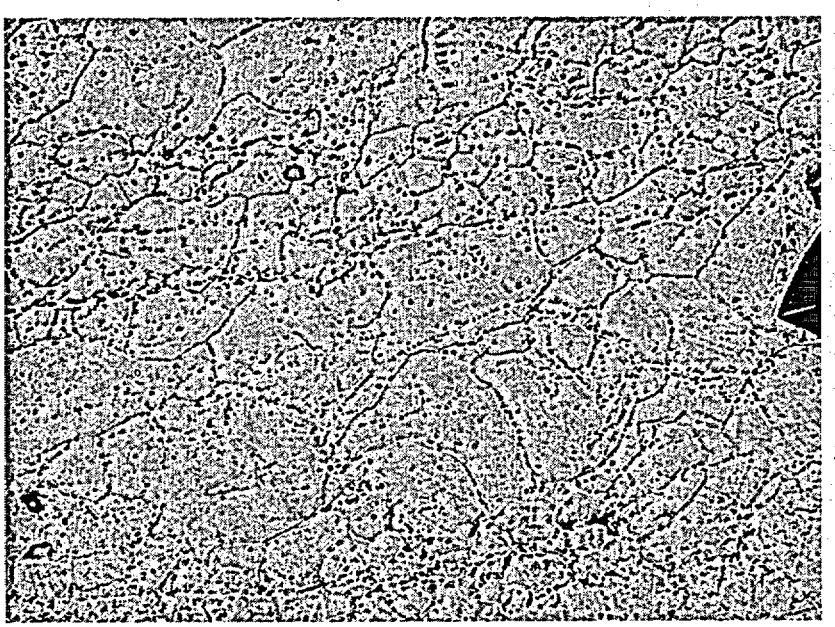

Figure 103. Grain boundary and carbide distribution in R35C57-9C3B1. 685X

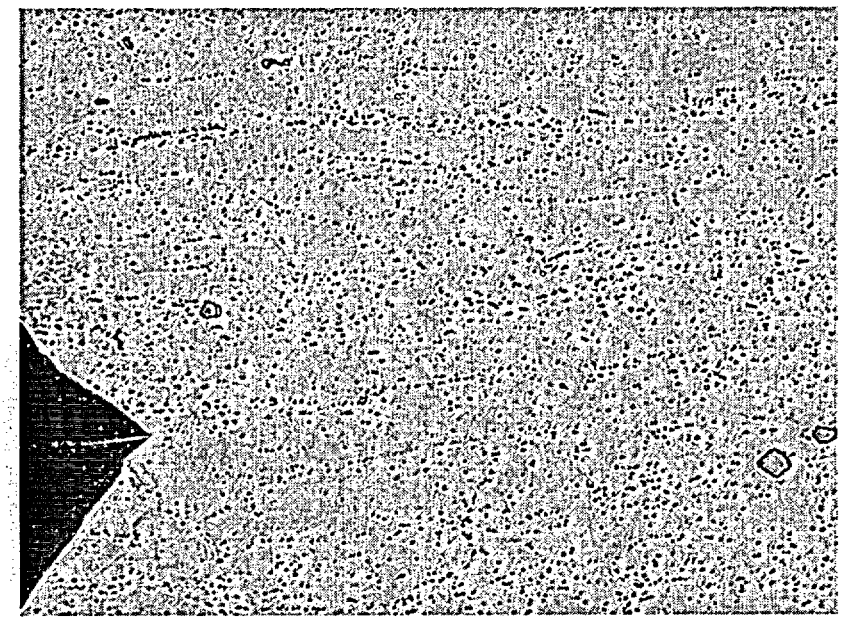

Figure 104. Carbide distribution in R44C45-14D2A. 685X

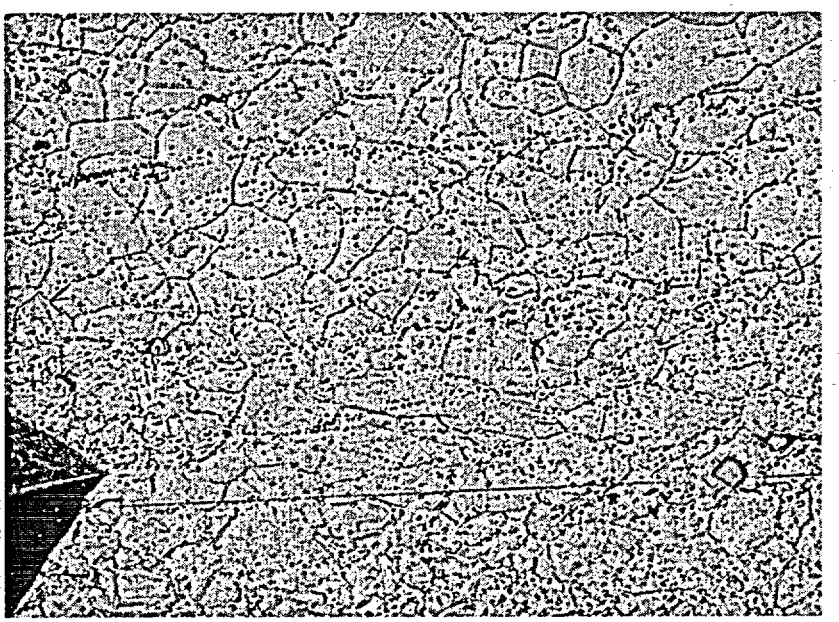

Figure 105. Grain boundary and carbide distribution \
in R44C45-14D2A. 685X

APPENDIX A

Evaluation of Crack Profiles[5]

[5] This evaluation was included as Sections 4.0 and 5.0 in FANP Document No. 51-5028414-01, *DCPP 2R11 DE Input Transmittal to Westinghouse*, 5/30/2003.

Crack Profile Results

Following leak rate testing the pulled tube burst test specimens were heated in air at 900°F for 1 hour to oxidize any ductile tearing crack extension that may have occurred at the differential pressures experienced during leak rate testing. Air oxidation at 900°F produces a straw color surface that is easily distinguishable from fresh ductile tearing surfaces. Following burst testing, the burst surfaces were examined via scanning electron spectroscopy (SEM). This allowed measurement of the crack profiles generated by intergranular cracking in service. Initially, the back scatter mode in the SEM was used to estimate areas of ductile tearing that were heavily oxidized, thus indicating the extent of ductile tearing during leak rate testing. Since optical stereo microscopy was used to benchmark acceptable oxidizing conditions (Ref. 3), a review and re-evaluation of suspected oxidized ductile tearing areas from SEM results was performed using optical stereo microscopy. These benchmarked optical results provide the best evaluation of ductile tearing during leak rate testing. Crack profiles for tubes 35-57 and 44-45 are shown in Figures 1 and 2. No ductile tearing during leak rate testing was observed for tube 35-47. A small patch of ductile tearing during leak rate testing was observed for tube 44-45. Tables 5 and 6 list the crack profile results. These tables include a re-evaluation of the extent of intergranular from SEM fractographs. They confirm the original results with only minor variation and are plotted in terms of %TW rather than absolute depth. The depth measurements were taken from photographic montages. The wall thickness was evident from locations of 100% TW cracking.

Both optical macrographs and SEM fractographs do not convey true nature of surface roughness both axially and through the wall thickness. Optical stereo microscopy shows that individual crack segments are displaced by about 0.025 inches in the hoop direction. Individual crack segments are about 0.10 inches in axial length. Crack segments have joined together by intergranular cracking. This is consistent with a large jump in bobbin voltage from EOC 10 to EOC 11. In tube 44-45, a small overall depth increased led to a throughwall crack length of 0.377 inches. This plus the loss of current paths from cracking of crack segment ligaments explains the large jump in bobbin (and Plus Point) voltage.

Figure 1

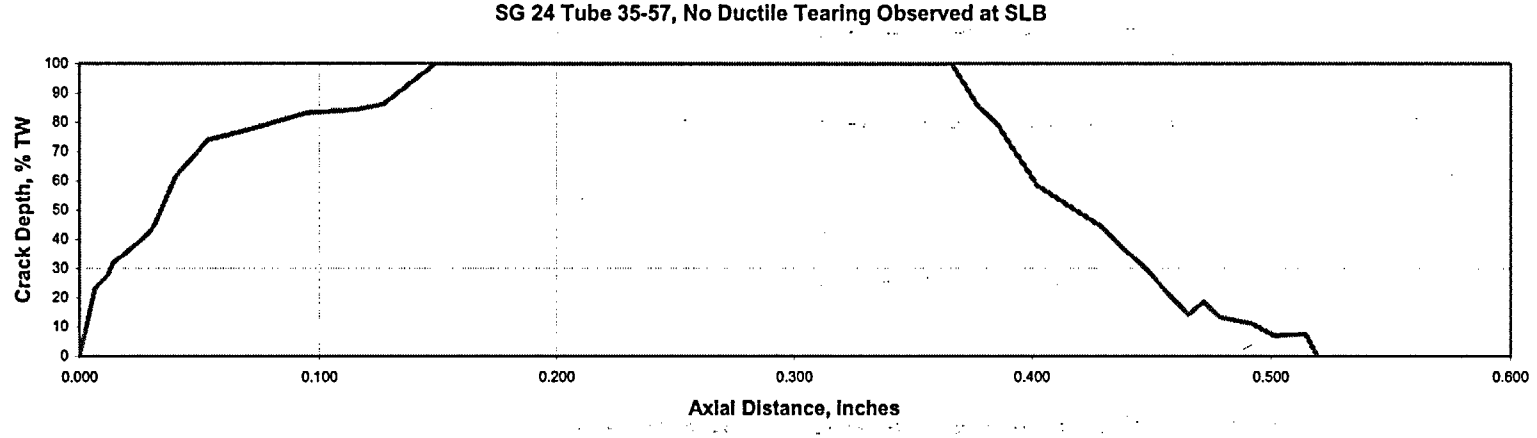

Figure 2

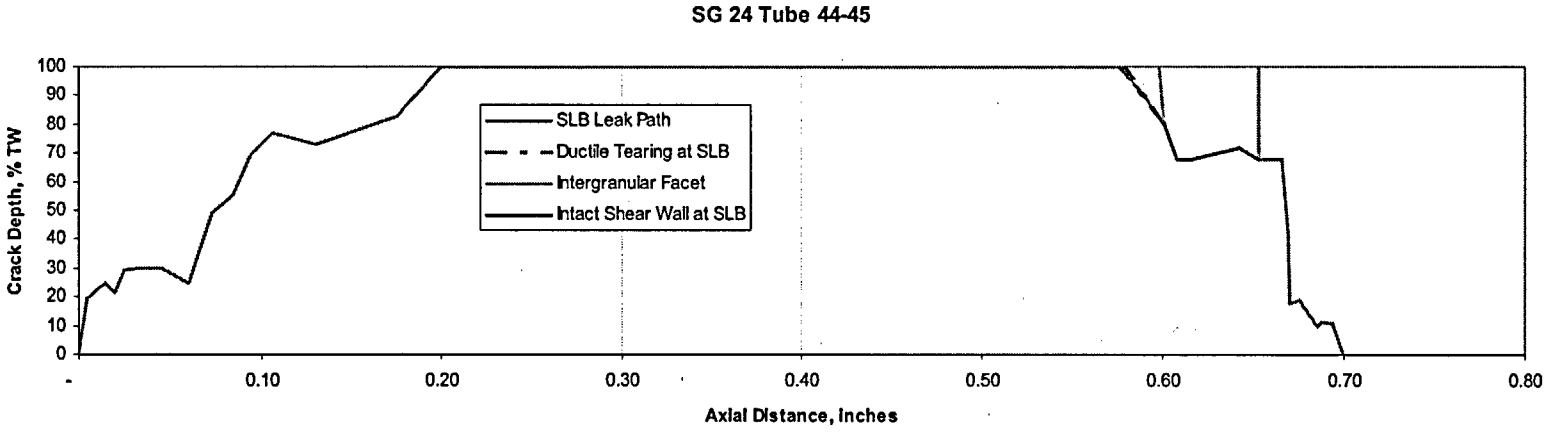

Notes for Figure 2: (1) The ductile tearing at SLB is essentially negligible

Table 5 Crack Profile Data for Tube No. R35C57

Intergranular Cracking	
Axial Distance	**Depth %TW**
0.000	0.0
0.007	23.4
0.012	27.7
0.014	32.0
0.021	36.8
0.029	42.4
0.031	45.0
0.040	61.5
0.054	74.0
0.073	77.9
0.094	83.1
0.116	84.4
0.127	86.1
0.149	100.0
0.158	100.0
0.176	100.0
0.195	100.0
0.224	100.0
0.249	100.0
0.276	100.0
0.301	100.0
0.329	100.0
0.351	100.0
0.366	100.0
0.378	85.0
0.386	79.2
0.402	58.4
0.429	44.2
0.438	37.2
0.447	30.1
0.465	14.2
0.472	18.6
0.479	13.3
0.492	11.1
0.501	7.1
0.514	7.5
0.519	0.0

Table 6 Crack Profile for Tube No. R44C45

SLB Leak Path Almost All Intergranular		High Shear Wall Intact at SLB		Intergranular Facet		Sliver of Ductile Tearing at SLB	
Axial Distance	Depth % TW	Axial Distance	Depth % TW	Axial Distance	Depth % TW	Axial Distance	Depth % TW
-	-	0.60	80.60	0.60	100.00	0.57	100.00
0.00	19.34	0.61	67.57	0.60	80.60	0.60	80.60
0.01	24.53	0.62	67.57	0.60	80.60	0.58	100.00
0.02	21.23	0.64	72.07	0.61	67.57		
0.03	29.25	0.65	67.57	0.62	67.57		
0.03	29.72			0.64	72.07		
0.05	29.72			0.65	67.57		
0.06	25.00			0.65	100.00		
0.07	49.06						
0.08	55.66						
0.09	68.87						
0.11	76.89						
0.13	73.11						
0.18	83.02						
0.20	100.00						
0.23	100.00						
0.27	100.00						
0.28	100.00						
0.30	100.00						
0.34	100.00						
0.35	100.00						
0.38	100.00						
0.41	100.00						
0.44	100.00						
0.46	100.00						
0.47	100.00						
0.50	100.00						
0.51	100.00						
0.53	100.00						
0.54	100.00						
0.56	100.00						
0.58	100.00						
0.60	80.60						
0.61	67.57						
0.62	67.57						
0.64	72.07						
0.65	67.57						
0.67	67.57						
0.67	42.34						
0.67	18.02						
0.68	18.92						
0.69	9.91						
0.69	11.71						
0.69	10.81						
0.70	-						

References

3. 7/8 OD RSG (Alloy 600) Oxidation Test Results, Framatome-ANP Report No. 51-5025213, March 2003.

SPECIAL REPORT 03-02

ENCLOSURE 6

DCPP UNIT 2 CYCLE 12 PROBABILISTIC RISK ASSESSMENT FOR SG TUBE SUPPORT PLATE AXIAL ODSCC INDICATIONS

1.0 INTRODUCTION

A PRA calculation is performed to determine the risk significance of operating a full cycle following 2R11, leaving in service steam generator (SG) tubes with axial outside diameter stress corrosion cracking (ODSCC) indications.

The results of the PRA are used to ascertain whether there is sufficient justification for providing relief from the prescriptive Probability of Burst (POB) requirements, while maintaining an acceptable level of safety, with ODSCC degraded SG tubes left in service. The calculation estimates the change in the large early release frequency (LERF) figure of merit, as a surrogate for risk.

2.0 EVALUATION

The impact of the SG tube condition on risk is assessed based on the impact on initiating event frequency (IEF) and accident mitigation capability. The evaluation of these impacts is presented below.

2.1 Impact on Spontaneous Tube Rupture Frequency

The degradation of tube integrity would have an impact on the steam generator tube rupture (SGTR) IEF, if the primary to the secondary leak via flaws in degraded tubes were not mechanically constrained. For example, flaws in the free span sections (straight sections between the tube support plates [TSPs]) may grow such that there is significant primary to secondary leakage. The impact of ODSCC flaws left in service on SGTR frequency is considered to be negligible based on:

- The tubes with axial ODSCC indications that are left in service are within the TSP sections of the tubes (See Segment 1a of Figure 1). These indications are covered by the TSPs, do not directly communicate with (i.e., leak to) the SGs, and their leakage to the SGs under normal operating conditions is restricted by the tight gap between the TSPs and the tubes. This is part of the basis in Generic Letter (GL) 95-05 (Reference 1) for allowing tubes with such indications to remain in service.

  Note that GL 95-05 performance criteria only addresses potential tube rupture following the worst-case design basis accident, Main Steam Line Break (MSLB), which implies that the potential tube rupture during normal operation is not of concern. In addition, WCAP-14707/14708 (Reference 2, or "the WCAP") concluded that DCPP's ODSCC leakage via through wall cracks is further restricted by the packed crevices.

  The in-situ pressure test results for the most degraded ODSCC crack (R44C45) on SG 2-4 showed a low leak rate of 0.004 gpm, which confirms the engineering judgments stated above. Indeed, most of the indications that were left in service following 2R11 are smaller at the beginning of cycle (BOC) 12 than the 2.0v BOC 11 indication for R44C45, due to the decrease in plugging limits following 2R11. Therefore, these smaller indications are not expected to grow as large as the R44C45 indication.

- The axial ODSCC indications in tubes that will be left in service will not propagate outside of the TSP area since there are no mechanisms that would facilitate such propagation. This judgment is supported by many years of in-service history that shows no significant outside of the TSP area.

2.2 Impact on Accident Mitigation Capability

The current prescriptive POB and leakage requirements for voltage-based ARC were established to ensure structural and leakage integrity for all postulated design basis events. The structural criteria are intended to ensure that indications subjected to the voltage repair limits will withstand pressure loadings consistent with the criteria of draft Regulatory Guide 1.121 (Reference 3). The leakage criteria ensure that for degraded tubes, induced leakage under worst-case MSLB conditions (calculated using licensing basis assumptions) will not result in offsite or control room dose releases that exceed the applicable limits of 10 CFR Part 100 and GDC 19. From the Probabilistic Risk Assessment (PRA) perspective, the risk significance of the POB requirements is analyzed for the following classes of events:

2.2.1 *Class 1 – Events with the Potential to Displace TSPs, Resulting in Exposure of Through-wall ODSCC Cracks, SGTR, But No Increase in ΔP across the TSPs*

The concern is that the challenge of mitigating the consequences of certain initiating events may be increased (i.e., probability of failure may be increased) if:

a. One or more ODSCC indications left in service were to grow and become long through-wall cracks (similar to the R44C45), and

b. The ODSCC through-wall crack(s) were exposed due to initiating event-induced, vertical displacement of one or more TSPs.

Note that for this class, there is no increase in differential pressure across the SG tubes.

Based on a review of Reference 4, it is concluded that seismic events are the only initiating events that can contribute to this class. The possibility of TSP movement due to a seismic event is judged not to be credible based on a review of Reference 5 and the WCAP.

2.2.2 *Class 2 – Secondary Side Depressurization Sequences with TSP Displacement, Resulting in Rupture of One or More Degraded Tubes*

The concern is that the presence of some degraded tubes may increase the potential for a consequential SGTR event. This potential increase is due to the pressure differential that is induced across the tubes following a plant trip (i.e., following a depressurization initiating event). For ODSCC flaws within the TSPs, this concern is only applicable if the TSPs are displaced. Based on a review of Table C.9-2A/B/C of Reference 4, it is concluded that SLB and Feedwater Line Break (FWLB) initiating events are the only DCPP PRA model initiators that potentially could displace the TSPs vertically concurrent with the SG tubes being subjected to higher differential pressure. This class of events is potentially affected by the integrity of those tubes with ODSCC indications that will be left in service following 2R11. The main concern for this event class is that forces

generated inside the SGs by the initiating event may result in displacement of the TSP relative to the tube, thereby exposing the ODSCC flaws, which would then be exposed to the high differential pressure induced by the initiating event.

The potential contribution of this class of events to the LERF figure of merit is discussed in Section 4.0.

2.2.3 *Class 3 – Severe Accident Thermal Challenge-Induced Tube Rupture Events*

This class includes tube ruptures that are induced during a severe accident where RCS pressure remains high and the secondary side has dried following failure of all feedwater (i.e., "high and dry" sequences). There are two possible tube rupture scenarios for these conditions: high pressure-induced ruptures and high temperature-induced ruptures (creep failures).

For this class, it is expected that there would be high temperatures in the tubes due to natural circulation of the hot gases from the reactor. However, the TSP performs the same reinforcing function for this class as stated in earlier sections of this calculation, just with lower material structural properties and a potential for creep to occur. In effect, there is a race to failure between different components of the primary pressure boundary due to the induced high temperature condition.

The issue is whether or not the primary piping or some other piping segment of the primary system would fail by creep rupture before SG tube failure occurred. One "rule-of-thumb" for this evaluation is that failure of the SG tubing is not expected to occur if performance criteria are met outside of consideration of severe accident conditions. The potential presence of a very large ODSCC indication within a TSP raises the question of considering the tube within the TSP. Although it is not known whether the flawed tube in the TSP is stronger than other primary components from the creep failure point of view, it is judged that, owing to the support provided by the TSP, the flawed tube would not fail. Therefore, the real question is whether the TSP would fail due to high temperature prior to failure of another segment of the RCS piping subjected to the same high temperature condition.

It is judged that the TSP will not fail prior to failure of another RCS piping segment. To illustrate, the material in the TSPs is stronger than the material in the unflawed free span of the SG tubes and is effectively very "thick" in the radial direction. In addition, the temperature gradient in the radial direction would further inhibit a thermally-induced reduction in strength of the TSP material relative to that of the free span tube material. This means that, in addition to the expectation that performance criteria will be met during normal operation, the barrier is also expected to stay intact for severe accident conditions.

The key is that the TSPs prevent or severely limit pressure-induced crack opening or tube deformation during a postulated severe accident. This prevents high-pressure tube ruptures and restraint of the deformation prevents high temperature tube ruptures by limiting the amount of creep deformation that could occur.

Note that based on a review of Reference 6, theoretical and experimental evidence suggests that creep failure of the surge line or hot leg would result in a large opening, and the resulting rapid depressurization of the RCS would eliminate any further threat to the SG tubes.

Based on the above, the contribution of this class of events to risk is not quantified. Note that the impact on the severe accident mitigation capability following a SLB-induced core damage is not evaluated on the basis that, the contribution from such a scenario to the risk would be even smaller than the contribution from the Class 2 events. This judgment is based on the observation that the conditional core damage probability for a SLB initiating event is less than 1.0E-4.

2.2.4 *Class 4 – Anticipated Transient Without Scram (ATWS) Sequences, Resulting in Tube Ruptures*

This class of events is caused by failure of the reactor protection system when all feedwater is lost. If the moderator temperature coefficient is also too low, RCS pressure could rise to create a pressure differential large enough to rupture one or more degraded tubes, creating a containment bypass.

For the ODSCC indications within the TSPs, this class of events is not of major concern since:

- Almost all ATWS events, other than the main feedwater (MFW) break ATWS, will not create a pressure differential within the SGs large enough to displace TSPs. As a result, any ODSCC indications left in service that may grow to degraded conditions will be covered by TSPs and will not be exposed to large differential pressures.

- The frequency of MFW break ATWS is very small (in the range of 1.0E-06 per year). Therefore, the contribution of this class of events is negligible when other probabilities (e.g., probability of TSP displacement and POB) are considered.

Based on the above, the contribution of this class of events to risk is not quantified.

3.0 MAJOR ASSUMPTIONS AND ASSERTIONS

The following assumptions and assertions are made for the evaluation.

1. Conservatively, the total contribution of non-isolated SGTR events to core damage frequency (CDF) is treated as the contribution to the LERF figure of merit.

2. Typically, in most risk-informed applications, the change in the figure of merit (LERF in this case) is calculated by subtracting a case figure of merit from a corresponding base case figure of merit. In this evaluation, this subtraction is not carried out and the entire contribution of the case figure of merit is conservatively considered to be the change in the figure of merit.

3. The ODSCC indications that are left in service are within the TSP sections of the tubes (See Segment 1a of Figure 1). Such indications are covered by the TSPs, do not directly communicate with (i.e., leak to) the SGs, and their leakage to the SGs under normal and most accident conditions is restricted by the gap between the TSP and the tube. However, following certain events, such as a major MSLB initiating event, the TSP may be displaced, exposing the cracks and potentially resulting in a SGTR event.

4. Based on a review of the WCAP (Reference 2), it is concluded that the likelihood that the TSPs would displace following a MSLB initiating event is small, and dented tubes or packed crevices would restrict leakage to negligible levels. The WCAP describes the results of work performed to assess potential TSP displacement in a postulated MSLB event for a generic Model 51 SG with dented or packed tube-to-TSP crevices. The generic analyses provided in the WCAP are applicable to DCPP as DCPP's SGs are Model 51 and have TSP corrosion. In essence, the WCAP concludes that the TSPs are essentially "locked" in place to the tubes. This conclusion is largely supported by the findings of the NRC's review of the WCAP (Reference 7). For example, page 6 of Reference 7 ("Staff Comments on Domestic Plant Pulled Tube Force Measurement" section) states that "the pull force measurements appear to support the licensee's contention that intersections packed with corrosion product (even non-dented intersections) offer significant resistance to tube displacement relative to the TSPs."

   The WCAP discusses the consequences of both MSLB and FWLB events, with MSLB loads being the highest (and therefore bounding). MSLB loads across the TSPs (about 60 psi) are well below the values required to overcome dented TSP contact pressures to permit TSP displacement. However, since the corrosion of TSPs is not an engineered safety feature, it is assumed that there is a probability (P_{DIS}) that TSPs will displace during a MSLB event given dented TSP intersections. Based on a review of Reference 8, P_{DIS} is assumed to be 0.001.

5. The postulated SLB has to be large enough to create sufficient force to displace the TSPs. It is asserted that the SLB break size must be at least as large as pipe ruptures that contribute to the medium LOCA initiating event (i.e., greater than 3 inches).

4.0 CALCULATIONS

Based on the evaluation presented above, the potential impact on LERF is calculated only for Class 2 events (See Section 2.2.2).

The delta LERF is calculated based on the equation below.

$$\Delta LERF_{C2} = F_{TSPIE} * P_{DIS} * P_{R/SLB} * CCDP_{C2} * CCBP_{C2}$$

Where,

F_{TSPIE} is the frequency of initiating events that could create load conditions with the potential to displace the TSP vertically, relative to the tubes.

P_{DIS} is the probability of TSP displacement.

$P_{R/SLB}$ is the probability of one or more tubes rupturing given TSP displacement.

$CCDP_{C2}$ is the conditional core damage probability given a Class 2 initiating event (scenario specific).

$CCBP_{C2}$ is the conditional containment bypass probability given core damage (scenario specific).

The result of a detailed calculation (Reference 7) is that the total delta LERF is 2.38E-9 per year.

5.0 CONCLUSIONS

The above results indicate that the safety significance, as measured by the change in the LERF figure of merit, associated with leaving tubes with ODSCC flaws in service after 2R11 is low. This conclusion is reached based on a comparison of the results of this calculation with the LERF safety (risk) insignificance criteria of 1.0E-7 presented in Reference 8.

Additionally, several sensitivity cases were run. The results indicate that the base case results are reasonable and, given the "locked" feature of the TSPs, the risk is low.

6.0 REFERENCES

1. Generic Letter 95-05, "Voltage-Based Repair Criteria for Westinghouse Steam Generator Tubes Affected by Outside Diameter Stress Corrosion Cracking"

2. WCAP-14707/14708, "Model 51 Steam Generator Limited Tube Support Plate Displacement Analysis for Dented or Packed Tube to Tube Support Plate Crevices," August 1996

3. Regulatory Guide 1.121, "Bases for Plugging Degraded PWR Steam Generator Tubes"

4. PG&E Calculation File C.9, "Quantification of CDF and LERF for the DCC0 Combined Internal, Seismic, and Fire Model," Revision 9

5. Email Rich Smith (Westinghouse) to Amir Afzali (PG&E), dated February 28, 2003, "Probability Assessment: Plate Displacement Under Seismic Loads" (stored in PRA03-02 subdirectory)

6. EPRI TR-107623-V1, "Steam Generator Tube Integrity Risk Assessment," Volume 1: General Methodology, Section 4.1.2, July 2000.

7. PRA Calculation File PRA03-02REV1, "Risk Significance of One Cycle Operation Given 2R11 SG ARC Issue".

8. Regulatory Guide 1.174, "An Approach for Using PRA in Risk Informed Decisions on Plant-Specific Changes to the Licensing Basis," dated July 1998.

Figure 1 - S/G Tube Degradation Mechanisms